2009-11-03

Caspase Mediated Cleavage, IAP Binding, Ubiquitination and Kinase Activation : Defining the Molecular Mechanisms Required for *Drosophila* NF-κB Signaling: A Dissertation

Nicholas Paul Paquette
University of Massachusetts Medical School Worcester

CASPASE MEDIATED CLEAVAGE, IAP BINDING, UBIQUITINATION AND KINASE ACTIVATION: DEFINING THE MOLECULAR MECHANISMS REQUIRED FOR *DROSOPHILA* NF-κB SIGNALING

A Dissertation Presented

By

Nicholas Paul Paquette

Submitted to the Faculty of the University of Massachusetts Medical School of Biomedical Sciences, Worcester in partial fulfillment of the requirements for the degree of

DOCTOR OF PHILOSOPHY

OCTOBER 22, 2009

INTERDISCIPLINARY GRADUATE PROGRAM

CASPASE MEDIATED CLEAVAGE, IAP BINDING, UBIQUITINATION AND KINASE ACTIVATION: DEFINING THE MOLECULAR MECHANISMS REQUIRED FOR *DROSOPHILA* NF-κB SIGNALING

A Dissertation Presented By

Nicholas Paul Paquette

The signatures of the Dissertation Defense Committee signifies completion and approval as to style and content of the Dissertation

Neal Silverman, Ph.D., Thesis Advisor

Michael Brodsky, Ph.D., Member of Committee

Y. Tony Ip, Ph.D., Member of Committee

Egil Lien, Ph.D., Member of Committee

Mary O'Riordan, Ph.D., Member of Committee

The signature of the Chair of the Committee signifies that the written dissertation meets the requirements of the Dissertation Committee

Jon Goguen, Ph.D., Chair of Committee

The signature of the Dean of the Graduate School of Biomedical Sciences signifies that the student has met all graduation requirements of the School.

Anthony Carruthers, Ph.D.
Dean of the Graduate School of Biomedical Sciences

Interdisciplinary Graduate Program

October 22, 2009

“You ever wonder why we're here?”

Dick Simmons and Michael J. Caboose

Acknowledgments

Foremost I would like to thank my advisor Dr. Neal Silverman for his superb advice and mentoring during my time in his lab. Although the road was not always clear he somehow always seemed to point me in the right direction. I would like to thank him for allowing me the freedom to work independently, make mistakes, and always come away learning something. His leadership and guidance have made me a better scientist, and a better thinker.

I thank my thesis advisory committee, Jon Goguen, Michael Brodsky, Egil Lien, and Tony Ip for their support during my graduate work as well as Mary O'Riordan, for taking the time to evaluate my dissertation.

I am deeply indebted to all the students, staff, professors, technicians and everyone else from the Silverman lab and the UMMS family who I have worked with and gotten to known over my time at the university. My thanks goes out to, Takashi Kaneko, Charles Sweet, Chan-Hee Kim, Florentina Rus, Kendi Okuda, Donggi Paik, Qi Wu, Deniz Erturk-Hasdemir, Kamna Aggarwal, Li Chan, Sandhya Ganesan, Chris Vriesema-Magnuson, Stefanie Crovello, Diane Hwang, Rosemary Behan, Norah Fogarty, Peihong Guan, Diana Wentworth, Andrea Pereira, Devon Slater, Bill Marshall, Kayla Morlock, Sanjay Ram, Lisa Lewis, Tathagat Dutta Ray, Ted Giehl, Susann Paul, Maryjean Capus Shedd-Lindem, Heather Montoya, Carol Jolly, Swati Joshi, Cathrine Knetter, Greg Vladimer, Zaida Ramirez, Nick Willis, Alex Keene, Dan Brewer, Krystin Bedard, and anyone

else I might have forgotten to mention. You have all made each day here a joy, a pleasure and an adventure.

I would also like to send out a special thanks to the people at Rooster Teeth. As most of my co-workers can attest your work always kept me laughing, quite loudly, and in a great mood, even when the experiments weren't going well. Thanks for being the humor in my ear over the years.

I was fortunate to have the opportunity to begin working at UMMS as a research intern while in high school at North High, in Worcester. This research sparked my curiosity and continued through my time in college at Worcester Polytechnic Institute where I earned a Bachelors of Science degree in Biology and Biotechnology. I would like to acknowledge the people who encouraged my interest during this time in my life; Mrs. Drake, Mrs. Clifford, Robert Zurier, Ron Rossetti, Jill Rulfs, and Dave Adams. Thank you for seeing the spark in me.

I am grateful my parents and family for their love, support and sacrifice over the years. Without you I wouldn't be where I am today. I am indebted to you always.

Lastly I would like to thank my wife Sara. When I started in graduate school I was unsure of what the future held for me. Little did I realize that the answer was right in front of me, well maybe off to the right. I thank you for your encouragement, your help, and your love. Although our studies were what brought us together, our love is what keeps us together. For that I am eternally grateful.

TABLE OF CONTENTS

LIST OF FIGURES

LIST OF PUBLICATIONS

- **Nicholas Paquette**, Meike Broemer, Kamna Aggarwal, Li Chen, Marie Husson, Deniz Ertürk-Hasdemir, Jean-Marc Reichhart, Pascal Meier, Neal Silverman. *Caspase Mediated Cleavage, IAP Binding and Ubiquitination: Linking Three Mechanisms Crucial for Drosophila NF-κB Signaling***.** Under review, 2009

- **Nicholas Paquette,** Charles Sweet, William Lane, Neal Silverman. *Serine/ Threonine Acetylation of Drosophila TAK1 by the Yersinia pestis protein YopJ.* In preperation, 2009

- Alain C Jung, Vanessa Gobert, Rui Zhou, **Nicholas Paquette**, Sophie Rutschmann, Marie-Claire Criqui, Marie-Céline Lafarge, Matthew Singer, David A Ruddy, Tom Maniatis, Jules A Hoffmann, Neal Silverman, Dominique Ferrandon, *Analysis of Drosophila TAB2 mutants reveals that IKK, but not JNK pathway activation, is essential in the host defense against Escherichia coli infections*. Under revision, 2009

- Joshua V. Troll, Eric H. Bent, **Nicholas Pacquette**, Andrew M. Wier, William E. Goldman, Neal Silverman and Margaret J. McFall-Ngai. *Taming the symbiont for Coexistence: A Host PGRP Neutralizes a Bacterial Symbiont Toxin*. Environmental Microbiology, 2009

- Deniz Erturk-Hasdemir, Meike Broemer, Francois Leulier, William S. Lane, **Nicholas Paquette**, Daye Hwang, Chan-Hee Kim, Svenja Stoven, Pascal Meier, and Neal Silverman *Two roles for the Drosophila IKK complex in the activation of Relish and the induction of antimicrobial peptide genes.* PNAS 2009 Jun; 106(24): 9779-9784

- Joshua V. Troll, Dawn M. Adin, Andrew M. Wier, **Nicholas Paquette**, Neal Silverman, William E. Goldman, Frank J. Stadermann, Eric V. Stabb and Margaret J. McFall-Ngai. *Peptidoglycan induces loss of a nuclear peptidoglycan recognition protein during host tissue development in a beneficial animal-bacterial symbiosis.* Cellular Microbiology 2009 Mar; 11(7): 1114-1127

- Kamna Aggarwal, Florentina Rus, Christie Vriesema-Magnuson, Deniz Ertuk-Hasdemir, **Nicholas Paquette**, and Neal Silverman. *Rudra Interrupts Receptor Signaling Complexes to Negatively Regulate the IMD pathway*. PLoS Pathog 2008 Aug; 4(8) :e1000120

- Neal Silverman and **Nicholas Paquette**. *The Right Resident Bugs*. *Science* 2008 Feb; 319(5864): 734-735

- Deniz Ertürk-Hasdemir, **Nicholas Paquette**, Kamna Aggarwal, and Neal Silverman. Bug versus Bug: Humoral Immune Responses in *Drosophila melanogaster*. Chapter in *Innate Immunity in Plants, Animals, and Man*, *Nucleic Acids and Molecular Biology, volume 21*, Edited by Holger Heine

ABSTRACT

Innate immunity is the first line of defense against invading pathogens. Vertebrate innate immunity provides both initial protection, and activates adaptive immune responses, including memory. As a result, the study of innate immune signaling is crucial for understanding the interactions between host and pathogen. Unlike mammals, the insect *Drosophila melanogaster* lack classical adaptive immunity, relying on innate immune signaling via the Toll and IMD pathways to detect and respond to invading pathogens. Once activated these pathways lead to the rapid and robust production of a variety of antimicrobial peptides. These peptides are secreted directly into the hemolymph and assist in clearance of the infection.

The genetic and molecular tools available in the *Drosophila* system make it an excellent model system for studying immunity. Furthermore, the innate immune signaling pathways used by *Drosophila* show strong homology to those of vertebrates making them ideal for the study of activation, regulation and mechanism. Currently a number of questions remain regarding the activation and regulation of both vertebrate and insect innate immune signaling. Over the past years many proteins have been implicated in mammalian and insect innate immune signaling pathways, however the mechanisms by which these proteins function remain largely undetermined.

My work has focused on understanding the molecular mechanisms of innate immune activation in *Drosophila*. In these studies I have identified a

number of novel protein/protein interactions which are vital for the activation and regulation of innate immune induction. This work shows that upon stimulation the *Drosophila* protein IMD is cleaved by the caspase-8 homologue DREDD. Cleaved IMD then binds the E3 ligase DIAP2 and promotes the K63-polyubiquitination of IMD and activation of downstream signaling. Furthermore the *Yersinia pestis* effector protein YopJ is able to inhibit the critical IMD pathway MAP3 kinase TAK1 by serine/threonine-acetylation of its activation loop. Lastly TAK1 signaling to the downstream Relish/NF-κB and JNK signaling pathways can be regulated by two isoforms of the TAB2 protein. This work elucidates the molecular mechanism of the IMD signaling pathway and suggests possible mechanisms of homologous mammalian systems, of which the molecular details remain unclear.

PREFACE TO CHAPTER I

Portions of this chapter have been published separately in:

Deniz Ertürk-Hasdemir, **Nicholas Paquette**, Kamna Aggarwal, and Neal Silverman. *Bug versus Bug: Humoral Immune Responses in Drosophila melanogaster*. Chapter in Innate Immunity in Plants, Animals, and Man, Nucleic Acids and Molecular Biology, volume 21, Edited by Holger Heine

Nicholas Paquette, Deniz Erturk Hasdemir, Kamna Aggarwal and Neal Silverman all contributed to the manuscript equally.

CHAPTER I

INTRODUCTION

A brief history of insects and immunity

In the last 200 years substantial focus has been placed on infection in insects for economic and public health reasons. In 1865 Louis Pasteur established that microsporidia was the causative agent of pébrine disease in silkworms resulting in decrease in silk production causing a significant economic impact (Brey, 1998). In the following decades Carlos Finlay showed that mosquitoes were vectors for yellow fever (Chaves-Carballo, 2005). As a result during the early 20th century a great deal of interest was placed on characterizing the microbial flora associated with insects with a view to their potential impact on human society (Steinhaus, 1940).

By the end of the 1960s, it had already been determined that pathogens such as fungi, protozoa, viruses and bacteria were capable of infecting insects. In response to these infections, insects activate cellular and humoral immune defenses including phagocytosis and the production of antimicrobial substances (Heimpel and Harshbarger, 1965). A milestone in the field of insect immunity was the study from Hans Boman and colleagues on the inducible antibacterial defense mechanisms of *Drosophila* (Boman *et al*., 1972). In subsequent years, a number of studies were undertaken to characterize insect specific antimicrobial peptides (AMPs) and the genes encoding them from various insect species including *Drosophila* (Hultmark *et al*., 1983; Kylsten *et al*., 1990; Samakovlis *et al*., 1990; Steiner *et al*., 1981; Sun *et al*., 1991).

Antimicrobial peptides are small, cationic molecules that are effective against specific classes of pathogens. For example, *Drosophila* express peptides against Gram-positive bacteria (Defensin) (Dimarcq *et al*., 1994), Gram-negative bacteria (Diptericin, Drosocin and Attacin) (Asling *et al*., 1995; Michaut *et al*., 1996; Wicker *et al*., 1990), fungi (Drosomycin) and both bacteria and fungi (Metchnikowin and Cecropin) (Ekengren and Hultmark, 1999; Levashina *et al*., 1995; Samakovlis *et al*., 1992). These antimicrobial peptides are critical for resistance to infection, such that transgenic expression of a single antimicrobial peptide can protect immunodeficient flies (Tzou *et al*., 2002). Since these early studies on antimicrobial peptides, two major questions have shaped the field of insect immunology; how are microbes recognized and how is antimicrobial peptide gene expression regulated? The powerful genetic and molecular tools available made *Drosophila* the preferred experimental system to address these issues.

While study in vertebrate systems is still essential, there are many advantages to using *Drosophila* as a model system. Although evolutionarily separated from vertebrate organisms, many major *Drosophila* pathways including those involved in immunity, DNA damage repair, and neurodegeneration are reasonably conserved. Moreover many vertebrate systems have developed multiple redundant proteins which can make analysis difficult. *Drosophila* often do not contain the same level of redundancy however. With a generation time of only two weeks, *Drosophila,* are quicker, cheaper and easier to maintain than

most mammals. *Drosophila* also offer a number of well established genetic tools such as balancers and P-elements, which allow for expedient genome wide screening in adult animals. Lastly, a number of well established *Drosophila* cell culture lines are also available for experimental use. Overall *Drosophila* provide versatility and control ideal for scientific research.

An Overview of the *Drosophila* immune response

Insects are exposed to a multitude of pathogens in their natural environment, and as a result they have developed sophisticated mechanisms to recognize and respond to infectious microorganisms. Although they lack a fully evolved adaptive immune response, insects do have highly effective innate immune responses to a wide range of pathogens. Moreover, the insect immune response has proven to be a useful and highly conserved model system for the study of innate immunity in general.

Drosophila have a multi-layered immune system to facilitate pathogen defense, with an initial physical barrier provided by the chitin-based exoskeleton and internal structures. If a pathogen breaches these barriers, several immune effector mechanisms respond, including cellular responses (*i.e.* phagocytosis, encapsulation and melanization) and humoral responses (*i.e.* antimicrobial peptides). Of these mechanisms, antimicrobial peptide synthesis is perhaps the most critical for protection from microbial infections. Antimicrobial peptides are produced both locally, at the site of infection, and systemically in the insect sera,

or hemolymph. Local induction of antimicrobial peptide gene expression takes place in epithelial tissues such as the trachea and gut (Ferrandon *et al*., 1998; Liehl *et al*., 2006; Tzou *et al*., 2000). Systemic humoral response is initiated in the fat body, the *Drosophila* liver-like organ, which is the major site of antimicrobial peptide production. Other tissues also contribute, including the malphigian tubules and circulating blood cells, known as hemocytes (Ferrandon *et al*., 2007).

Recognition of pathogens is the first step in a cascade of events that lead to immune response. Microbial products, often cell surface components, are detected by recognition receptors, which in turn stimulate signaling pathways that culminate in the induction of antimicrobial peptide gene expression. There are at least two different pathways that regulate the expression of AMP genes in *Drosophila*, the Toll and IMD pathways. The Toll pathway is stimulated by fungal and many Gram-positive bacterial pathogens, while the IMD pathway is triggered by the DAP-type peptidoglycan common to most Gram-negative bacteria (Kaneko *et al*., 2004; Michel *et al*., 2001; Levitin and Whiteway, 2008). Once activated, these pathways trigger an intracellular cascade, culminating in the rapid and robust production of antimicrobial peptides.

The signaling pathways of mammalian and insect innate immune responses show a great deal of overall similarity. After binding and activation of receptors, various adaptor proteins stimulate downstream kinases. These kinases in turn activate NF-κB proteins, leading to their nuclear localization and

transcription of immune genes. Of particular interest is the ubiquitination of signaling proteins, a step which play a critical role in mammalian innate immunity. Although ubiquitination has been implicated in signaling within the insect innate immune response no ubiquitinated target proteins have thus far been identified.

Ubiquitination

Polyubiquitination of target proteins plays an important role in many mammalian innate immune signaling pathways, and is also implicated in insect immunity. Ubiquitin is an evolutionarily conserved 76 amino acid polypeptide, found in all eukaryotic organisms. Originally identified as a cellular label of proteins designated for destruction, ubiquitination has also been shown to play an additional regulatory role. In order to covalently bind a ubiquitin moiety to a target protein, a multi-step enzymatic cascade must first occur (Figure 1.1) (Hershko, 1983). Initially ubiquitin is produced as a poly-protein which is recognized by endogenous *ubiquitin specific protease* (USP) (Varshavsky, 2000). USP cleaves the polypeptide just after the double glycine residues present at the C-terminal of each individual ubiquitin sequence, releasing mono-ubiquitin polypeptides. This liberated ubiquitin then binds to the ubiquitin activating enzyme (E1) via a thioester bond between the active cysteine of the E1 and the C-terminal glycine of the ubiquitin moiety. This ‘activated’ ubiquitin is then transferred to a ubiquitin conjugating enzyme (E2) via the formation of an additional thioester bond. Lastly the C-terminal glycine of the ubiquitin is

Figure 1.1

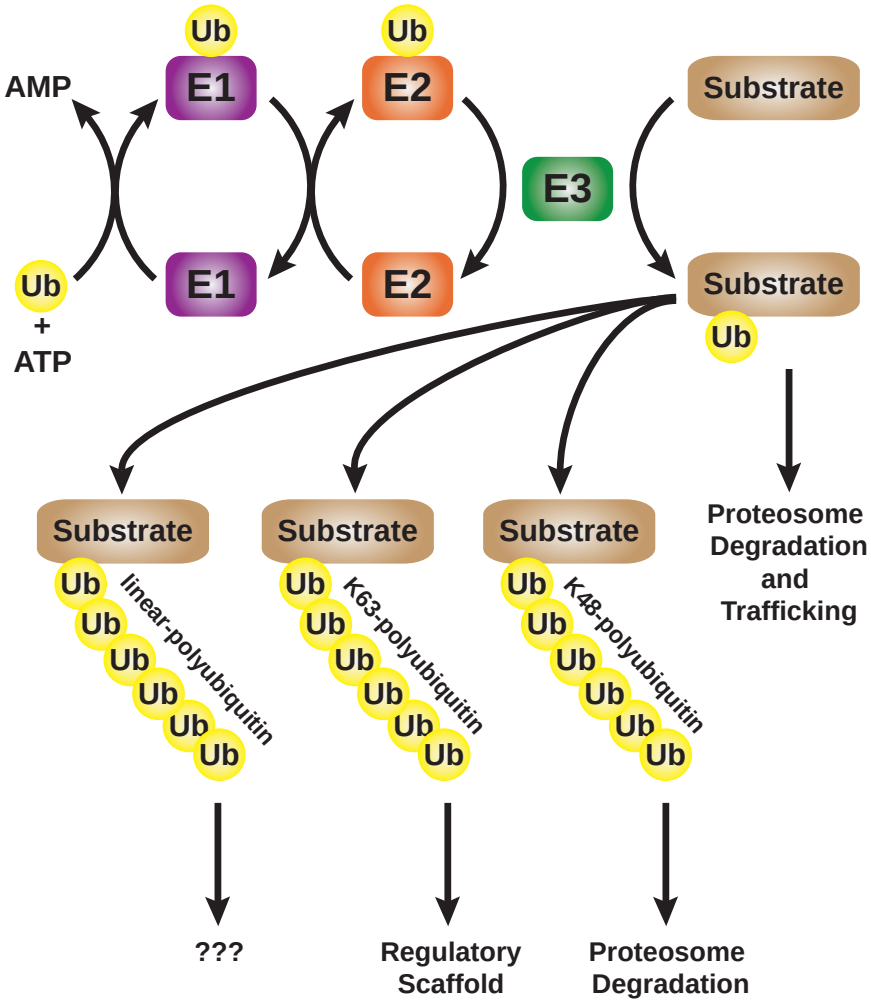
Ub
Ub
AMP
E1
E2
Substrate
E3
Ub
+
ATP
E1
E2
Substrate
Ub
Substrate
Substrate
Substrate
Proteosome
Degradation
and
Trafficking
Ub
Ub
Ub
Ub
Ub
Ub
linear-polyubiquitin
Ub
Ub
Ub
Ub
Ub
Ub
K63-polyubiquitin
Ub
Ub
Ub
Ub
Ub
Ub
K48-polyubiquitin
???
Regulatory
Scaffold
Proteosome
Degradation

Figure 1.1 Protein ubiquitination

Ubiquitination of a target substrate protein is a multistep enzymatic process. In the first setup free ubiquitin is conjugated to a ubiquitin activating enzyme (E1) in an ATP-dependent process. The ubiquitin is then passed to a ubiquitin-conjugating enzyme (E2). Utilizing a ubiquitin ligase (E3) the ubiquitin is then bound to a lysine on the substrate protein via a isopeptide bond. Mono-ubiquitinated substrate proteins can then be degraded by the proteosome or marked for cellular trafficking. Alternatively, lysine 48 or lysine 63 of the conjugated ubiquitin can act as sites for binding further ubiquitin moieties resulting in K48- or K63-polyubiquitination respectively. While K48-polyubiquitin chains have been shown to play a role in protein degradation via the proteosome, K63-polyubiquitin chains appear to act as scaffolds to recruit downstream singling components. The N-terminal amino group of an initial conjugated ubiquitin protein can also bind further ubiquitin moieties resulting in linear (or head to tail) polyubiquitin chains. The physiological relevance of linear polyubiquitin chains remains unclear.

covalently bound to the ε-amino group of a lysine on the target protein via an isopeptide bond with the assistance of a ubiquitin protein ligase (E3). Two classes of E3 enzymes have currently been identified. Those containing a HECT domain mediate the transfer of ubiquitin via the formation of a ubiquitin-E3 intermediate (Bernassola *et al*., 2008). While E3 enzymes containing a RING domain catalyze the attachment of ubiquitin directly from the E2 conjugating enzyme to the target protein (Petroski and Deshaies, 2005).

Currently a number of ubiquitin modification types have been identified, all of which play different regulatory roles. The binding of a single ubiquitin moiety to a target protein can serve as a flag for protein destruction via the proteosome, while also marking proteins for cellular localization or transport (Hicke, 2001). The ubiquitin protein also carries seven lysine residues which can themselves be the target of further ubiquitination, resulting in the formation of polyubiquitin chains. Two types of lysine-mediated polyubiquitin chains have been widely described, lysine 48 (K48) and lysine 63 (K63). K48-mediated polyubiquitin chains play a major role in targeting proteins for destruction via the 26S-proteasome (Glickman and Ciechanover, 2002). K63-mediated chains do not target proteins for destruction however, and instead seem to play an alternative role (Chiu *et al*., 2009; Mukhopadhyay and Riezman, 2007). Implicated in a number of intracellular pathways K63-polyubiquitin chains are thought to act as scaffolds, recruiting downstream proteins together via ubiquitin binding domains. Once in proximity, these proteins (which are often kinases) are activated,

initiating downstream signaling. It is currently unclear if the remaining five lysine residues present in ubiquitin also mediate the production of polyubiquitin chains. It also remains to be resolved what functions polyubiquitin chains mediated from these lysines serve.

The most recently discovered type of polyubiquitin chains are linear (or head-to-tail) chains (Kirisako *et al*., 2006; Rahighi *et al*., 2009; Komander *et al*., 2009; Tokunaga *et al*., 2009). Unlike K48- and K63-polyubiquitin chains which require binding of a lysine residue, linear ubiquitin chains result from the binding of the C-terminal glycine of a free ubiquitin protein to the N-terminal amino group of a previous conjugated ubiquitin. Little is known about the functional relevance of these linear polyubiquitin chains, however; there is some evidence that they may play a role in immune signaling (Tokunaga *et al*., 2009; Rahighi *et al*., 2009; Komander *et al*., 2009).

Evidence has come to light indicating that the substrate proteins to which polyubiquitin chains are conjugated may not be as critical as once thought. Work done by Xia and colleagues (2009), shows that unanchored polyubiquitin chains (*i.e.* polyubiquitin chains which are not conjugated to a target protein) are able to recruit and activate downstream kinases. In at least one case, these unachored polyubiquitin chains have been shown to form after stimulation of mammalian HEK cells (Xia *et al*., 2009). These data strongly indicate that the presence or absence of polyubiquitin chains is in some cases more important than the substrate protein to which they are conjugated.

Protein ubiquitination is a reversible reaction. Deubiquitinating enzymes (DUBs) catalyze the removal of ubiquitin from target proteins via protease or metalloprotease activity (Amerik and Hochstrasser, 2004). Deubiquitination is a critical step in many signal transduction pathways. In particular at least 2 DUBs have been described as playing integral roles in mammalian immunity (Kovalenko *et al*., 2003; Trompouki *et al*., 2003; Krikos *et al*., 1992). Recently a *Drosophila* DUB, USP36, was identified as playing a role in the IMD innate immune signaling pathway (discussed further in Chapter 2). This protein is shown to remove K63-polyubiquitin chains in order to down regulate signaling (Thevenon *et al*., 2009).

***Drosophila* Toll signaling**

The *Drosophila* Toll pathway responds to Gram-positive bacterial and fungal infections (Lemaitre *et al*., 1996). Unlike human Toll-like receptors (TLRs), *Drosophila* Toll does not directly bind pathogens or microbe-derived compounds. Instead Toll is activated by the serum protein Spätzle. Spätzle is secreted into the extracellular environment as a pro-protein, with a disulfide-linked dimeric structure. In order to activate the Toll pathway, pathogens activate serine protease cascades that culminate in the cleavage of Spätzle, liberating the mature Toll ligand (C-terminal 106 amino acids) (Hu *et al*., 2004; Weber *et al*., 2003).

Recognition of Gram-positive bacteria involves the receptors PGRP-SA and PGRP-SD (Bischoff *et al*., 2004; Gobert *et al*., 2003; Michel *et al*., 2001; Pili-Floury *et al*., 2004). These receptors can function individually, or in the case of PGRP-SA as part of a complex with Gram-Negative Binding Protein 1 (GNBP-1), which is a peptidoglycan (PGN) processing enzyme. Both the PGRP-SA and PGRP-SD receptors recognize lysine-type PGN, found in the cell wall of most Gram-positive bacteria, although their specificities probably differ slightly (Michel *et al*., 2001; Bischoff *et al*., 2004). Once activated, the receptors and associated proteins lead to Spätzle cleavage by activating serine protease cascades (Lemaitre *et al*., 1996; Ligoxygakis *et al*., 2002; Kambris *et al*., 2006; Jang *et al*., 2006).

Once cleaved, Spätzle binding induces dimerization of the Toll receptor. Although the ligand is a symmetric dimer, biophysical studies indicate that the Spätzle-induced Toll dimer is asymmetrical (Weber *et al*., 2003). It is not yet clear if this asymmetric aspect of the ligand-induced Toll dimer is critical for the activation of intracellular signaling. Dimerization of the Toll receptor is believed to recruit a pre-existing MyD88/Tube complex (Figure 1.2) and also associates with the kinase Pelle (the homolog of mammalian IRAK). The assembly of the resulting receptor complex occurs via two distinct functional domains on each protein. While the interaction between Toll and MyD88 occurs via their Toll/IL-1R (TIR) domains, Myd88, Tube, and Pelle interact in a trimeric complex via Death Domains (DD) found in each protein (Sun *et al*., 2002a; Sun *et al*., 2002b;

Figure 1.2

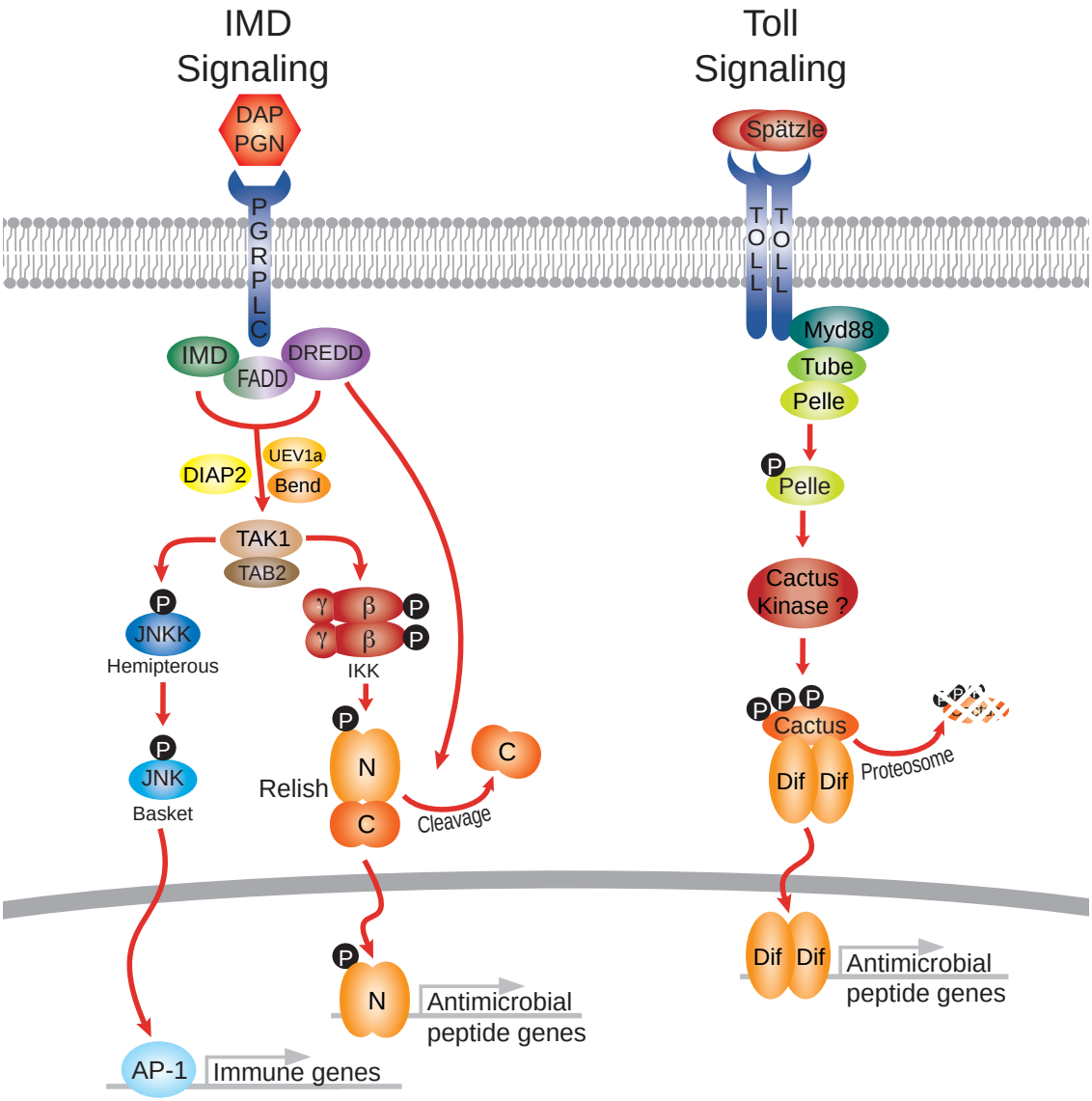
IMD
Signaling
Toll
Signaling
DAP
PGN
PGRPLC
IMD
FADD
DREDD
DIAP2
UEV1a
Bend
TAK1
TAB2
JNKK
Hemipterous
JNK
Basket
AP-1
Immune genes
γ
β
IKK
Relish
N
C
Cleavage
N
Antimicrobial
peptide genes
Spätzle
TOLL
TOLL
Myd88
Tube
Pelle
Pelle
Cactus
Kinase ?
Cactus
Dif
Dif
Proteosome
Dif
Dif
Antimicrobial
peptide genes

Figure 1.2 *Drosophila* NF-κB signaling

(Left) In the presence of Gram-negative bacteria, the receptor PGRP-LC binds DAP type peptidoglycan (PGN). Binding of PGN to the receptor recruits the adaptor proteins IMD, FADD, and the caspase DREDD. Through an undefined mechanism requiring Uev1A and Bendless (Ubc13 homologue), the MAP3 kinase TAK1 is then activated. The protein DIAP2 is also thought to play a role in this activation. TAK1 then phosphorylates and activates the IKK complex leading to the phosphoryation of the NF-κB protein Relish. In a separate arm of the pathway, Relish is cleaved in a DREDD dependent manner. Cleaved/ phosphorylated Relish translocates into the nucleus activating antimicrobial peptide production. TAK1 also phosphorylates the JNK kinase Hemipterous leading to the phosphorylation of the JNK protein Basket and activation of AP1 dependent immune genes. (Right) In the presence of Gram-positive bacteria and fungus, the secreted cytokine Spätzle is proteolytically cleaved. Cleaved Spätzle then acts as the Toll receptor ligand inducing dimerization. Activated Toll recruits the adaptor proteins MyD88, Tube and Pelle. Activation of Pelle leads to the phosphorylation of the IκB protein Cactus. Phosphorylation of Cactus promotes its K48-polyubiquitination and proteosomal degradation allowing the NF-κB homologue Dif (or Dorsal) to translocate into the nucleus and activate AMP production.

Tauszig-Delamasure *et al*., 2002; Towb *et al*., 1998). Although the DDs of these proteins are necessary for their interactions, Myd88 and Pelle do not interact directly; Tube acts as the core of the trimeric complex. The mammalian homolog IRAK displays similar recruitment via an adapter complex in the mammalian Myd88-dependent TLR signaling.

Insect infections by Gram-positive bacteria and fungi culminate in the nuclear translocation of the NF-κB proteins DIF and/or Dorsal. DIF is the main regulator of Toll signaling in both adults and larvae, whereas Dorsal is specifically required for the immune response in larvae. Dorsal was first identified for its role in dorso-ventral patterning of the developing embryo (Santamaria and Nusslein-Volhard, 1983). The intracellular signaling components that lead to the activation of Dorsal are the same in both early embryo development and the immune response (Drier and Steward, 1997). In the absence of stimulation, DIF/Dorsal are sequestered in the cytoplasm by their interaction with the IκB protein Cactus via six-ankyrin repeats. Upon signaling, Cactus is degraded and DIF/Dorsal then translocates to the nucleus (Belvin *et al*., 1995; Bergmann *et al*., 1996; Gillespie and Wasserman, 1994; Reach *et al*., 1996; Wu and Anderson, 1998). The degradation of Cactus, like that of IκBs, is controlled by phosphorylation and K48-polyubiquitination with subsequent protesome-mediated degradation. Unlike mammalian IκBα which contains a single phosphorylation site responsible for its eventual degradation, Cactus contains two sites. Phosphorylation of the PEST domain, found at the C-terminus of Cactus, is also implicated in its signal-

independent degradation (Liu *et al*., 1997).

Unlike mammalian TLR signaling, neither of the two *Drosophila* IKK-related kinases (IKKε and IKKβ) are required for Toll-mediated Cactus phosphorylation and degradation. Although *Drosophila* IKKβ can phosphorylate Cactus *in vitro* (Kim *et al*., 2000), it is not required for drosomycin expression in cultured cells or flies (Lu *et al*., 2001; Rutschmann *et al*., 2000b; Silverman *et al*., 2000). The sequence motifs that are phosphorylated in Cactus show a high level of similarity to those critical for IκBα phosphorylation in human cells. It remains to be determined if Pelle or some other kinase is responsible for Cactus phosphorylation. Once phosphorylated Cactus is likely ubiquitinated via the Slimb-SCF E3-ligase complex, as *Drosophila* embryos mutant for *slimb* (βTrCP homolog), are unable to activate the Dorsal target genes *twist* and *snail* (Spencer *et al*., 1999).

Degradation of Cactus and nuclear translocation of DIF (and Dorsal) leads directly to the transcriptional induction of many immune-responsive genes (De Gregorio *et al*., 2002; De Gregorio *et al*., 2001; Irving *et al*., 2001). For example, the well-characterized AMP genes *Defensin, Drosomycin*, *Cecropin* and *Metchnikowin* are all activated as a consequence of Toll signaling, with DIF or Dorsal binding the κB-sites within the promoter/enhancer regions of these AMP genes (Senger *et al*., 2004). Toll signaling leads to the activation of other less-well characterized genes as well, some of which might be AMPs while others

may control different facets of the immune response such as the activation of the cellular immune response and the proliferation of hemocytes (Qiu *et al*., 1998; Zettervall *et al*., 2004). In addition, many components of the Toll pathway are regulated by Toll signaling (De Gregorio *et al*., 2002; Lemaitre *et al*., 1996). Most notable is the upregulation of Cactus in response to an immune challenge, which generates a negative feedback loop to down-modulate the cascade (Nicolas *et al*., 1998).

The Toll and IMD pathways are thought to be activated independently and initiate specific responses to different microorganisms. However, some AMPs are activated by both the Toll and IMD pathways. Tanji *et al*. (2007) have demonstrated that some antimicrobial peptide genes have distinct κB elements in their enhancer region (*e.g. Drosomycin*). These elements respond to either Relish or DIF, with optimal gene induction occurring only when both the Toll (DIF) and IMD (Relish) pathways are activated, suggesting synergistic regulation of AMPs by two pathways (Tanji *et al*., 2007)**.**

***Drosophila* IMD signaling**

The IMD pathway is activated by DAP-type PGN derived from Gram-negative and certain Gram-positive bacteria, such as *E. coli* and *Bacillus spp.* Initially, it was believed that the IMD pathway was activated by lipopolysaccharide (LPS) (Silverman *et al*., 2000; Werner *et al*., 2003). However, this did not account for the activation of the IMD pathway by certain Gram-positive bacteria

(Kaneko *et al*., 2004; Lemaitre *et al*., 1997; Leulier *et al*., 2003). It was subsequently demonstrated that the commercial LPS preparations often used to experimentally stimulate the IMD pathway are contaminated with PGN, and it is this PGN that activates the IMD pathway (Kaneko *et al*., 2004; Leulier *et al*., 2003; Werner *et al*., 2003).

Recognition of DAP-type PGN involves the receptors PGRP-LC and PGRP-LE (Choe *et al*., 2002; Gottar *et al*., 2002; Leulier *et al*., 2003; Ramet *et al*., 2002; Takehana *et al*., 2002). *PGRP-LC* encodes three alternatively spliced transcripts *PGRP-LCa*, *-LCx* and *–LCy*, which produce single pass transmembrane cell surface receptors. Each have a distinct extracellular PGRP domain anchored to identical transmembrane and cytoplasmic domains (Werner *et al*., 2003). PGRP-LE encodes a single protein which lacks both a signal sequence and a transmembrane domain. Although *PGRP-LC* null flies, which lack all three isoforms, induce dramatically reduced levels of antimicrobial peptide following infection with Gram-negative bacteria, such as *E. coli* and *Agrobacterium tumefaciens,* they are not particularly susceptible to infection with all Gram-negative bacteria. For example, *PGRP-LC* mutants are sensitive to *A. tumefaciens, Erwinia carotovora carotovora,* and *Enterobacter cloacae* but not *E. coli and B. megaterium.* (Choe *et al*., 2002; Gottar *et al*., 2002; Takehana *et al*., 2004). Mutants that abolish signaling through the IMD pathway, such as null alleles in IKK genes, are highly susceptible to all Gram-negative bacteria. It was therefore hypothesized that another receptor must also recognize and respond to

Gram-negative bacteria. Moreover, it suggests that relatively low levels of antimicrobial peptide gene induction, as observed in *PGRP-LC* mutants, are sufficient to protect against infection from many Gram-negative bacteria. Genetic experiments suggest that PGRP-LE is the alternate receptor for the IMD pathway. Double *PGRP-LC, PGRP-LE* mutants are hyper-susceptible to most Gram-negative bacteria, similar to other null mutants in the IMD pathway, and these double mutants do not induce detectable levels of antimicrobial peptide genes following infection (Takehana *et al*., 2004). Over expression of either PGRP-LC or PGRP-LE, in flies or in cell culture, is sufficient to drive AMP expression through the IMD pathway.

It has been shown that PGRP-LC and PGRP-LE serve to recognize different forms (monomeric and polymeric) of DAP-type PGN and to protect distinct niches. In cell culture and in flies, only the PGRP-LCx isform is required for recognizing polymeric PGN (isolated from *E. coli*). However, both PGRP-LCx and -LCa are required in cultured cells for the recognition of the monomeric fragment of DAP-type PGN known as TCT (Trachael Cyto-Toxin) (Kaneko *et al*., 2004; Stenbak *et al*., 2004). The role of PGRP-LCy in microbial recognition is still unknown.

The molecular mechanism by which PGN binding to either PGRP-LC or PGRP-LE leads to activation of the IMD pathway is still unclear. However, it is known that the cytoplasmic domain of PGRP-LC is responsible for initiating this signal transduction cascade (Choe *et al*., 2005). Epistatic experiments suggest

that the *imd* protein functions immediately downstream of PGRP-LC and upstream of all other known members of the pathway. IMD is a death domain protein similar to mammalian Receptor Interacting Protein 1 (RIP1) (Georgel *et al*., 2001) and immunoprecipitation experiments have shown that PGRP-LC and IMD interact (Aggarwal *et al*., 2008; Choe *et al*., 2005; Kaneko *et al*., 2006). Kaneko *et al*. (2006) identified a RIP Homotypic Interaction Motif (RHIM)-like domain that is crucial for signaling by PGRP-LC when over expressed or following infection. The RHIM domain, a motif of approximately 35 amino acids, was first identified in mammalian proteins RIP1, RIP3 and in the adaptor protein TRIF (Meylan *et al*., 2004; Sun *et al*., 2002b). The RHIM domain of TRIF interacts with RIP1 and RIP3, while RIP1 and RIP3 also interact with each other through their RHIM domains. The TRIF-RIP1 interaction is implicated in TLR3-induced NF-κB activation (Meylan *et al*., 2004). Likewise, the RHIM-like domain of PGRP-LC is critical for signaling, however it is not necessary for the interaction between PGRP-LC and IMD. Instead, PGRP-LC interacts with IMD via a region that is not required for signaling , and thus, the PGRP-LC/IMD interaction appears be superfluous for the activation of the pathway (Kaneko *et al*., 2006). Although the N-terminal signaling domains of PGRP-LC and PGRP-LE are not homologous, a RHIM-like motif was also identified in PGRP-LE. Mutation of the PGRP-LE RHIM-like motif blocks signaling induced by forced expression of this intracellular receptor. However it remains unclear exactly how the RHIM-like domains of PGRP-LC and -LE function to transduce IMD signaling, but it can be

speculated that the RHIM-like domain might interact with some unidentified component of the pathway.

Downstream of PGRP-LC and the *imd* protein, signal transduction through the IMD pathway leads to the *Drosophila* MAP3 kinase TAK1 and activation of the *Drosophila* IKK complex (Figure 1.2) (Silverman and Maniatis, 2001; Silverman *et al*., 2003; Vidal *et al*., 2001). RNAi-based experiments suggest that ubiquitination may play a key role in the activation of TAK1. Work by Zhou and colleagues has indicated that the E2 ubiquitin conjugating enzyme complex of UEV1A and Bendless (the *Drosophila* Ubc13 homolog) functions downstream of IMD yet upstream of TAK1 in the IMD pathway (Zhou *et al*., 2005). The mammalian homologs of this E2 complex, Uev1A and Ubc13, are responsible for the K63-polyubiquitination of many immune proteins, such as RIP1, TRAF2 and TRAF6. Unlike K48-polyubiquitination, which leads to proteasomal degradation, K63-polyubiquitin chains often have a regulatory function and are used to recruit and activate other signaling components. It is highly probable that K63-polyubiquitination plays an important role in the IMD signaling pathway between IMD and TAK1.

The *Drosophila* Inhibitor of Apoptosis Protein 2 (DIAP2) has also been identified as a member of the IMD signaling pathway (Gesellchen *et al*., 2005; Kleino *et al*., 2005; Leulier *et al*., 2006; Valanne *et al*., 2007). Similar to other E3 IAP proteins, DIAP2 contains 3 baculovirus IAP repeat (BIR) domains as well as a RING motif that is required for IMD signaling (Huh *et al*., 2007). Thus, although

DIAP2 has not yet been epistatically placed in the IMD signaling cascade, it is a good candidate for the missing IMD pathway E3 ligase, perhaps functioning along with the dUEV1A/Bendless E2 complex. Analysis of these proteins and their roles in IMD pathway ubiquitination can be found in Chapter 2. A deubiquitinating enzyme, USP36 has also been identified as playing a role in IMD pathway signaling. Functioning as a K63-polyubiquitin protease, USP36 acts to down regulate IMD pathway signaling, further implicating the importance of K63-polyubiquitination for IMD pathway activation (Thevenon *et al*., 2009).

The apical caspase DREDD has been shown to play a role in the pathway between IMD and TAK1, perhaps functioning as an E3-ligase accessory factor (Zhou *et al*., 2005). The mammalian homologue of DREDD, caspase-8, has been implicated NF-κB signaling pathways, many of which are thought to involve ubiquitination. Taken together, it becomes an attractive hypothesis that the E2/E3 complex of UEV1A, Bendless, DIAP2 and perhaps DREDD may mediate the K63-poly-ubiquitination of some member of the IMD pathway. This ubiquitinated protein is likely to be critical for signaling to TAK1, the next component in the pathway.

TAK1 is believed to function in a complex with the *Drosophila* TAB2 homolog (Zhuang *et al*., 2006). Similar to mammalian TAB2, which was originally identified as a TAK1 binding protein, *Drosophila* TAB2 contains a conserved C-terminal K63-polyubiquitin binding domain (Wang *et al*., 2001; Zhou *et al*., 2005), again suggesting that ubiquitination may play a crucial role in IMD signaling.

Signaling by the TAK1/TAB2 complex leads to the simultaneous induction of two downstream branches of the IMD pathway, which culminate in JNK and NF-κB/ Relish activation (Silverman *et al*., 2003).

The JNK arm of the IMD pathway is activated by TAK1-mediated signaling to Hemipterous, the *Drosophila* MKK7/JNKK homolog (Chen *et al*., 2002; Holland *et al*., 1997; Sluss *et al*., 1996). Hemipterous then phosphorylates the *basket* protein (JNK), which activates the *Drosophila* AP-1 transcription factor. Signaling through the IMD/JNK pathway has been linked to the up-regulation of wound repair and stress response genes (Boutros *et al*., 2002; Silverman *et al*., 2003), yet the precise role that JNK signaling plays in the IMD pathway remains controversial. Several reports have concluded that JNK signaling is not involved in AMP gene induction, instead it is suggested that AMP gene expression relies entirely on the NF-κB/Relish branch of the IMD pathway (Boutros *et al*., 2002; Silverman *et al*., 2003). In fact, an unidentified product of the Relish branch of the IMD pathway was proposed to inhibit JNK signaling (Park *et al*., 2004), while the JNK pathway was proposed to directly inhibit AMP gene expression by recruiting histone deacetylases (Kim *et al*., 2005). Alternatively, Delaney and colleagues (2006) concluded that the TAK1/JNK branch of the IMD pathway is critical for AMP gene induction, at least in clones of JNK-deficient cells within the larval fat body (Delaney and Mlodzik, 2006). The role of the JNK pathway in antimicrobial gene expression remains controversial and further work will be

necessary to clarify whether JNK has positive and/or negative role in this process.

In parallel to JNK activation, TAK1 is also required for induction of the NF-κB/Relish branch of the IMD pathway, through activation of the *Drosophila* IKK complex (Silverman *et al*., 2003; Vidal *et al*., 2001). The *Drosophila* IKK complex contains two subunits, a catalytic kinase subunit encoded by *ird5* (IKKβ) and a regulatory subunit encoded by *kenny* (IKKγ) (Rutschmann *et al*., 2000a; Silverman *et al*., 2000). In the *Drosophila* S2* cell line, it was demonstrated that the IKK complex is activated rapidly following immune stimulation and this activation requires TAK1 (Silverman *et al*., 2000; Silverman *et al*., 2003). Activated IKK complex can then directly phosphorylate Relish.

Relish is a bipartite protein similar to mammalian NF-κB precursors p100 and p105. It contains an N-terminal Rel homology domain (RHD) and an inhibitory IκB domain with six ankyrin repeats that retain the protein in the cytoplasm. Upon infection with Gram-negative bacteria, *Relish* expression is strongly induced in adult flies (Dushay *et al*., 1996). *Relish* mutant flies show extreme sensitivity to infections and fail to induce antimicrobial genes after bacterial infection (Hedengren *et al*., 1999). Although the *Relish* locus encodes an embryo specific isoform, *Relish* does not appear to have a role in development as homozygous Relish mutants continue to be viable and fertile.

In mammals, the NF-κB precursors p100 and p105 are processed by the proteasome and their C-terminal region is degraded to produce p50 and p52, respectively. This processing is regulated by phosphorylation of C-terminal serine residues, which leads to ubiquitination and partial proteasome degradation of the C-terminus (Perkins *et al*., 1997). In contrast, Relish processing does not depend on proteasomal degradation. Relish is instead endo-proteolytically cleaved by a caspase, producing an N-terminal RHD transcription factor module that translocates to the nucleus to activate immune genes, while the stable C-terminal domain remains in the cytoplasm (Stöven *et al*., 2000). Relish cleavage occurs after residue D545, within a typical caspase target motif, $_{542}$LQHD$_{545}$. DREDD, in addition to its previously mentioned role upstream in the pathway, also appears to function downstream and is a likely candidate for the caspase responsible for cleavage of Relish. DREDD and Relish physically interact under cell culture conditions and *Dredd* RNAi prevents antimicrobial peptide gene expression induced by an activated allele of TAK1 (Zhou *et al*., 2005). *Dredd* mutants also fail to cleave Relish, are unable to induce AMP gene expression and are highly sensitive to Gram-negative bacterial infections (Leulier *et al*., 2000; Stöven *et al*., 2003). Furthermore, over expression of DREDD is sufficient to cause Relish cleavage and purified DREDD cleaves Relish in vitro (Erturk-Hasdemir *et al*., 2009).

Phosphorylation of Relish occurs in a signal dependent manner by the *Drosophila* IKK complex and the C-terminus of Relish is required for both its

phosphorylation and cleavage (Stöven *et al*., 2003). Recently, studies have identified 2 serine residues, 528 and 529, in the N-terminal transcription factor module of Relish that are phosphorylated by *Drosophila* IKKβ yet are dispensable for the Relish cleavage. Instead, phosphorylation appears critical for the proper transcriptional activation of Relish targets via efficient recruitment of RNA polymerase II to the promoters of antimicrobial peptide genes. Apart from its role in phosphorylation, the IKK complex also functions noncatalytically in the cleavage of Relish (Erturk-Hasdemir *et al*., 2009). In total, Relish activity is coordinately regulated by 2 distinct mechanisms; cleavage by DREDD and phosphorylation by the IKK complex.

While Relish is activated by caspase-dependent cleavage, the ubiquitin-proteasome pathway may target Relish for destruction. It was established that inhibiting the SCF E3-ubiquitin-ligase complex caused the constitutive expression of antimicrobial peptide genes and increased levels of Relish (Khush *et al*., 2002). Thus, the ubiquitin proteosome pathway may be important for down-regulating the IMD pathway.

Mammalian NF-κB signaling

Mammals rely largely on an adaptive immune response, including B-cells, T-cells, and antibodies to provide long lasting protective immunity from pathogens. However, the first line of defense against a pathogenic invasion is largely delegated to the innate immune response. Unlike the adaptive immune

response, which tends to be slow acting, yet entail a very specific defense against a particular pathogen, the innate immune response is much faster yet less specific, activating defenses against a wide variety of pathogens.

Mammals have developed an intricate series of receptors and cell signaling events which respond to a range of microbial products, known as pathogen associated molecular patterns (PAMPs). When these receptors bind their PAMP ligand a signaling cascade is triggered causing the production of both pro- and anti-inflammatory cytokines and chemokines which modulate the immune response. This leads to the recruitment and activation of cells involved in both innate and adaptive immune response, the activation of complement to promote the removal of foreign organisms, and serves to prime the adaptive immune response.

The NF-κB signaling pathway is perhaps the most well defined mammalian innate immune signaling pathway (Figure 1.3). Signaling through the canonical NF-κB pathway can occur via a number of cellular receptors including tumor necrosis factor receptors (TNFR), the interleukin-1 receptor (IL-1R), or the toll like receptors (TLRs). Currently eleven human and thirteen mouse TLRs have been identified each of which contain leucine rich repeat (LRR) motifs in their extracellular domains which are used bind a variety of PAMPs. Alternatively, TNFR and IL-1R do not bind PAMPs but instead bind the cytokines TNF and IL-1, respectively, which are produced during an infection. Although the extracellular domains of TLRs and IL-1R show striking differences, a cytoplasmic domain

Figure 1.3

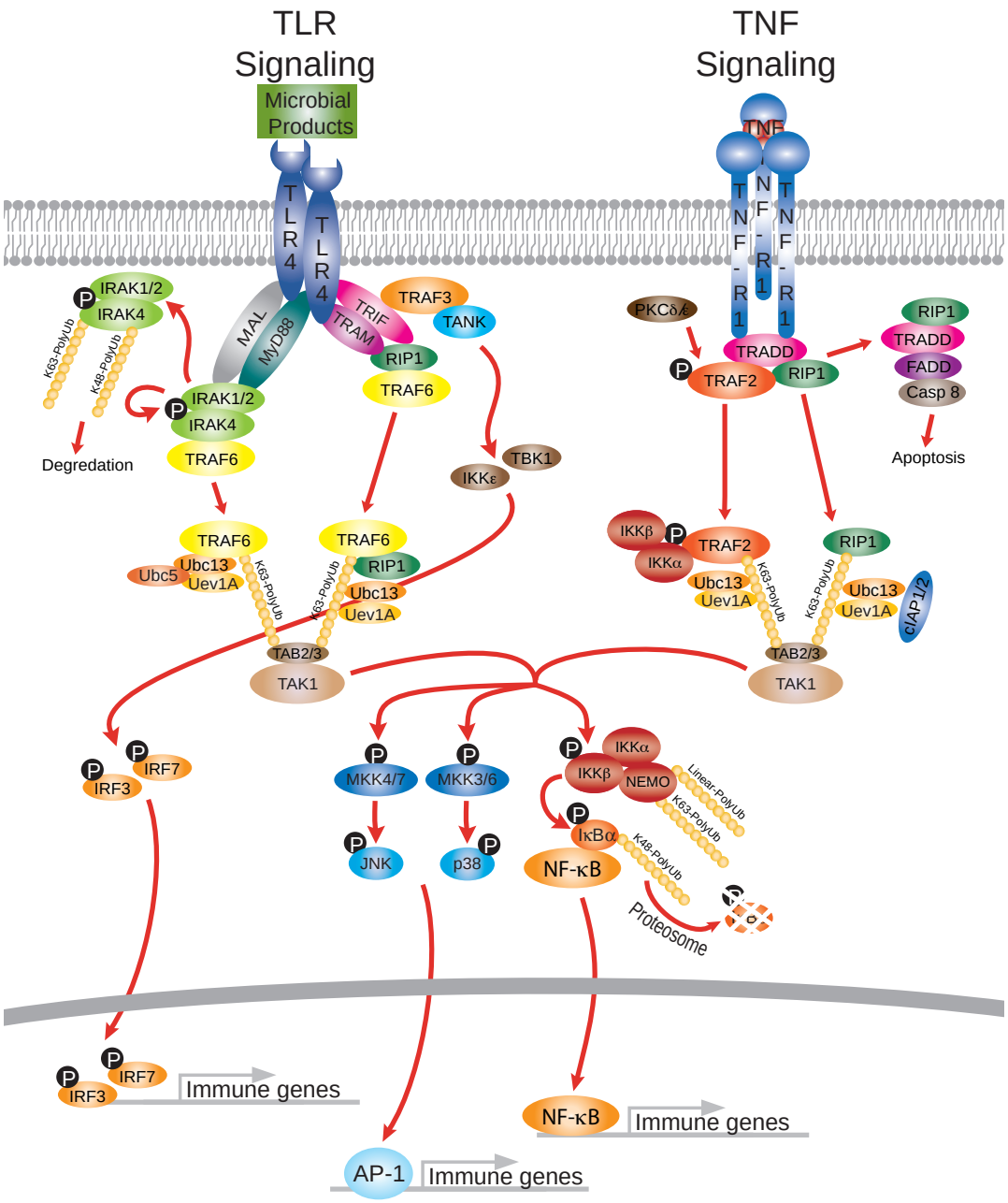
TLR
Signaling
Microbial
Products
TLR4
TLR4
MAL
MyD88
TRIF
TRAM
TRAF3
TANK
RIP1
TRAF6
IRAK1/2
IRAK4
TRAF6
K63-PolyUb
K48-PolyUb
Degredation
TBK1
IKKε
TRAF6
Ubc5
Ubc13
Uev1A
K63-PolyUb
TRAF6
RIP1
Ubc13
Uev1A
K63-PolyUb
TAB2/3
TAK1
IRF3
IRF7
MKK4/7
MKK3/6
JNK
p38
IKKα
IKKβ
NEMO
Linear-PolyUb
K63-PolyUb
IκBα
K48-PolyUb
NF-κB
Proteosome
IRF3
IRF7
Immune genes
AP-1
Immune genes
TNF
Signaling
TNF
TNF-R1
TNF-R1
PKCδ/ε
TRADD
TRAF2
RIP1
RIP1
TRADD
FADD
Casp 8
Apoptosis
IKKβ
IKKα
TRAF2
Ubc13
Uev1A
K63-PolyUb
RIP1
K63-PolyUb
Ubc13
Uev1A
cIAP1/2
TAB2/3
TAK1
NF-κB
Immune genes

Figure 1.3 Mammalian NF-κB signaling

(Left) Upon recognition of microbial products TLR4 dimerizes and leads to the recruitment of the adaptor proteins MyD88 and Mal. MyD88 interacts with IRAK via homeotypic death domain interactions and binds TRAF6. Activated IRAK auto-phosphorylates and TRAF6 is then released into the cytoplasm. Phosphorylated IRAK stays near the membrane and is polyubiquitinated and degraded. In the cytoplasm, TRAF6 interacts with the E2 enzymes Uev1a, Ubc13, and Ubc5 promoting its own K63-polyubiquitination. In a second MyD88 independent pathway TLR4 activation leads to the recruitment of the adapters TRIF and TRAM. These adaptors then interact with the proteins RIP1 and TRAF6. Via interactions with Uev1A and Ubc13, RIP1 and TRAF6 are K63-polyubiquitinated. (Right) Binding of the cytokine TNF to its receptor TNF-R1 leads to recruitment of the adaptor protein TRADD which in turn interacts with TRAF2 and RIP1. Activation of TNF-R1 leads to the PKCδ/ε dependent phosphorylation of TRAF2. Phosphorylated TRAF2 is K63-polyubiquitinated in a Uev1A/Ubc13 dependent manner. RIP1 is also K63-polyubiquitinated in an event which requires Uev1A/Ubc13 and cIAP1/2. (Bottom) In all cases K63-polyubiquitination of upstream pathway members leads to the recruitment of TAK1 via ubiquitin binding domains found in TAB2/3. Activated TAK1 then phosphorylates and activates the IKK complex resulting in the phosphorylation and K48-polyubiquitin mediated degradation of IκBα, releasing NF-κB into the nucleus. TAK1 also phosphorylates MKK3, -4, -6 and -7 activating JNK/p38 mediated AP1 signaling.

found in both receptors, which is critical for downstream signaling, shows a high degree of similarity and has been named the Toll/IL-1 receptor (TIR) domain (O'Neill and Bowie, 2007; Dunne and O'Neill, 2003). Although these receptors may bind different ligands they are able to activate similar downstream signaling pathways.

Upon binding ligand, TLRs (in particular TLR4) oligomerize causing a conformational change which results in the recruitment of the downstream adaptor myeloid differentiation primary response protein 88 (MyD88) and MyD88 adaptor-like protein (Mal, also known as TIRAP) (Akira *et al*., 2006; O'Neill and Bowie, 2007; Kawai *et al*., 1999; Fitzgerald *et al*., 2001; Horng *et al*., 2002; Kim *et al*., 2007; Park *et al*., 2009). MyD88 recruits IL-1 receptor-associated kinase (IRAK) and tumor necrosis factor receptor associated factor 6 (TRAF6) via interactions in the death domains of MyD88 and IRAK (Burns *et al*., 1998; Wesche *et al*., 1997; Cao *et al*., 1996). Four members of the IRAK family have been identified (IRAK-1, IRAK-2, IRAK-M, IRAK-4), two of which, IRAK-1 and IRAK-4, show serine/threonine kinase activity (Suzuki *et al*., 2002; Kawagoe *et al*., 2008; Keating *et al*., 2007; Qin *et al*., 2004; Cheng *et al*., 2007). MyD88 recruited IRAK4 and IRAK1/2 are phosphorylated and along with TRAF6 disassociate from the receptor complex (Cheng *et al*., 2007; Kollewe *et al*., 2004; Li *et al*., 1999). IRAK remains on the membrane becoming polyubiquitinated and degraded, whereas TRAF6 migrates into the cytoplasm (Li *et al*., 1999; Yamin and Miller, 1997). Varying reports have indicated the formation of both K48- and

K63-polyubiquitin chains on IRAK however multiple groups have concluded that IRAK degradation does not appear proteasome-dependent (Ordureau *et al*., 2008; Windheim *et al*., 2008; Yamin and Miller, 1997).

Once disassociated from the receptor, TRAF6 interacts with the ubiquitin E2 complex of Uev1A and Ubc13. Using its own ring finger to act as an E3 ligase, TRAF6 promotes its own K63-polyubiquitination (Lamothe *et al*., 2007; Deng *et al*., 2000; Wang *et al*., 2001; Wooff *et al*., 2004). Although the E2 Uev1A/Ubc13 complex has been shown to be sufficient for TRAF6 polyubiquitination, a third E2, UbcH7, is also thought to be involved (Geetha *et al*., 2005). In addition, the E2 enzyme UbcH5, which is known to generate various types of polyubiquitin chains, is also thought to play a role in TRAF6 polyubiquitination and subsequent downstream activation (Xia *et al*., 2009; Chen *et al*., 1996).

Polyubiquitinated TRAF6 acts as a scaffold, recruiting downstream kinases. The MAP3 kinase TAK1 is recruited by ubiquitin-binding motifs in its binding partners TAB2 and TAB3 (Kanayama *et al*., 2004). Serving as adaptors between TRAF6 and TAK1, the TAB2 and TAB3 proteins contain two ubiquitin-binding motifs, an N-terminal CUE domain and a C-terminal nuclear protein localization four zinc finger (NZF) (Ishitani *et al*., 2003; Takaesu *et al*., 2000; Kanayama *et al*., 2004; Cheung *et al*., 2004). Although the NZF appears to play a significant role in binding TAB2/3 to ubiquitinated TRAF6, the CUE domain

appears to be dispensable for NF-κB signaling (Kanayama *et al*., 2004; Kishida *et al*., 2005).

Binding of the TAB2/3-TAK1 complex to ubiquitinated TRAF6 leads to activation loop auto-phosphorylation of TAK1, and initiation of downstream signaling pathways (Takaesu *et al*., 2000; Jiang *et al*., 2002; Wang *et al*., 2001; Sakurai *et al*., 2000; Kishimoto *et al*., 2000; Xia *et al*., 2009). TAK1 phosphorylates the multi-protein IKK complex composed of three proteins; two kinases, IKKα and IKKβ, and a scaffold protein IKKγ (NEMO) (Hacker and Karin, 2006; Mercurio *et al*., 1997; Rothwarf *et al*., 1998; Zandi *et al*., 1997). One main site of IKK phosphorylation occurs in the activation loop of IKKβ which allows the protein to become active and further phosphorylate downstream proteins (Wang *et al*., 2001).

It is widely thought that the ubiquitin-binding motif found on NEMO is responsible for bringing the IKK complex into proximity with TAK1 by binding K63-polyubiquitinated TRAF6 (Wu *et al*., 2006; Windheim *et al*., 2008; Xia *et al*., 2009; Laplantine *et al*., 2009). A number of reports, however, have indicated that NEMO may instead bind linear-polyubiquitin chains (Rahighi *et al*., 2009). Surprisingly NEMO has been the only protein within the NF-κB pathway shown to be modified by linear polyubiquitin. Linear polyubiquitination of NEMO occurs in concert with the E3 proteins HOIL-1L and HOIP in a Ubc13 dependent manner, and in the absence of linear polyubiqiutination of NEMO, NF-κB responses are severely depleted (Tokunaga *et al*., 2009). It is currently unclear what

physiological role, if any, linear polyubiquitin plays in NF-κB signaling, or why there is such a discrepancy between the reported ubiquitin binding preference of NEMO. One possible explanation could be the use of NEMO protein fragments used in *in-vitro* linear ubiquitin binding assays which may show an altered binding specificity when compared to the full length protein.

Evidence has been presented indicating that the mere presence or absence of polyubiquitin chains may be more important than the substrates to which they are conjugated. Work by Xia *et al*. (2009), shows that unanchored polyubuiqitin chains are able to recruit and activate both TAK1 and IKK kinases. While unanchored K63-polyubiquitin chains generated by the E2 complex of Uev1A and Ubc13 alone were able to activate TAK1 (and to a lesser degree IKK), the E2 enzyme UbcH5 was required to generate polyubiquitin chains which activated the IKK complex robustly in a NEMO-dependent manner. The chains generated by UbcH5 however appeared to be neither K48 or K63-polyubiquitin chains, indicating that they could be either linear, or some alternative polyubiquitin linkage (Xia *et al*., 2009).

It has also been shown that NEMO can become K63-polyubiquitinated in a TRAF6 dependent fashion, a step that appears to be crucial for maximal IKK kinase activity (Sun *et al*., 2004). Once activated by phosphorylation and perhaps ubiquitination, the IKK complex phosphorylates the NF-κB inhibitory protein IκB, signaling the protein to become K48-polyubiquitinated and degraded by the proteosome (Chen, 2005; Hacker and Karin, 2006). NF-κB can then freely

translocate into the nucleus where it binds any number of κB sites activating various inflammatory cytokines and cell survival genes (Hoffmann and Baltimore, 2006).

Aside from NF-κB signaling, activated TAK1 also phosphorylates various MAP2 kinase proteins, such as MKK3, -4, -6, and -7 (Chang and Karin, 2001). Phosphorylation of these proteins leads to the activation of both c-Jun N-terminal kinase (JNK) and p38. This results in the activation and nuclear translocation of activator protein 1 (AP1), which promotes the induction of various pro-inflammatory cytokines (Chang and Karin, 2001; Shim *et al*., 2005).

MyD88-independent signaling pathways are also present downstream of TLR4 (and TLR3). In one of these pathways the adaptors TRIF and TRAM associate with the proteins TRAF3 and TANK to induce signaling to the IKK-like proteins TBK1 and IKKε (Yamamoto *et al*., 2003; Hacker *et al*., 2006; Oganesyan *et al*., 2006; Sato *et al*., 2003). These kinases phosphorylate the transcription factors interferon regulatory factor 3 and 7 (IRF3 and IRF7), causing them to dimerize and translocate into the nucleus where they activate the production of type I interferons (Sharma *et al*., 2003; Fitzgerald *et al*., 2003). MyD88-independent signaling can also lead to the activation of the NF-κB pathway. In this case TRIF/TRAM bind the receptor interacting protein 1 (RIP1) and in association with the E3 ligase TRAF6 promote the K63-polyubiquitination of RIP1, leading to the recruitment and activation of TAB2/3 and TAK1 and activation of NF-κB (Meylan *et al*., 2004; Sato *et al*., 2003).

Aside from acting in MyD88-independent TLR signaling, the adaptor RIP1 also plays a significant role in the activation of NF-κB by tumor necrosis factor (TNF), utilizing a signaling pathway that has many overlapping components. TNF, binding as a trimer, forces the trimerization of the death domain containing TNF receptor (TNF-R1), which then interacts with the death domains of the adaptor protein TRADD leading to the recruitment of TRAF2 and RIP1 (Hsu *et al*., 1996a; Hsu *et al*., 1996b; Idriss and Naismith, 2000). Activation of TNF-R1 also leads to protein kinase C (PKC)δ/ε-dependent phosphorylation of TRAF2 (Li *et al*., 2009). PKCs have traditionally been thought to be involved in T-cell and B-cell mediated NF-κB signaling. It is therefore unclear precisely how activation of TNF-R1 recruits/activates PKCδ/ε. Phosphorylated TRAF2 then interacts with IKKα and IKKβ through an undetermined mechanism. Furthermore, phosphorylation of TRAF2 is required for its K63-polyubiquitination, and subsequent recruitment of TAB2/3 and TAK1 (Li *et al*., 2009). In parallel, RIP1 is also K63 polyubiquitinated, leading to recruitment of TAB2/3-TAK1 and NEMO/IKK (Lee *et al*., 2004; Kanayama *et al*., 2004; Ea *et al*., 2006; Wu *et al*., 2006). TAK1 then goes on to activate signaling as previously discussed.

After TNF signaling has been activated TRADD, RIP1 and TRAF2 disassociate from TNF-R1. TRADD then utilizes its death domains to bind the adaptor protein FADD, recruiting caspase-8 and allowing the induction of apoptosis (Hsu *et al*., 1996a). Although caspase-8 has traditionally been implicated as an activator of apoptosis, a growing body of literature indicates that

it also plays a role in NF-κB signaling in B-cells, T-cells and lipopolysaccharide (LPS) signaling. Cells from mice or humans which lack caspase-8 show defects in immune activation, cytokine production and nuclear translocation of NF-κB (Chun *et al*., 2002; Sun *et al*., 2008; Su *et al*., 2005; Bidere *et al*., 2006; Lemmers *et al*., 2007). However, the precise function of caspase-8 in NF-κB signaling remains unclear.

Polyubiquitination of RIP1 after TNF-R1 activation was largely thought to be the result of the E2 complex of Uev1A and Ubc13 utilizing TRAF2 as an E3 ligase. Recent data however shows that TRAF2 may only play a minor role as the E3 ligase for RIP1. Instead the proteins cIAP1 and cIAP2 seem to play more significant roles in TNF induced RIP1 K63-polyubiquitination (Bertrand *et al*., 2008). Inhibitor of apoptosis (IAP) proteins have been largely thought to act in the inhibition of apoptosis by blocking the activity of caspases. However, a number of IAP proteins have recently been implicated in signaling outside of cell death. While all IAP proteins are characterized by the presence of baculovirus IAP repeat (BIR) domains, a number of them (including cIAP1/2) have also been shown to carry putative E3 ubiquitin ligase RING finger motifs strongly implicating them in ubiquitination. cIAP1/2, for example, have also been associated with the K63-polyubiquitination of the RIP family member RIP2, following NOD signaling (Bertrand *et al*., 2009). Although they rely on many of the same downstream signaling components, unlike TLR and TNF receptors which are membrane bound, nucleotide-binding and oligomerization (NOD)-like receptors (NLRs) act

as cytosolic intracellular receptors. Upon activation of NLRs, RIP2 is K63-polyubiquitinated by the E3 proteins cIAP1/2. However, the precise mechanism by which RIP1/2 and cIAP2/3 interact remains to be resolved.

Thesis objective

Currently a number of unanswered questions remain regarding the activation and regulation of innate immune signaling in both mammals and *Drosophila.* Many homologous proteins have been shown to play roles in both mammalian and insect innate immunity, however, the significance, interaction and physiological relevance of these proteins have not been completely elucidated. The work described in the following chapters was designed to utilize *Drosophila* as a model system for better understanding innate immunity of both vertebrates and invertebrates. By studying *Drosophila* innate immune signaling I aim to elucidate novel mechanisms by which many of these proteins interact and are regulated. It is my hope that this work can contribute to the ever growing body of knowledge regarding innate immunity and ultimately be used to develop effective and efficient treatments for pathogenic diseases.

PREFACE TO CHAPTER II

This chapter has been submitted for publication:

Nicholas Paquette, Meike Broemer, Kamna Aggarwal, Li Chen, Marie Husson, Deniz Ertürk-Hasdemir, Jean-Marc Reichhart, Pascal Meier, Neal Silverman. *Caspase Mediated Cleavage, IAP Binding and Ubiquitination: Linking Three Mechanisms Crucial for Drosophila NF-κB Signaling***.** (2009)

Meike Broemer performed IMD/DIAP2 BIR interaction analysis

Kamna Aggarwal performed Northern blots on IMD mutants

Li Chen performed IMD/Ub Western blots and Northern blots on E2 RNAi samples

Marie Husson performed transgenic IMD experiments

Nicholas Paquette performed the remaining experiments

Nicholas Paquette and Neal Silverman designed the experiments and wrote the manuscript

CHAPTER II

Caspase Mediated Cleavage, IAP Binding and Ubiquitination: Linking Three Mechanisms Crucial for *Drosophila* NF-κB Signaling.

Abstract

Innate immune responses are critical for the immediate protection against microbial infection. In *Drosophila*, infection leads to the rapid and robust production of antimicrobial peptides, through two NF-κB signaling pathways - IMD and Toll. The IMD pathway is triggered by DAP-type peptidoglycan, common to most Gram-negative bacteria. Signaling downstream from the peptidoglycan receptors is thought to involve K63-ubiquitination and caspase-mediated cleavage, but the molecular mechanisms remain obscure. We now show that PGN-stimulation causes caspase-mediated cleavage of the *imd* protein, exposing a highly conserved IAP-binding motif (IBM) at its neo-N-terminus. A functional IBM is required for the association of cleaved-IMD with the ubiquitin E3 ligase DIAP2. Through its association with DIAP2, IMD is rapidly conjugated with K63-linked polyubiquitin chains. These results mechanistically connect caspase-mediated cleavage and K63-ubiquitination in immune-induced NF-κB signaling.

Introduction

Activation of the *Drosophila* IMD pathway by DAP-type peptidoglycan (PGN) leads to the robust and rapid production of a battery of antimicrobial peptides (AMPs) and other immune responsive genes (Ferrandon *et al*., 2007; Lemaitre and Hoffmann, 2007). Two members of the peptidoglycan recognition protein (PGRP) family of receptors are responsible for the recognition of DAP-type PGN, the cell surface receptor PGRP-LC and the cytosolic receptor PGRP-LE (Kaneko *et al*., 2006). DAP-type PGN binding causes these receptors to multimerize or cluster (Chang *et al*., 2006; Lim *et al*., 2006), and trigger signal transduction. IMD signaling culminates in activation of the NF-κB precursor Relish and transcriptional induction of AMP genes.

Currently, the molecular mechanisms linking these PGN-binding receptors and activation of Relish remain unclear. Genetic experiments suggest that the most receptor proximal component of the pathway is the *imd* protein (Georgel *et al*., 2001), while the MAP3 kinase TAK1 appears to function further downstream (Silverman *et al*., 2003; Vidal *et al*., 2001). In addition to NF-κB signaling, TAK1 also mediates immune-induced JNK signaling (Silverman *et al*., 2003). The role, if any, that JNK signaling plays in AMP gene expression is controversial (Delaney *et al*., 2006; Kim *et al*., 2005). More central to AMP gene induction, TAK1 is required for activation of the *Drosophila* IKK complex, which in turn is essential for the immune-induced cleavage and activation of the NF-κB precursor Relish,

the key transcription factor required for immune-responsive AMP gene expression (Silverman *et al*., 2000).

Other major components in the IMD pathway include the caspase-8 like DREDD and its adapter FADD. Cell-based RNAi studies suggest that these proteins have two distinct roles in IMD pathway signaling, one relatively early in the cascade and the second further downstream. Using RNAi, DREDD and FADD were shown to be required for immune-induced activation of the IKK complex (Zhou *et al*., 2005). These data further suggested that DREDD and FADD function downstream of IMD but upstream of TAK1, however their precise function remained unclear. In its second role, DREDD is thought to play a key role in the endoproteolytic cleavage of Relish, the ultimate cytoplasmic event in IMD signaling (Stöven *et al*., 2003; Erturk-Hasdemir *et al*., 2009).

In addition to the components outlined above, several studies have suggested that ubiquitination plays a critical, positive role in the IMD signaling cascade. Recently, *Drosophila* Inhibitor of Apoptosis 2 (DIAP2) was shown to be a crucial component of the IMD pathway (Gesellchen *et al*., 2005; Huh *et al*., 2007; Kleino *et al*., 2005; Leulier *et al*., 2006). Typical of IAP proteins, DIAP2 has three N-terminal BIR domains, which are involved in interactions with other proteins carrying conserved IAP binding motifs (IBMs) (Wu *et al*., 2000). In addition, some IAPs, including DIAP2, carry a C-terminal RING finger domain that provides these proteins with ubiquitin E3 ligase activity (Vaux and Silke, 2005). Although it is not precisely clear where in the pathway DIAP2 functions,

one study showed that the RING finger is indispensable for its role in the immune response, suggesting it operates as an E3 ubiquitin ligase in IMD signaling (Huh *et al*., 2007). Also, Zhou *et al*. (2005) showed, using RNAi-based approaches, that the E2 ubiquitin conjugating enzymes Uev1a and Ubc13 (*bendless*) are critical components of the IMD pathway. Notably, Ubc13 and Uev1a function together in a complex to generate K63-linked polyubiquitin chains. K63-polyubiquitin chains are not linked to proteasomal degradation but, instead, are thought to play regulatory roles (Chiu *et al*., 2009; Mukhopadhyay and Riezman, 2007; Xia *et al*., 2009). Although no connection between DIAP2 and the Ubc13/ Uev1a E2 complex has been established, one attractive scenario is that DIAP2 functions as an E3 together with the Ubc13-Uev1a E2 complex.

Previous work has suggested that Ubc13, Uev1a, DREDD and FADD all function downstream of IMD but upstream of TAK1. In fact, it was predicted that DREDD may play a role as an accessory protein for K63-ubiquitination in IMD signaling (Zhou *et al*., 2005). However, it was not established if the upstream role for DREDD involves its protease activity. Moreover, no K63-ubiquitinated target protein(s) have been identified in the IMD pathway. Thus, the molecular mechanisms that link the caspase DREDD and K63-ubiquitination to the activation of the IMD pathway are undefined.

The *imd*^{1} allele is a strong hypomorphic mutation that impairs innate immune responses. Surprisingly, this allele encodes a conservative amino acid substitution, alanine (A) to valine (V) at position 31, which lies outside the death

domain of IMD and is positioned in a region with no obvious structural motifs (Georgel *et al*., 2001). Thus, the reason for the strong hypomorphic phenotype associated with the A31V substitution remains unclear. In this work, we demonstrate that *imd* protein is rapidly cleaved following PGN-stimulation. Cleavage requires the caspase DREDD and occurs at caspase recognition motif, $_{27}$LEKD/A$_{31}$, creating a neo-N-terminus at A31 that is critical for the immune-induced association of IMD with DIAP2. Substitution of the neo-N-terminus with valine, as in *imd*^{1}, disrupts the IMD-DIAP2 interaction. Moreover, once associated with DIAP2, cleaved-IMD is rapidly K63-polyubiquitinated. Together, these data resolve a number of outstanding questions in IMD signal transduction and present a novel molecular mechanism linking caspase-mediated-cleavage to NF-κB activation.

Results

Signal-induced modification of IMD

Previous evidence suggested that the apical caspase DREDD plays a crucial role in the IMD pathway upstream of TAK1 activation (Zhou *et al*., 2005). To determine if proteolytic activity is required upstream in the IMD pathway, the caspase inhibitor zVAD-FMK was utilized. Immune responsive *Drosophila* S2* cells were treated with zVAD-FMK (or vehicle control) prior to stimulation with *E. coli* peptidoglycan (PGN). Treatment with caspase inhibitor suppressed the

activation of TAK1 kinase, as monitored by *in-vitro* IP-kinase assay. zVAD-fmk also prevented accumulation of phospho-JNK (Figure 2.1A)

Hypothesizing that IMD signaling results in the DREDD-mediated cleavage of an upstream signaling component, we next examined the fate of endogenous *imd* protein. Peptidoglycan stimulation of S2* cells resulted in the rapid, signal dependent modification of IMD (Figure 2.1B). The faster migrating IMD product did not accumulate in the presence of caspase inhibitor (Figure 2.1C), suggesting that it represents an IMD cleavage product. Cleavage of IMD appeared very rapidly, within one minute, and peaked between 10 and 30 minutes. Treatment of S2* cells with RNAi targeting either DREDD and FADD, prior to stimulation with peptidoglycan, resulted in a noticeable decrease in IMD cleavage, and accumulation of full length IMD (Figure 2.1D). Furthermore, over expression of wild type DREDD (WT), but not a catalytically inactive mutant (CA) or the the caspase DRONC, from the copper inducible metallothionein promoter resulted in the cleavage of IMD, independent of any immune stimulus (Figure 2.1E). Together these results suggest that the proteolytic activity of DREDD is required for the cleavage of IMD.

A slower migrating form of IMD was also detectable following immune stimulation. λ phosphatase treatment resolved this higher molecular weight species, indicating that it is a phosphorylated isoform of IMD (Figure 2.2). Interestingly, RNAi-mediated knockdown of TAK1, DIAP2 or Uev1a and Ubc13 resulted in reduced levels of phospho-IMD (Figure 2.1D), suggesting that TAK1

Figure 2.1

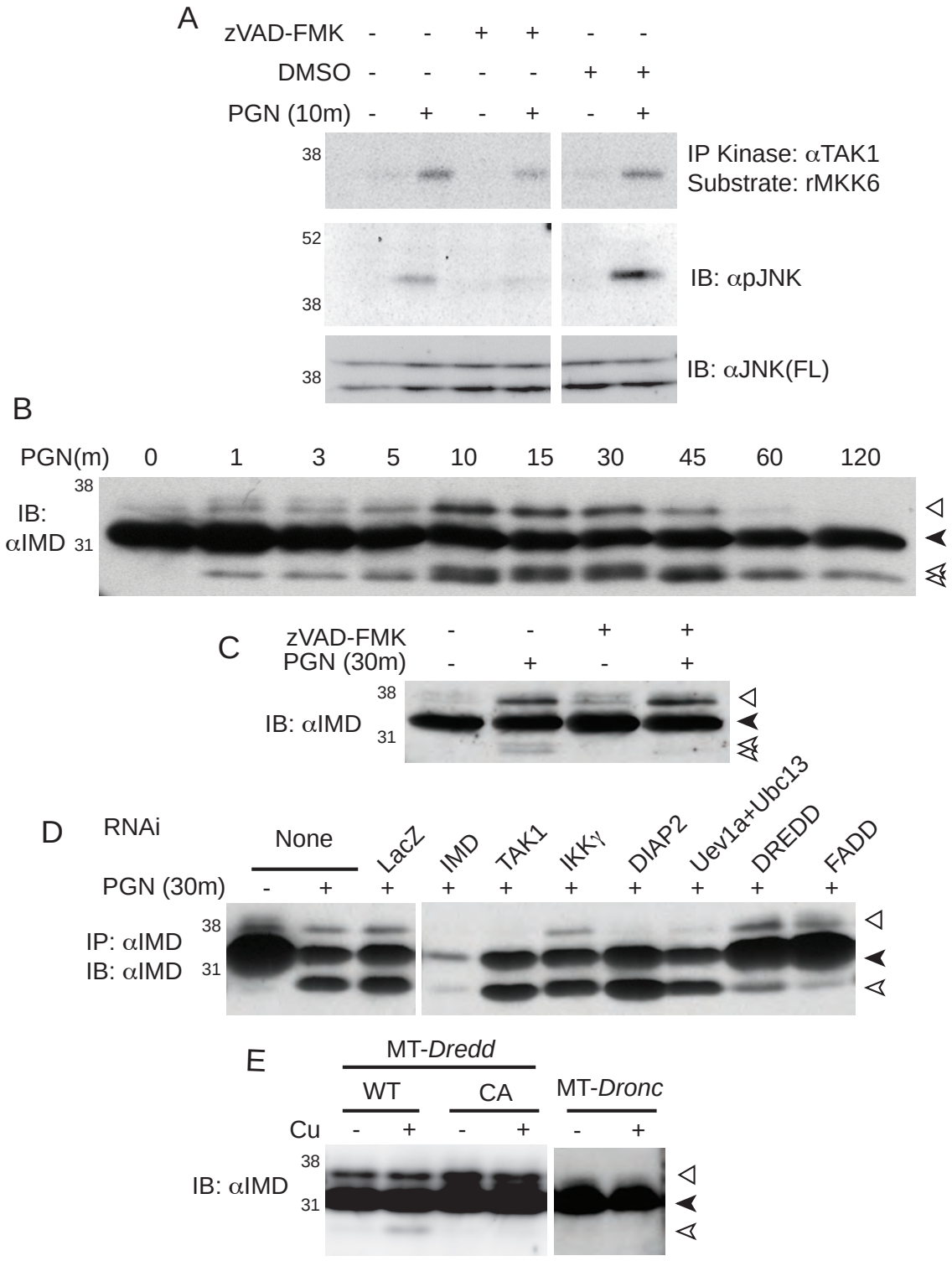
A
zVAD-FMK - - + + - -
DMSO - - - - + +
PGN (10m) - + - + - +
38
IP Kinase: αTAK1
Substrate: rMKK6
52
38
IB: αpJNK
38
IB: αJNK(FL)
B
PGN(m) 0 1 3 5 10 15 30 45 60 120
38
IB:
αIMD 31
C
zVAD-FMK - - + +
PGN (30m) - + - +
38
IB: αIMD
31
D
RNAi
None
LacZ
IMD
TAK1
IKKγ
DIAP2
Uev1a+Ubc13
DREDD
FADD
PGN (30m) - + + + + + + + + +
IP: αIMD
IB: αIMD
38
31
E
MT-Dredd
WT
CA
MT-Dronc
Cu - + - + - +
IB: αIMD
38
31

Figure 2.1 Dredd-dependent cleavage of IMD

(A) S2* cells were treated with zVAD-FMK or vehicle control (DMSO) prior to stimulation with peptidoglycan for 30 minutes. TAK1 kinase activity, assayed by TAK1 IP-kinase assay, was reduced in the presence of zVAD-FMK, compared to controls. Similarly, a reduction of phospho-JNK was also observed, by immunoblotting.

(B) S2* cells were stimulated with peptidoglycan from 0 to 120 minutes, as indicated, and endogenous-IMD was monitored in whole cell lysates by immunoblotting.

(C) Endogenous IMD was monitored in S2* cell lysates after pretreatment with zVAD-FMK followed by PGN stimulation.

(D) Endogenous IMD was monitored by IP-immunoblotting in lysates from S2* cells after treatment with RNAi against various IMD pathway components, as indicated.

(E) Endogenous IMD was monitored in S2* cell lysates after expression of DREDD-WT, DREDD-CA or DRONC. Caspases were expressed from the metallothionein promoter by addition of copper sulfate for 6 hours. DREDD-CA is a catalytically inactive mutant. All 3 caspases were robustly expressed (data not shown).

In all cases, ◀ marks unmodified full length IMD, ◁ highlights phosphorylated IMD, and ◁ marks the cleaved-IMD products.

Figure 2.2

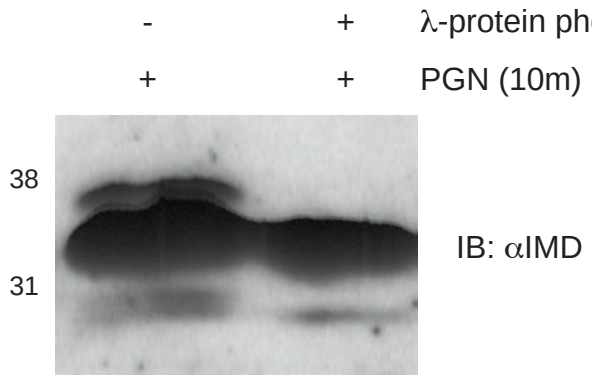

Figure 2.2 IMD is phosphorylated

Whole cell lysates from PGN-stimulated S2* cell lysates were treated with λ-protein phosphatase and immunoblotted with IMD antisera.

may be responsible for phosphorylating IMD in some sort of regulatory loop. This phosphorylation event may regulate signaling, but will require further study.

DIAP2 functions between IMD and TAK1

To examine how IMD cleavage might be linked to downstream signaling events such as K63-ubiquitination, we sought to more carefully characterize the role of DIAP2, a putative ubiquitin E3-ligase, in this pathway. As previously shown, DIAP2 RNAi markedly inhibited the induction of the antimicrobial peptide gene *Diptericin* following immune stimulation with DAP-type peptidoglycan, similar to RNAi targeting PGRP-LC or IKKγ, as analyzed by Northern blotting, (Figure 2.3A) (Gesellchen *et al*., 2005; Huh *et al*., 2007; Kleino *et al*., 2005; Leulier *et al*., 2006). Using a stable S2* cell line that expresses *imd* from the metallothionein promoter, AMP gene expression can be induced by the addition of copper (Zhou *et al*., 2005). DIAP2 RNAi also inhibited *Diptericin* induction in this assay (Figure 2.3B), similar to RNAi targeting Uev1a and Ubc13 or TAK1, as shown previously (Zhou *et al*., 2005). In contrast, RNAi mediated knockdown of PGRP-LC did not inhibit IMD-induced signaling. These results suggest that DIAP2, TAK1, Ubc13 and Uev1a, but not PGRP-LC, function downstream of IMD.

In addition, the activation of the two downstream kinases, TAK1 and IKK, was directly assayed by immunoprecipitation-kinase assays. PGN-induced activation of both kinases required DIAP2 (Figure 2.3C). Together these data

Figure 2.3

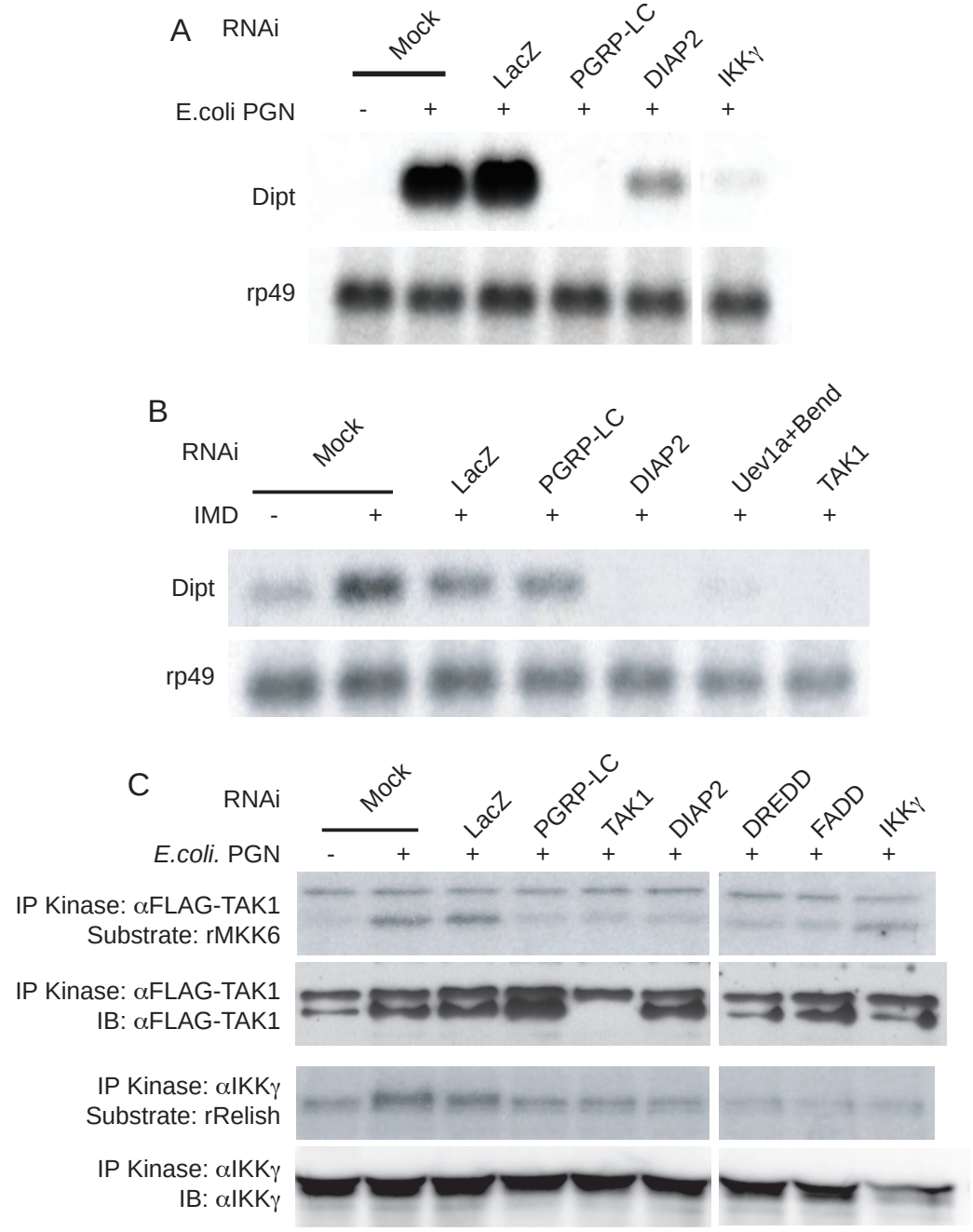
A
RNAi
Mock
LacZ
PGRP-LC
DIAP2
IKKγ
E.coli PGN
- + + + + +
Dipt
rp49
B
RNAi
Mock
LacZ
PGRP-LC
DIAP2
Uev1a+Bend
TAK1
IMD
- + + + + + +
Dipt
rp49
C
RNAi
Mock
LacZ
PGRP-LC
TAK1
DIAP2
DREDD
FADD
IKKγ
E.coli. PGN
- + + + + + + + +
IP Kinase: αFLAG-TAK1
Substrate: rMKK6
IP Kinase: αFLAG-TAK1
IB: αFLAG-TAK1
IP Kinase: αIKKγ
Substrate: rRelish
IP Kinase: αIKKγ
IB: αIKKγ

Figure 2.3 DIAP2 functions between IMD and TAK1

(A) S2* cells were treated with RNAi against various IMD pathway components, as indicated, prior to stimulation with *E.coli* peptidoglycan (PGN) for 6 hours. Induction of the AMP gene *Diptericin* was monitored by Northern blotting. *rp49* levels were monitored as a loading control.

(B) S2* cells stably expressing metallothionein IMD were treated with RNAi against various IMD pathway components, as indicated. Then cells were stimulated with copper sulfate for 6 hours to induce IMD expression. Expression of the AMP gene *Diptericin* and *rp49* were monitored by Northern blotting.

(C) The activation of TAK1 or IKK kinases was monitored by immunoprecipitation-*in vitro* kinase assays, after stimulation with *E. coli* PGN for 10 minutes. Recombinant $MKK6^{K28A}$ and recombinant Relish were used as substrates for TAK1 and IKK, respectively. RNAi was used to target various IMD pathway components, as indicated

argue that DIAP2 functions downstream of IMD but upstream of TAK1, similarly to Ubc13 and Uev1a (Zhou *et al*., 2005).

Cleaved IMD associates with DIAP2 and is ubiquitinated

As IMD is rapidly cleaved following immune stimulation and DIAP2 appears to function immediately downstream, we hypothesized that these two proteins may associate. To that end, endogenous DIAP2 was immunoprecipitated from PGN-stimulated and unstimulated S2* cells. Endogenous IMD co-precipitated with DIAP2 in a signal dependent fashion (Figure 2.4A). Strikingly, DIAP2 preferentially associated with cleaved-IMD. Overall, the amount of IMD cleavage observed in whole cell lysates varied, ranging from 5% to 15% of the total, while the cleaved IMD was preferentially (50-70%) associated with immunoprecipitated DIAP2.

These results, linking cleaved IMD and the E3-ligase DIAP2, suggest that one or both of these proteins may be conjugated with ubiquitin. Using immunoprecipitation followed by immunoblotting for total ubiquitin, IMD was found to be ubiquitinated rapidly and robustly after PGN stimulation of S2* cells (Figure 2.4B). DIAP2 was also ubiquitinated, but to a lesser extent (Figure 2.4C and Figure 2.5A). This modification occurs within one minute of stimulation, reaching a maximum at 5-10 minutes, and is lost in approximately 30 minutes. IMD ubiquitination is stable after boiling in 1% SDS, further arguing that it is directly conjugated (Figure 2.5B). IMD cleavage, DIAP2 association, and

Figure 2.4

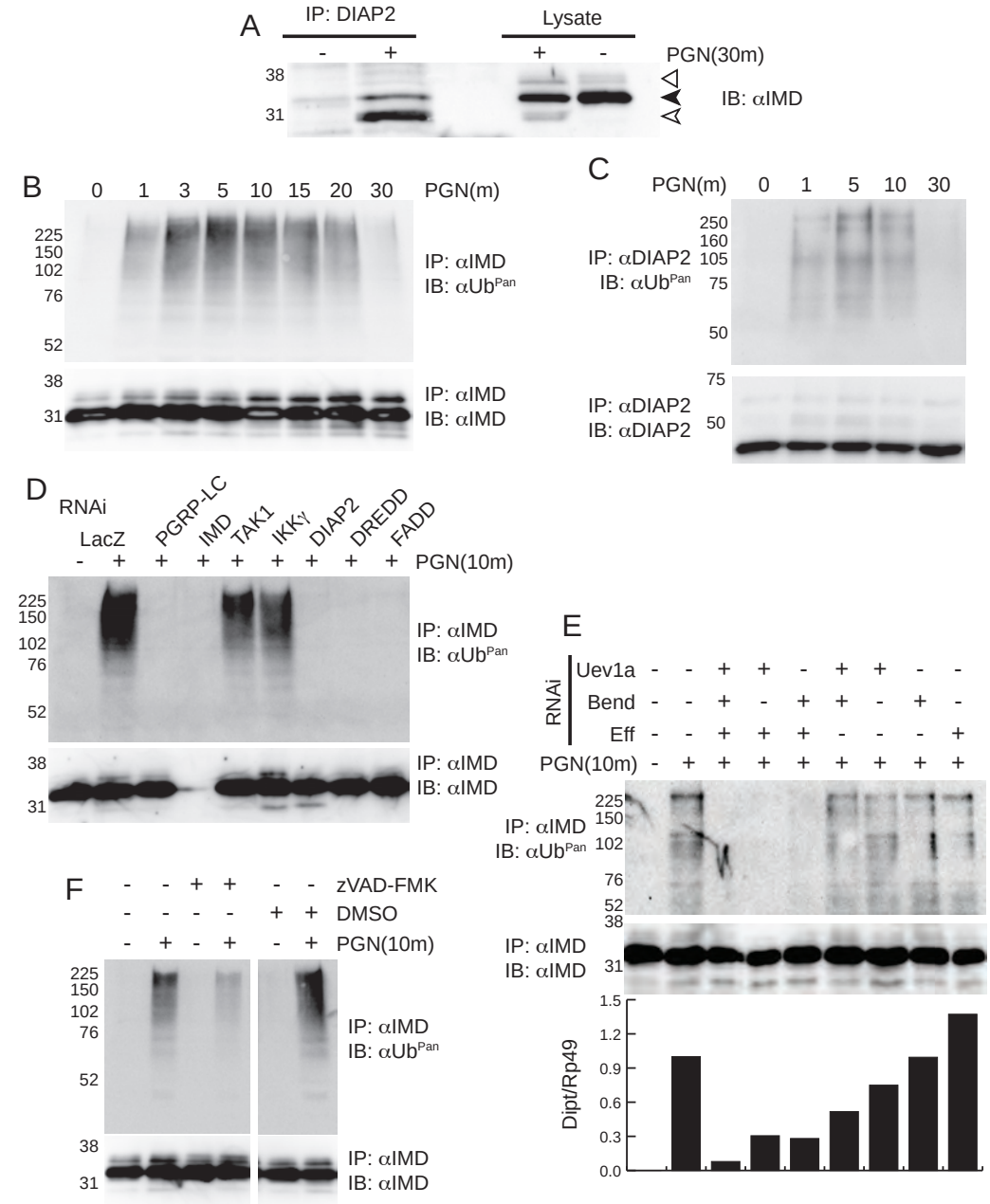
A
IP: DIAP2
Lysate
PGN(30m)
IB: αIMD
B
PGN(m)
IP: αIMD
IB: αUbPan
IP: αIMD
IB: αIMD
C
PGN(m)
IP: αDIAP2
IB: αUbPan
IP: αDIAP2
IB: αDIAP2
D
RNAi
LacZ
PGRP-LC
IMD
TAK1
IKKγ
DIAP2
DREDD
FADD
PGN(10m)
IP: αIMD
IB: αUbPan
IP: αIMD
IB: αIMD
E
RNAi
Uev1a
Bend
Eff
PGN(10m)
IP: αIMD
IB: αUbPan
IP: αIMD
IB: αIMD
Dipt/Rp49
F
zVAD-FMK
DMSO
PGN(10m)
IP: αIMD
IB: αUbPan
IP: αIMD
IB: αIMD

Figure 2.4 Association of DIAP2 and cleaved-IMD leads to IMD ubiquitination

(A) Endogenous DIAP2 was immunoprecipitated from whole cell lysates prepared from S2* cells before or after a 10 minute stimulation with *E. coli* PGN, and associated IMD was monitored by immunoblotting (left lanes). For comparison, levels of full length and cleaved IMD in whole cell lysates are shown on the right. ◀ marks unmodified full length IMD, ◁ highlights phosphorylated IMD, and ◁ marks the cleaved-IMD products.

(B) Ubiquitination of endogenous IMD was monitored in lysates from S2* cells after stimulation with *E. coli* PGN for various times (as indicated) by anti-IMD immunoprecipitation followed by immunoblotting with anti-Ub^{Pan} (top). An anti-IMD immunoblot serves as a loading control (bottom).

(C) Ubiquitination of endogenous DIAP2 was monitored in lysates from S2* cells after stimulation with *E. coli* PGN for various times (as indicated) by anti-DIAP2 immunorecipitation followed by immunoblotting with anti-Ub^{Pan}. An anti-DIAP2 immunoblot serves as a loading control (bottom).

(D) Ubiquitination of endogenous IMD in PGN-stimulated S2* cells was monitored after RNAi targeting various pathway members (top). An anti-IMD immunoblot serves as a loading control (bottom).

(E) Ubiquitination of endogenous IMD after PGN-stimulation was monitored after treatment with RNAi targeting various E2-ubiquitin conjugating enzymes (top). An anti-IMD immunoblot serves as a loading control (middle). In parallel, IMD

Figure 2.4 Association of DIAP2 and cleaved-IMD leads to IMD ubiquitination (cont.)

pathway activation was also monitored by Northern blotting for the AMP gene *Diptericin*. The ratio of *Diptericin* to *Rp49* message was quantified by phosphoimager and plotted (bottom). Y-axis is arbitrary normalized phosphoimager units.

(F) Ubiquitination of endogenous IMD in S2* cells was monitored after treatment with zVAD-FMK, or vehicle control (DMSO) (top). An anti-IMD immunoblot serves as a loading control (bottom)**.**

Figure 2.5

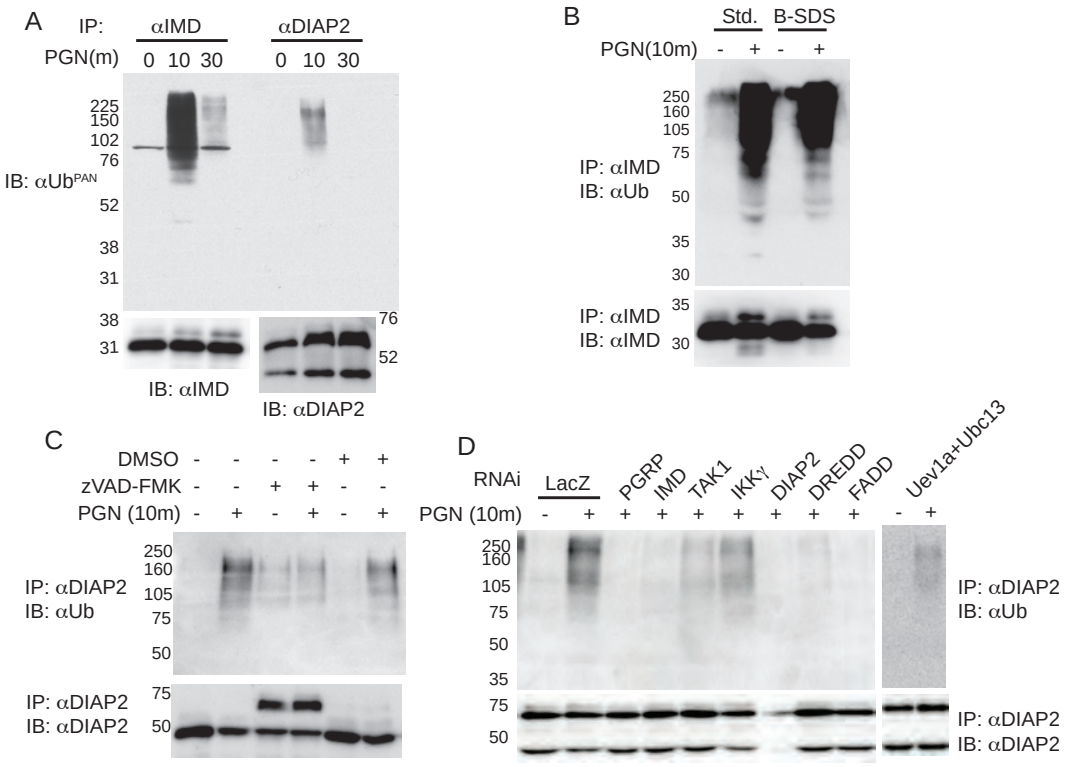
A
IP:
αIMD
αDIAP2
PGN(m)
0 10 30
0 10 30
225
150
102
76
IB: αUbPAN
52
38
31
38
31
76
52
IB: αIMD
IB: αDIAP2
B
Std.
B-SDS
PGN(10m)
- + - +
250
160
105
75
IP: αIMD
IB: αUb
50
35
30
35
30
IP: αIMD
IB: αIMD
C
DMSO - - - - + +
zVAD-FMK - - + + - -
PGN (10m) - + - + - +
250
160
105
75
50
IP: αDIAP2
IB: αUb
75
50
IP: αDIAP2
IB: αDIAP2
D
RNAi
LacZ
PGRP
IMD
TAK1
IKKγ
DIAP2
DREDD
FADD
Uev1a+Ubc13
PGN (10m) - + + + + + + + + - +
250
160
105
75
50
35
IP: αDIAP2
IB: αUb
75
50
IP: αDIAP2
IB: αDIAP2

Figure 2.5 DIAP2 is ubiquitinated

(A) 200 µg or 600µg of S2* cell lysates were immunoprecipiated for endogenous IMD or DIAP2, respectively. Samples were then run side-by-side and immunoblotted with endogenous ubiquitin antibody. IMD and DIAP2 blots are also shown as a loading control, lower panels.

(B) Endogenous IMD was immunoprecipitated from standard S2* lysate (Std.) or lysates that had been boiled with 1% SDS (B-SDS). Samples were then immunoblotted for endogenous ubiquitin. IMD blots are shown as a loading control, below.

(C) PGN-induced ubiquitination of endogenous DIAP2 in lysates from S2* cells was monitored after pretreatment with zVAD-FMK, or vehicle control (DMSO). An anti-DIAP2 immunoblot serves as a loading control.

(D) PGN-induced ubiquitination of endogenous DIAP2 in lysates from S2* cells treated with RNAi to various IMD pathway. An anti-DIAP2 blot serves as a loading control.

ubiquitination were also all analyzed together (Figure 2.6). This experiment demonstrates that IMD ubiquitination peaks shortly after cleavage and maximal DIAP2 association.

In order to determine which members of the IMD pathway are required for PGN-induced IMD ubiquitination, S2* cells were treated with RNAi targeting various pathway components, and then analyzed by IMD immunoprecipitation and ubiquitin immunoblotting. PGRP-LC, IMD, DREDD, FADD, and DIAP2 RNAi markedly reduced IMD ubiquitination. Conversely, targeting of downstream components, such as TAK1 or IKKγ, did not robustly affect IMD ubiquitination (Figure 2.4D). Previously, the E2 complex of Ubc13, and Uev1a was implicated in IMD pathway ubiquitination. RNAi treatment targeting both of these proteins (separately and together), reduced but did not eliminate the ubiquitination of IMD after stimulation (Figure 2.4E, lanes 6-8) similar to their partial effect on immune-induced *Diptericin* expression (Zhou *et al*., 2005 and Figure 2.4E). Recently, it has been suggested that another E2, Ubc5, may also form K63-ubiquitin chains (Xia *et al*., 2009). Therefore, we determined if the *Drosophila* Ubc5 homologue, Effete, was also required for IMD ubiquitination. RNAi targeting Effete, in concert with Ubc13, or Uev1a (together or separately) were able to completely inhibit ubiquitination of IMD (Figure 2.4E, lanes 3-5). Similarly, when *Diptericin* induction was analyzed, RNAi targeting Uev1a, Bend or Effete alone or in pairs only partially inhibited IMD signaling, while treatment with all three RNAis nearly abolished immune-induced *Diptericin* expression (Figure 2.4E, bottom).

Figure 2.6

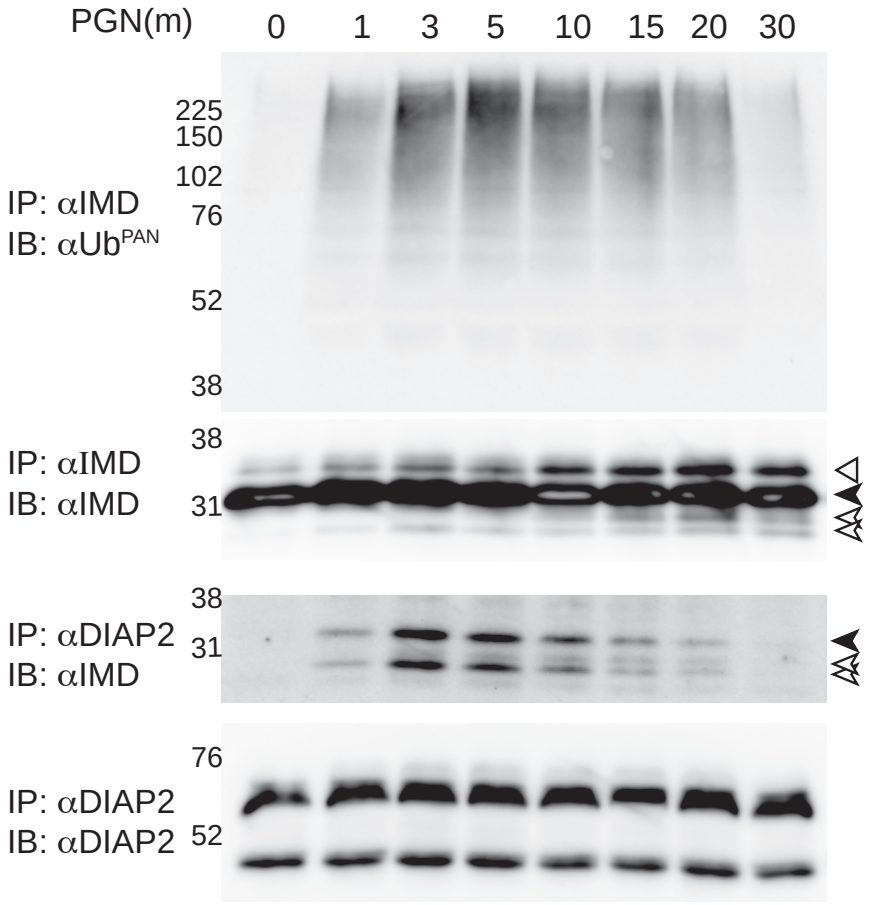
PGN(m)
0
1
3
5
10
15
20
30
225
150
102
76
52
38
IP: αIMD
IB: αUb^PAN
38
31
IP: αIMD
IB: αIMD
38
31
IP: αDIAP2
IB: αIMD
76
52
IP: αDIAP2
IB: αDIAP2

Figure 2.6 Coincident IMD ubiquitination, cleavage and DIAP2 association

Lysates from S2* cells stimulated with PGN for various times (as indicated) were immunoprecipitated for endogenous IMD or DIAP2. Immunoprecipiated IMD samples were then immunoblotted for endogenous ubiquitin and endogenous IMD. Immunoprecipitated DIAP2 samples were probed with endogenous IMD and DIAP2. ◀ marks unmodified full length IMD, ◁ highlights phosphorylated IMD,and ◁ marks the cleaved-IMD products.

Moreover, pretreatment with the caspase inhibitor zVAD-FMK reduced the amount of ubiquitinated IMD observed (Figure 2.4F), consistent with above data. DIAP2 ubiquitination similarly required these same factors (Figure 2.5C and 2.5D). Together, these results indicate that cleaved IMD and DIAP2 associate, triggering their Uev1a/Bend/Ubc5 dependent ubiquitination.

DIAP2 is the E3 for IMD K63-polyubiquitination *in vivo*

Strikingly, infection-induced IMD ubiquitination was readily detectable when IMD was immunoprecipitated from lysates extracted from adult flies, 30 minutes after septic infection with *E. coli*. As expected, *diap2* null flies, $diap2^{7c}$, show no IMD-ubiquitination following infection with *E. coli* (Figure 2.7A). Previously, the RING finger of DIAP2 was shown to play an important role in the IMD pathway (Huh *et al*., 2007). Therefore, we next sought to determine if this domain was required for IMD-ubiquitination. Transgenic rescue flies, expressing wild type DIAP2 from the daughterless-gal4/UAS system were able to rescue the $diap2^{7c}$ IMD ubiquitination phenotype. However expression of a RING finger mutant of DIAP2 ($DIAP2^{C466Y}$) was unable to rescue this phenotype (Figure 2.7A, right panels). These data demonstrate that IMD is ubiquitinated in a signal-dependent manner in flies, and that the DIAP2 RING finger is critical for this ubiquitination. These results strongly suggest that DIAP2 is the E3-ligase involved in for IMD modification.

Figure 2.7

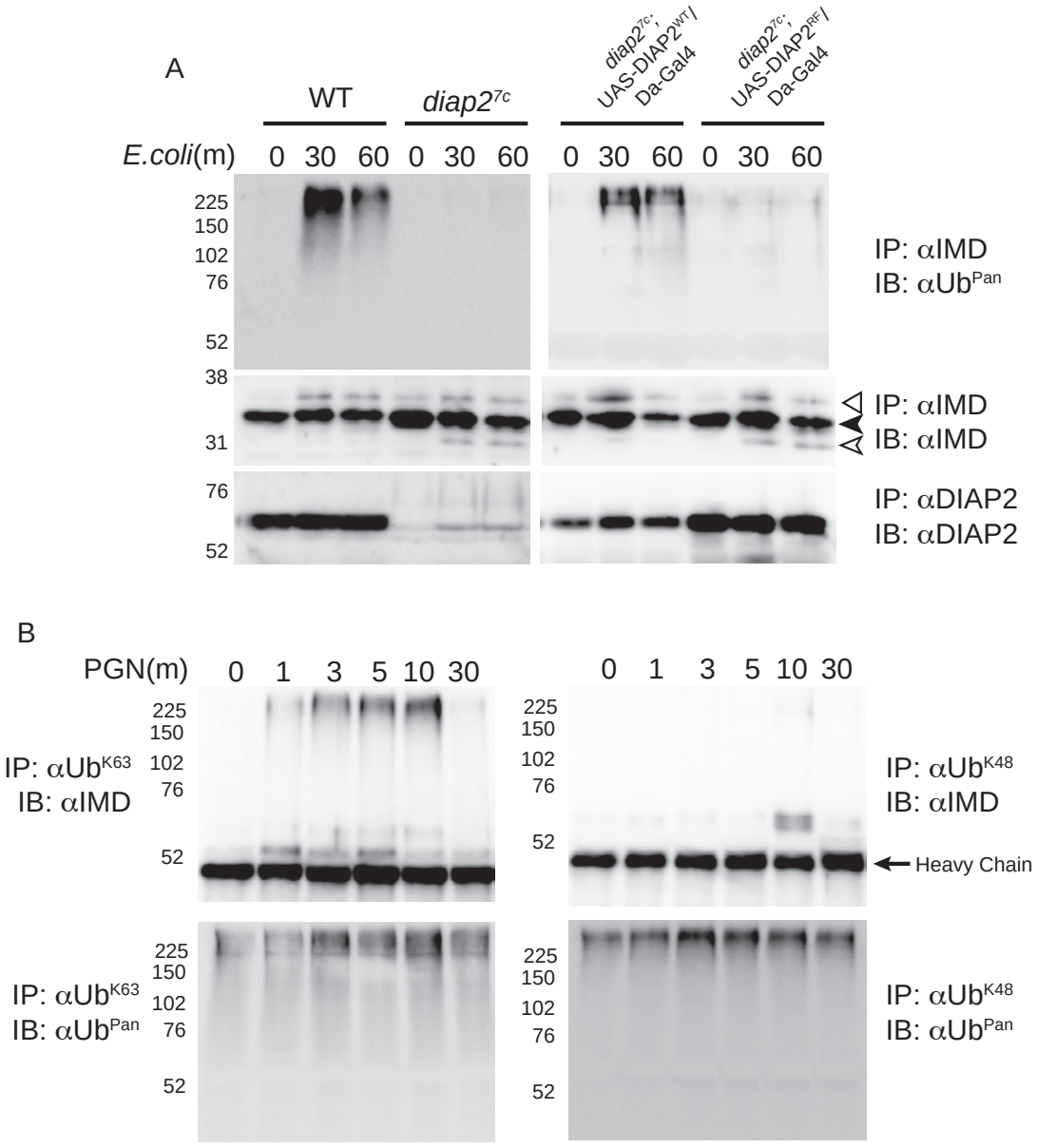
A
WT
diap2^7c
diap2^7c; UAS-DIAP2^WT/ Da-Gal4
diap2^7c; UAS-DIAP2^RF/ Da-Gal4
E.coli(m)
0 30 60 0 30 60 0 30 60 0 30 60
225
150
102
76
52
38
31
76
52
IP: αIMD
IB: αUb^Pan
IP: αIMD
IB: αIMD
IP: αDIAP2
IB: αDIAP2
B
PGN(m)
0 1 3 5 10 30
0 1 3 5 10 30
IP: αUb^K63
IB: αIMD
IP: αUb^K48
IB: αIMD
Heavy Chain
IP: αUb^K63
IB: αUb^Pan
IP: αUb^K48
IB: αUb^Pan

Figure 2.7 IMD is K63-polyubiquitinated

(A) Ubiquitination of endogenous IMD from adult flies was monitored after infection with live *E. coli* (top). An anti-IMD immunoblot serves as a control (middle, ◀ marks unmodified full length IMD, ◁ highlights phosphorylated IMD,and ◁ marks the cleaved-IMD product). IMD ubiquitination was monitored in wildtype (DD1), *diap2*^{7c} (null), and *diap2*^{7c} expressing transgenic wildtype (WT) or RING-finger mutated (RF) DIAP2. anti-DIAP2 immunoprecipitation verifies the presence/absence of DIAP2 protein in the various mutant *Drosophila* lines, as indicated.

(B) Total K63-linked (left) or K48-linked (right) polyubiquitin chains were immunoprecipiated from denatured cell lysates prepared from S2* cells stimulated with PGN for various times, as indicated. The presence of IMD was then monitored by IMD immunoblotting (top). Subsequently the same membranes were then probed for total ubiquitin as a control (bottom).

The data implicating Ubc13 (*bendless)* and Uev1a in this pathway (Zhou *et al*., 2005), suggest that IMD may be modified with K63-linked polyubiquitin chains. In order to clarify if IMD is conjugated with K48- or K63-polyubiquitin chains, we took advantage of two monoclonal antibodies that are specific to either K48- or K63-polyubiquitin chains (Mollah *et al*., 2007). After denaturing lysis, these antibodies were used to immunoprecipitate ubiquitin conjugated proteins from PGN-stimulated S2 cells. These immunoprecipitated samples were then analyzed by immunoblotting for IMD. These experiments demonstrate that IMD is strongly K63-ubiquitinated in a PGN-inducible manner, peaking at approximately 10 minutes after stimulation (Figure 2.7B), while negligible IMD was detected in the K48-immunoprecipitated samples. Control probing of these blots, with an antibody that recognizes all ubiquitin forms, showed that the K63- and K48-specific antibodies immunopurified similar amounts of ubiquitin-conjugated material. These data demonstrate that IMD is conjugated with K63-linked polyubiquitin chains.

Non-cleavable IMD prevents signaling

We next sought to identify the IMD cleavage site and determine how IMD cleavage might be linked to association with DIAP2 and K63-ubiquitination. Based on experiments with either N- or C-terminally epitope-tagged IMD (data not shown) and the size of the cleaved product (~30 kDa), the site of cleavage was tentatively mapped to the N-terminal region of IMD. The involvement of the

caspase DREDD further suggested a candidate cleavage site after residue 30, in the motif $_{27}$LEKD/A$_{31}$. Wild type or D30A mutant versions of IMD, with epitope tags at both the C- and N-termini, were expressed in S2* cells by stable transfection, using the constitutive actin promoter. Double-tagged wild type IMD showed the expected cleavage and ubiquitination kinetics after stimulation with PGN, as detected with the C-terminal FLAG-tag (Figure 2.8A). The N-terminal T7-tag did not detect cleaved-IMD (data not shown). With the aspartate at the putative cleavage site substituted with alanine (D30A), no PGN-induced cleavage was observed (Figure 2.8A, lower panel, right lanes), suggesting that caspase-mediated cleavage of IMD occurs at this position. Furthermore, IMD^{D30A} acted as a dominant negative, blocking the PGN-induced ubiquitination of endogenous IMD (Figure 2.8A, upper panel, right lanes), and blocking downstream IMD signaling as monitored by analysis of *Diptericin* expression (Figure 2.8B). Similarly, transgenic flies, over expressing IMD^{D30A} show a marked inhibition of *Diptericin* induction following *E. coli* challenge (Figure 2.8C). These data strongly argue that cleavage of IMD occurs between residues 30 and 31, and that this cleavage is required for ubiquitination and activation of downstream target genes.

Using a series of IMD deletion mutants we also analyzed which regions of IMD were required for signal induced ubiquitination (Figure 2.8D). As shown previously, over expression of wild type IMD drives IMD pathway signaling (Figure 2.3B). Interestingly only IMDΔ1 and IMDΔ5 were unable to drive signaling after over expression (Figure 2.8E and data not shown). The region

Figure 2.8

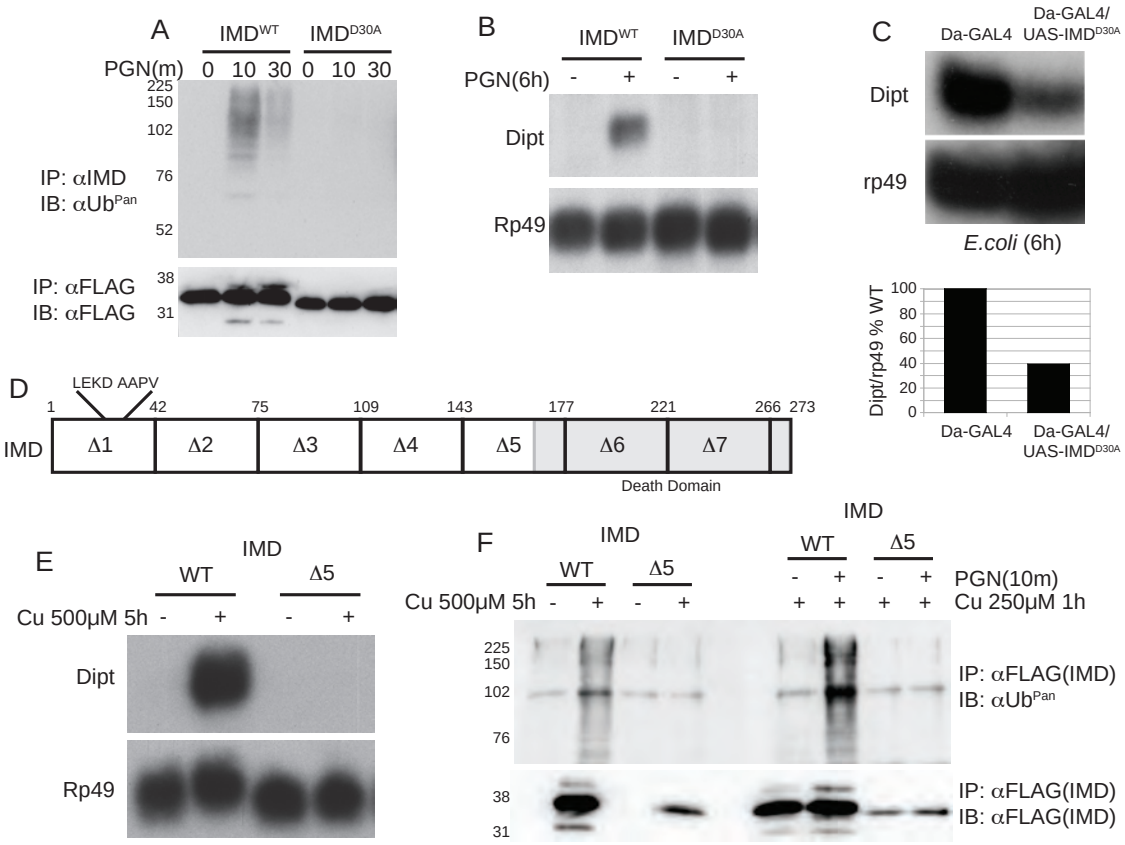
A
IMD^WT
IMD^D30A
PGN(m) 0 10 30 0 10 30
225
150
102
76
52
IP: αIMD
IB: αUb^Pan
38
31
IP: αFLAG
IB: αFLAG
B
IMD^WT
IMD^D30A
PGN(6h) - + - +
Dipt
Rp49
C
Da-GAL4
Da-GAL4/ UAS-IMD^D30A
Dipt
rp49
E. coli (6h)
Dipt/rp49 % WT
100
80
60
40
20
0
Da-GAL4
Da-GAL4/ UAS-IMD^D30A
D
LEKD AAPV
1
42
75
109
143
177
221
266
273
IMD
Δ1
Δ2
Δ3
Δ4
Δ5
Δ6
Δ7
Death Domain
E
IMD
WT
Δ5
Cu 500μM 5h - + - +
Dipt
Rp49
F
IMD
WT
Δ5
Cu 500μM 5h - + - +
IMD
WT
Δ5
- + - + PGN(10m)
+ + + + Cu 250μM 1h
225
150
102
76
IP: αFLAG(IMD)
IB: αUb^Pan
38
31
IP: αFLAG(IMD)
IB: αFLAG(IMD)

Figure 2.8 Uncleavable IMD is a dominant negative

(A) Total ubiquitinated IMD was monitored by immunoprecipitation/Ub^{pan} immublotting, in cells stably expressing either WT or mutant (D30A) IMD from the actin promoter (top). The lower anti-FLAG blot monitors cleavage of the WT or D30A IMD.

(B) Northern blot analysis of *Diptericin* expression was used to monitor IMD pathway signaling in cells over expressing WT or D30A IMD, before and after stimulation with *E. coli* PGN.

(C) Northern blot analysis of *Diptericin* expression was used to monitor IMD pathway signaling in flies expressing a transgenic copy of UAS-IMD^{D30A} under the control of ubiquitous daughterless-Gal4 driver (top). Quantitation of these data is presented below.

(D) A map of IMD deletions used to analyze signaling activity is shown. The caspase cleavage (LEKD) and IAP binding motif (AAPV) domains are indicated. The C-terminal death domain is indicated in grey.

(E) Wile type IMD or IMDΔ5 was stably expressed in S2* cells from the copper inducible metallothionein promoter. Activation of immune signaling was monitored by Northern blotting for *Diptericin. Rp49* blot serves as a loading control.

(F) Ubiquitination of wild type IMD or IMDΔ5 was monitored in two conditions. (Left) IMD protein was expressed at high level by addition of high copper for 5 hours, identical to that seen in panel E. (Right) IMD protein was moderately expressed, with lower copper for only 1 hour, and then cells were stimulated with PGN. In both cases, IMD was then immunoprecipitated with FLAG antibody, and ubiquitination levels were assayed by immunoblotting for ubiquitin. FLAG blot (bottom) serves as a control for the levels of IMD immunoprecipitated.

removed in the IMDΔ1 construct contains the IMD cleavage site, which is critical for signaling, as shown above, via its involvement in DIAP2 interaction (see below for more details). In order to determine if the region removed in IMDΔ5 functions in ubiquitination, *imd* protein was analyzed in two ways. First, IMD was strongly over expressed from the metallothionein promoter, at a level strong enough to induce AMP expression (Figure 2.8F, left). Second, IMD was expressed at lower levels, before cells were stimulated with PGN (Figure 2.8F, right). In both cases wild type IMD shows robust ubiquitination after activation, while IMDΔ5 shows no ubiquitination over background. These data indicated that this region of IMD is crucial for signal induced ubiquitination and the induction of downstream target genes.

IMD Cleavage Exposes an IAP-Binding Motif

BIR domains, such as those found in DIAP2, preferentially bind to unblocked N-terminal alanines, generated either by removal of the initiating methionine or endoproteolytic cleavage. These exposed neo-N-terminal alanines are invariant components of IAP-binding motifs (IBMs), which also include a strong preference for proline at position 3 (Shi, 2004). In particular, the DIAP1 BIR1 domain associates with the neo-N-termini IBM of the cleaved caspases drICE and DCP-1 (Tenev *et al*., 2005). Likewise, cleavage of IMD at D30 exposes a putative IBM sequence with an initial alanine and a proline at position three (AAPV). Moreover, both the proposed caspase cleavage site and this IBM

are highly conserved in the *imd* protein from 12 *Drosophila* species and the *Anopheles* mosquito (Figure 2.9A, highlighted in blue and red respectively).

Interestingly, the *imd*^{1} allele substitutes alanine 31 with valine, altering the key residue of the IBM. Although a fairly conservative change, this substitution generates a strong hypomorphic phenotype through unknown mechanisms (Georgel *et al*., 2001). To test whether cleaved IMD exposes a *bona fide* IBM we assessed whether DIAP2 interacted with cleaved-wild type IMD (A31) or cleaved-mutant (V31) IMD. To this end, we used the ubiquitin-fusion technique to express IMD$^{31\text{-}273}$ (Varshavsky, 2000), which generates IMD with an unblocked N-terminal IBM. In this system, ubiquitin is fused to the test proteins A31-IMD$^{31\text{-}273}$ or V31-IMD$^{31\text{-}273}$. Ubiquitin-specific proteases co-translationally cleave these fusion proteins at the C-terminus of the Ub moiety (Bachmair *et al*., 1986; Hershko, 1983), yielding the test protein A31-IMD$^{31\text{-}273}$ or V31-IMD$^{31\text{-}273}$ (Figure 2.10). Wild type A31-IMD$^{31\text{-}273}$ robustly interacted with DIAP2 (Figure 2.9B, lane marked AAPV). However, V31-IMD$^{31\text{-}273}$, equivalent to the cleavage product expected from the *imd*^{1} allele, showed markedly reduced binding to DIAP2 (Figure 2.9B, lane marked VAPV). Also, in transient transfections, full length IMD was spontaneously cleaved at a low level (Figure 2.9B, lower left panels), and only the cleaved product associated with cotransfected DIAP2, consistent with the data examining the endogenous proteins.

In order to verify the importance of the neo-N-terminal alanine on IMD pathway signaling, we over expressed IMD-A31V in S2* cells from the actin

Figure 2.9

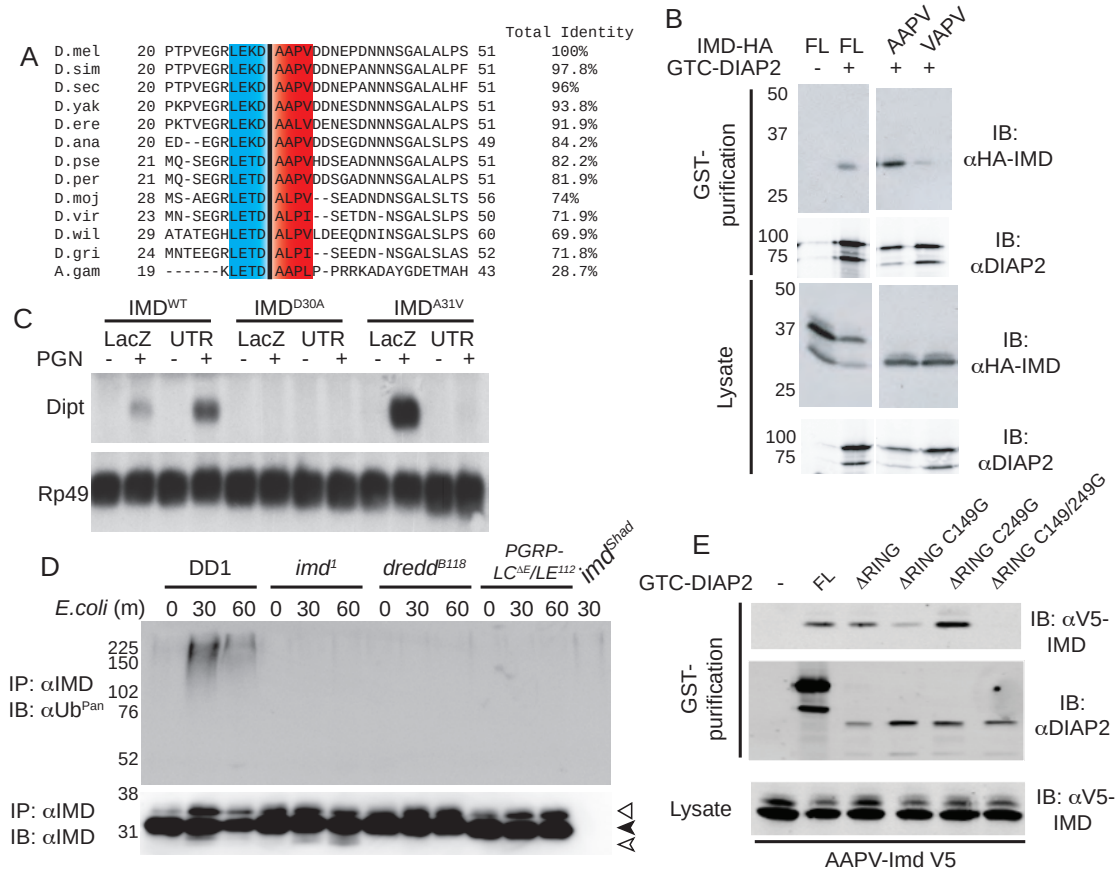
A
Total Identity
D.mel 20 PTPVEGRLEKD AAPVDDNEPDNNNSGALALPS 51 100%
D.sim 20 PTPVEGRLEKD AAPVDDNEPANNNSGALALPF 51 97.8%
D.sec 20 PTPVEGRLEKD AAPVDDNEPANNNSGALALHF 51 96%
D.yak 20 PKPVEGRLEKD AAPVDDNESDNNNSGALALPS 51 93.8%
D.ere 20 PKTVEGRLEKD AALVDNESDNNNSGALALPS 51 91.9%
D.ana 20 ED--EGRLEKD AAPVDDSEGDNNNSGALSLPS 49 84.2%
D.pse 21 MQ-SEGRLETD AAPVHDSEADNNNSGALALPS 51 82.2%
D.per 21 MQ-SEGRLETD AAPVDDSGADNNNSGALALPS 51 81.9%
D.moj 28 MS-AEGRLETD ALPV--SEADNDNSGALSLTS 56 74%
D.vir 23 MN-SEGRLETD ALPI--SETDN-NSGALSLPS 50 71.9%
D.wil 29 ATATEGHLETD ALPVLDEEQDNINSGALSLPS 60 69.9%
D.gri 24 MNTEEGRLETD ALPI--SEEDN-NSGALSLAS 52 71.8%
A.gam 19 ------KLETD AAPLP-PRRKADAYGDETMAH 43 28.7%
B
IMD-HA
GTC-DIAP2
FL FL AAPV VAPV
- + + +
GST-purification
Lysate
50
37
25
100
75
IB: αHA-IMD
IB: αDIAP2
C
IMD^WT IMD^D30A IMD^A31V
LacZ UTR LacZ UTR LacZ UTR
PGN - + - + - + - + - + - +
Dipt
Rp49
D
DD1 imd^1 dredd^B118 PGRP-LC^ΔE/LE^112 imd^Shad
E. coli (m) 0 30 60 0 30 60 0 30 60 0 30 60 30
225
150
102
76
52
38
31
IP: αIMD
IB: αUb^Pan
IP: αIMD
IB: αIMD
E
GTC-DIAP2 - FL ΔRING ΔRING C149G ΔRING C249G ΔRING C149/249G
GST-purification
Lysate
IB: αV5-IMD
IB: αDIAP2
IB: αV5-IMD
AAPV-Imd V5

Figure 2.9 IMD A31 is required for DIAP2 association

(A) An alignment of IMD from 12 *Drosophila* species and the *Anopheles* mosquito show conservation in the caspase cleavage site (blue), and IAP-binding motif (red).

(B) The binding of WT and mutant cleaved-IMD proteins was monitored using the ubiquitin-cleavage technique. HA tagged full length (FL), A31-IMD$^{31\text{-}273}$ (AAPV) or V31-IMD$^{31\text{-}273}$ (VAPV) were co-expressed in cells along with GTC-DIAP2. GST purification and immunoblotting for anti-HA were used to monitor IMD/ DIAP2 association.

(C) Northern blot analysis of *Diptericin* expression was used to monitor IMD signaling in cells expressing WT, D30A or A31V IMD after treatment with RNAi to *LacZ* or *imd* 3' UTR.

(D) Ubiquitination of endogenous IMD from WT (DD1) and various mutant adult flies was motioned after infection with live *E. coli* via IMD immunoprecipitation followed by Ub^{Pan} immunoblotting (top). IMD immunoblot is shown as a loading control (bottom). ◀ marks unmodified full length IMD, ◁ highlights phosphorylated IMD,and ◁ marks the cleaved-IMD product.

(E) Association of IMD and DIAP2 mutants was monitored via GST-coprecpitation, as in panel B.

Figure 2.10

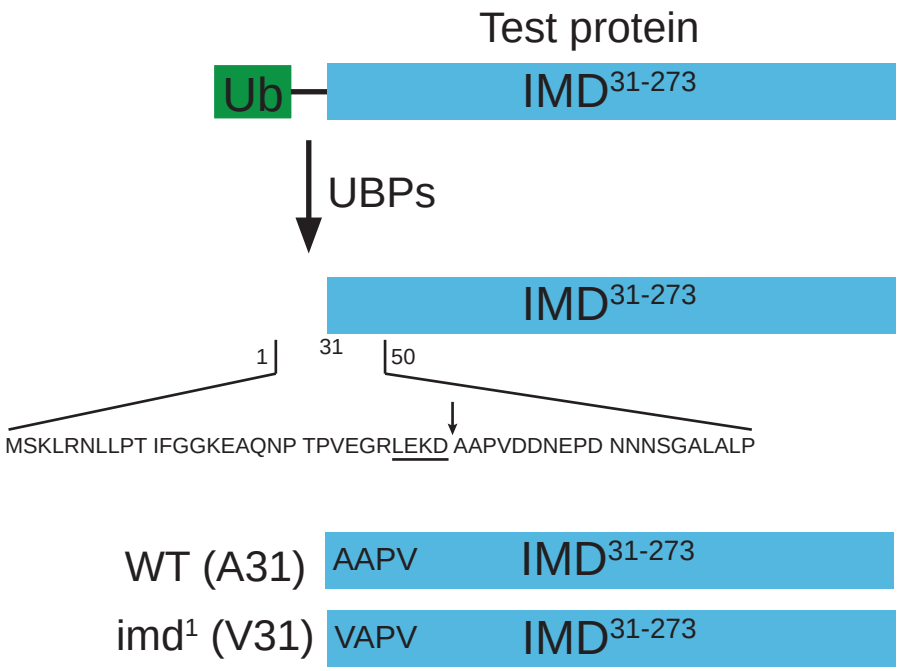
Test protein
Ub
IMD31-273
UBPs
IMD31-273
1
31
50
MSKLRNLLPT IFGGKEAQNP TPVEGRLEKD AAPVDDNEPD NNNSGALALP
WT (A31)
AAPV
IMD31-273
imd1 (V31)
VAPV
IMD31-273

Figure 2.10 Ubiquitin fusion technique

imd protein from residues 31-273 was expressed with the N-terminal ubiquitin fusion technique. Once translated, ubiquitin-specific proteases (UBPs) remove the ubiquitin moiety. The remaining target protein is left with an exposed neo-N-terminal residue. Two such proteins were expressed in this fashion, A31-IMD$^{31\text{-}273}$ (WT) and V31-IMD$^{31\text{-}273}$ (*imd*^{1}).

promoter. Cells were treated with RNAi against the 3' UTR region of IMD, to remove the endogenous wild type protein, or LacZ (as a control) prior to stimulation with PGN. As expected, expression of IMD-D30A shows a strong dominant negative phenotype, consistent with previous data. On the other hand, cells expressing IMD-A31V and treated with the control LacZ RNAi showed a strong *Diptericin* induction. Treatment with IMD 3'UTR RNAi, which selectively degrades endogenous, but not ectopically expressed IMD, resulted in a near complete inhibition of *Diptericin* induction, showing that IMD-A31V is not sufficient for signaling in cells, as observed in flies (Figure 2.9C).

In order to probe whether or not these same mechanisms are involved in immune signaling in the whole animal, IMD cleavage and ubiquitination was also probed in the the *imd*^{1} strain, which carries the A31V substitution. In lysates prepared from these flies, cleaved IMD was readily detected following *E. coli* infection but ubiquitinated IMD was completely absent (Figure 2.9D). In fact, the cleaved IMD product appears to accumulate in the *imd*^{1} animals, relative to the wild type control, presumably because cleaved IMD is rapidly and efficiently ubiquitinated in wild type but not *imd*^{1} animals. Likewise, cleaved IMD is more easily detected in the *diap2* mutant strain (Figure 2.7A). On the other hand, neither cleaved nor ubiquitinated IMD was detectable in either *dredd*, or *PGRP-LE*;*PGRP-LC* mutant animals, consistent with the results from cell culture.

In order to determine which domains of DIAP2 are required for the binding of cleaved IMD, a series of DIAP2 mutations were generated. A C149G mutation

of BIR2, predicted to abrogate its IBM binding (Ribeiro *et al*., 2007), reduced IMD^{31-273} association. Under the same conditions, mutation of the BIR3 domain (C249G) did not affect the interaction with IMD^{31-273}. When both BIR2 and BIR3 domains were altered (C149/249G), IMD^{31-273} completely failed to interact (Figure 2.9E). As expected, the RING finger domain did not contribute to IMD binding, since its deletion had no noticeable effect on IMD^{31-273} binding. Together these results indicate that cleaved IMD carries a *bona fide* IBM at its neo-N-terminus, which preferentially binds to the BIR2 of DIAP2, and to some extent also binds the BIR3 domain. The alanine at the N-terminus of the IMD cleavage product is critical for this binding, while valine at this position, as in imd^{1}, weakens with the interaction.

Discussion

In previous work, we demonstrated that the caspase-8 like protease DREDD and its binding partner FADD are required upstream in the IMD pathway, at a position similar to Ubc13 and Uev1a (Zhou *et al*., 2005). However it was not clear from these studies if the protease activity of DREDD is also required in this role upstream in the IMD pathway. Here, we show that upon immune stimulation the *imd* protein is rapidly cleaved in a DREDD and FADD dependent manner. In fact, expression of DREDD, without immune stimulation, was sufficient to cause IMD cleavage. A caspase recognition site was identified in IMD, with cleavage predicted to occur after aspartate 30. Substitution of this residue with alanine

prevents signal-induced cleavage and creates a dominant-negative allele of *imd*. This putative cleavage site in IMD ($_{27}$LEKD/A$_{31}$) is similar to the Relish cleavage site ($_{542}$LQHD/G$_{546}$), consistent with the notion that both proteins are cleaved by the same protease. Likewise, when IMD cleavage was blocked by caspase inhibitors, IMD was no longer ubiquitinated. Alignment of *imd* protein sequences from 12 *Drosophila* species and the *Anopheles* mosquito showed that the cleavage site is highly conserved (LEKD or LETD in all cases). These findings strongly argue that IMD cleavage after position 30 is mediated by DREDD, and that this cleavage is critical for further downstream signaling events.

Cleavage of IMD exposes a highly conserved IAP-binding motif (IBM) (Figure 2.9A), which then binds the BIR 2/3 domains of DIAP2. In the context of programmed cell death regulation, these IBM motifs are best defined by their neo-N-terminal alanine as well as the proline at position 3, both of which are also present in cleaved-IMD, supporting the notion that IMD includes an IBM starting at position 31. The notion that IMD carries an IBM also provides a molecular explanation for the hypomorphic phenotype observed in the *imd*^{1} mutant, which carries a valine substitution for this alanine at position 1 of cleaved IMD. Although several IAP proteins have been implicated in mammalian innate immune/NF-κB signaling (Deveraux and Reed, 1999; Verhagen *et al*., 2001; Bertrand *et al*., 2008; Bertrand *et al*., 2009), the significance of their associated BIR domains, as well as their possible binding to proteins with exposed IBMs, has remained largely unexplored. We show here, for the first time, that the BIR/

IBM association plays a crucial role in innate immune NF-κB signaling in *Drosophila*. These findings present a novel role for the BIR-IBM interaction module outside of the cell death arena.

Furthermore, characterization of signaling in the *imd*^{1}*, diap2, dredd* and *PGRP-LC/LE* mutant flies provides critical *in vivo* verification of the cell culture data and leads to the model presented in Figure 2.11. In particular, the molecular mechanism we propose suggests that immune stimulation leads to the DREDD-dependent cleavage of IMD, perhaps by recruiting IMD, FADD and DREDD to a receptor complex. Consistent with this aspect of the model, *dredd* mutants and receptor mutants failed to cleave (or ubiquitinate) IMD following infection. Once cleaved, the exposed IBM of IMD interacts with BIRs 2 & 3 of DIAP2. Currently, we do not know precisely where in the cell the IMD/DIAP2 association occurs. In Figure 2.11, this interaction is diagramed as occurring away from the receptor proximal complex, but this is only for illustrative purposes. Once associated with DIAP2, cleaved IMD is rapidly K63-ubiquitinated. As the RING mutated version of *diap2* failed to support IMD ubiquitination in flies, DIAP2 likely functions as the E3 for this reaction. In addition, the *imd*^{1} allele, which fails to interact with DIAP2 because of a mutation in the IBM, demonstrates the critical nature of the IMD-DIAP2 interaction for innate immune signaling. Consistent with the notion that cleavage precedes ubiquitination, mutants that fail to generate ubiquitinated IMD (*i.e. diap2 and imd*^{1}*)* actually accumulate more cleaved IMD than is observed in wild type flies. Presumably, in wild type animals, cleaved IMD is efficiently

Figure 2.11

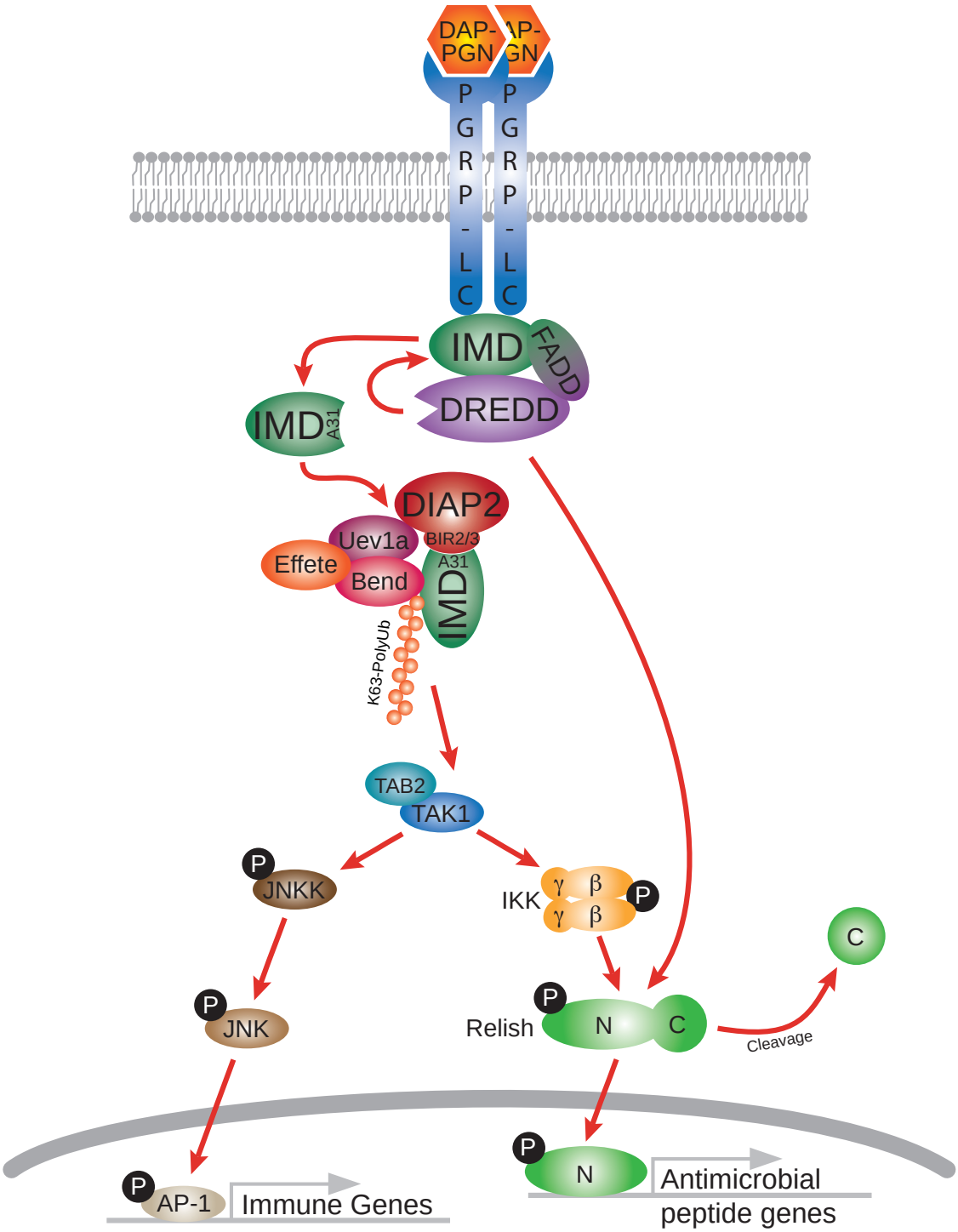
DAP-PGN
AP-GN
PGRP-LC
PGRP-LC
IMD
FADD
DREDD
IMD A31
DIAP2
Uev1a
BIR2/3
Effete
Bend
A31
IMD
K63-PolyUb
TAB2
TAK1
P
JNKK
IKK
γ β
γ β
P
C
P
JNK
P
Relish
N
C
Cleavage
P
AP-1
Immune Genes
P
N
Antimicrobial
peptide genes

Figure 2.11 IMD pathway model

DAP-type PGN binding causes multimerization or clustering of PGRP receptors. This likely recruits the adapter proteins IMD, FADD and the caspase DREDD. Once in proximity, DREDD cleaves IMD, generating an exposed neo-N-terminal A31 residue. This neo-N-terminus then binds the E3 ligase DIAP2 via its BIR2/3 domains. In conjuction with the E2-ubiquitin conjugating enzymes UEV1a, Bendless (Ubc13) and Effete (Ubc5), IMD (and to a lesser degree DIAP2) are then K63-polyubiquitinated. This polyubiquitin chain then leads to the activation of downstream kinases ultimately leading to the phosphorylation and activation of Relish and induction of downstream targets, like the AMP genes.

ubiquitinated, and thus is difficult to detect in our assays. On the other hand, *dredd* mutants or mutants lacking the key immunoreceptors (*PGRP-LC/LE)* failed to cleave and ubiquitinate IMD, consistent with our cell culture data.

Previous work has suggested that ubiquitination plays a critical role in IMD signaling in the *Drosophila* immune response (Gesellchen *et al*., 2005; Huh *et al*., 2007; Kleino *et al*., 2005; Leulier *et al*., 2006; Zhou *et al*., 2005). However, the molecular target(s) of ubiquitination and the mechanisms of its activation have remained elusive. As discussed above, the data presented here indicate that DIAP2 functions as the E3-ligase in the IMD pathway, a function usually attributed to the TRAF or, more recently, cIAP proteins in mammalian NF-κB signaling pathways (Bertrand *et al*., 2009). The E2 complex of Ubc13 and Uev1a also appears to be involved in IMD ubiquitination. RNAi targeting of these K63-ubiquitinating enzymes reproducibly decreases IMD ubiquitination and the induction of target genes, however the degree of inhibition is variable and never complete (data herein and Zhou *et al*., 2005). We now show that a third E2 enzyme, Effete, the *Drosophila* Ubc5 homologue, also plays a vital role in ubiquitination of IMD. RNAi treatment targeting Effete, in concert with Uev1a and/or Bendless reproducibly eliminated IMD ubiquitination and the induction of *Diptericin*.

Several lines of evidence argue that IMD is the critical target for K63-ubiqutination in this pathway. First, IMD is by far, the most robustly modified component that we have identified, and the only one in which modifications can

be detected in whole animals. Second, the protein produced as a result of the *imd*^{1} mutation, which does not signal, is also not ubiquitinated. Third, we present a deletion mutant, IMDΔ5, that is not ubiquitinated and fails to signal. Finally, Thevenon *et al*. (2009) recently identified the *Drosophila* ubiquitin specific protease, USP36, as a negative regulator of IMD ubiquitination. Functionally, USP36 is able to remove K63-polyubiquitin chains from IMD, promoting K48-mediated polyubiquitination and degradation of IMD. Consistent with our model, animals which over express USP36 show decreased levels of IMD ubiquitination, reduced IMD pathway activation as monitored by *Diptericin* RNA expression, and are susceptible to bacterial infection. Together, these data strongly argue that IMD is the critical substrate for K63-polyubiqutination in IMD pathway signaling, although other proteins may also be conjugated to lesser degree (as shown here for DIAP2) and could potentially substitute for IMD as the platform for ubiquitin conjugation. Interestingly, Xia and colleagues, recently showed that unanchored K63-polyubiquitin chains (i.e. ubiquitin chains which are not conjugated to a target substrate) are sufficient to activate the mammalian TAK1 and IKK kinase complexes. Furthermore they show that unanchored polyubiquitin chains are produced after stimulation of HEK cells with IL-1β (Xia *et al*., 2009). Thus, the presence (or absence) of K63-polyubiquitin chains may be more important than their conjugation substrate.

K63-polyubiquitin chains are likely to serve as scaffolds to recruit the key kinases TAK1 and IKK, in the IMD pathway. Both of these kinases include

regulatory subunits with highly conserved K63-polyubiquitin binding domains. *Drosophila* TAB2, which complexes with TAK1, and the IKKγ subunit are predicted to contain conserved K63-polyubiquitin binding domains (Ea *et al*., 2006; Kleino *et al*., 2005; Zhou *et al*., 2005; Zhuang *et al*., 2006). Thus, we hypothesize that K63-polyubiquitin chains will recruit both the TAB2/TAK1 complex and the IKK complex, creating a local environment for optimal kinase activation and signal transduction, however this aspect of our model is still speculative.

Although mammalian caspase-8 and FADD are best known for their role in apoptosis, a growing body of literature indicates that these factors, along with RIP1 (which has some homology to IMD), also function in RIG-I signaling to NF-κB (Balachandran *et al*., 2004; Takahashi *et al*., 2006). In addition, caspase-8 has been implicated in NF-κB signaling in B-cell, T-cell and LPS signaling (Bidere *et al*., 2006; Chun *et al*., 2002; Lemmers *et al*., 2007; Salmena *et al*., 2003; Su *et al*., 2005; Sun *et al*., 2008). Cells, from mice or humans, lacking caspase-8 have defects in immune activation, cytokine production and nuclear translocation of NF-κB p50/p65 (Chun *et al*., 2002; Lemmers *et al*., 2007). Furthermore, recent evidence also shows that during mammalian NOD signaling the RIP2 protein is ubiquitinated in a cIAP1/2 dependent manner (Bertrand *et al*., 2009). Given that *Drosophila* homologs of RIP1, FADD and capase-8 also function in the IMD pathway, the results presented here may help elucidate the mechanism by which these factors function in these mammalian immune signaling pathways.

Material and Methods

Fly Stocks

The following fly strains were used in this work. DD1 (labeled as WT in most cases) (Gottar *et al*., 2002; Rutschmann *et al*., 2000), *diap2*^{7c} (Leulier *et al*., 2006), *diap2*^{7c}; UAS-DIAP2^{C466Y}/UAS-DIAP2^{C466Y} or TM6-Tb (Leulier *et al*., 2006), *imd*^{1} (Georgel *et al*., 2001), *imd*^{shadok} (Kaneko *et al*., 2006), *daughterless*-GAL4/UAS-IMD^{D30A}, *dredd*^{B118} (Leulier *et al*., 2000), and double PGRP-LC, PGRP-LE mutant flies (*pgrp-le*^{112};+;*pgrp-lc*$^{\Delta E}$) (Takehana *et al*., 2004).

RNAi

RNAi to IMD pathway components, and LacZ as a control, were produced using T7 RiboMAX Express Large Scale RNA Production System (Promega). S2* cells were split to 0.5x10^{6} cells per ml and allowed to incubate for ~24 hours at 27°C. 2µg/ml RNAi was then delivered by calcium phosphate transfection and cells were allowed to recover for ~24 hours at 27°C. 1µM 20-hydroxyecdysone was then added to the cells for ~24 hours. Finally cells were stimulated with either *E.coli* peptidoglycan (100ng/ml) or induced with copper, for 6 hours, before being isolation of RNA or whole cell lysate for Northern blotting or immunoprecipitation/immunoblot/kinase assays as described below.

RNA Analysis

Total RNA was isolated with the TRIzol reagent (Invitrogen) as previously described (Silverman *et al*., 2000) and expression of *Dpt* and *Rp49* was analyzed by Northern blot analysis followed by autoradiography.

IMD Antibody

For the production of anti-IMD polyclonal antibodies, the full-length imd coding sequence was cloned in the *E. coli* expression vector pDS56/RBII, 6xhis. His-tagged-IMD was expressed in M15 *E. coli* (strain M15) and purified by nickel chelate chromatography. Purified proteins were used to immunize rabbits. Nucleotide sequence of all constructs was confirmed by sequencing.

TAK1 Antibody

For the production of the anti-TAK1 polyclonal antibody, the peptide KSDGRERLTVTDTKP was generated an used to immunize rabbits (Open Biosystems, Inc.). Serum was then pooled and purified via affinity purification.

Protein and Immunoprecipitation Assays

Following stimulation with PGN (100ng/ml) or $CuSO_4$ (500µM), S2* cells were lysed in buffer (10% glycerol, 1% Triton X-100, 20mM Tris, 150mM NaCl, 25mM β-glycerolphosphate, 2mM EDTA, 1mM DTT, 1mM Sodium Orthovanadate, 1X Protease Inhibitor Cocktail). For total protein analysis, 50-100µg of total protein were prepared as previously described (Kaneko *et al*., 2006) and immunoblotted with anti-IMD, anti-pJNK (Santa Cruz), or anti-JNK(FL) (Santa Cruz). For immunoprecipitations, 200-600µg of total protein extract was immunoprecipitated as previously described (Kaneko *et al*., 2006) with anti-DIAP2 (Leulier *et al*., 2006) , anti-IMD or anti-FLAG-M5 (Sigma), before immunoblotting with anti-DIAP2, anti-Ubiquitin (Santa Cruz), or anti-IMD. For adult flies, a 4mL culture of *E. coli* 1106 was grown up to an approximate OD595

of 1. Bacteria were then pelleted, washed once with PBS and pelleted a second time. A stainless steel needle was then dipped into the bacterial pellet and used to infect flies by pricking their abdomen. Post infection, 10-15 frozen adult male flies were ground in 500µL of 2X lysis buffer. 400-600µg of total protein were then immunoprecipitated in 2X lysis buffer overnight at 4°C with anti-IMD. Immunoprecipitated IMD was then washed 2 times 500µL with lysis buffer and analysed as described above.

K48- and K63-polyubiquitin Immunoprecipitation Assays

Following stimulation with PGN (100ng/ml), S2* cells were lysed in buffer (10% glycerol, 1% Triton X-100, 20mM Tris, 150mM NaCl, 25mM β-glycerolphosphate, 2mM EDTA, 1mM DTT, 1mM Sodium Orthovanadate, 1X Protease Inhibitor Cocktail) containing 6M UREA and 2mM NEM. 900µg of total protein extract was then diluted to 3M UREA (using lysis buffer) and immunoprecipitated overnight at room temperature with K48- or K63-polyubiquitin antibody. Samples were then spun at ~14000xg to remove any possible UREA precipitate. Protein A sepharose was added to each sample and samples were allowed to roll at room temperature for 8 hours to overnight. Finally samples were washed 3x 500µl in lysis buffer containing 3M UREA and 2mM NEM before running on SDS-PAGE and immunoblotting for IMD (as above).

Kinase Assays

Activity of kinases was assayed as previously described (Silverman *et al*., 2000; Wang *et al*., 2001). Briefly, cultured S2* cells or S2* cells stability transfected with inducible metallothionein FLAG-TAK1 were pretreated with 1µM 20-hydroxyecdysone for 24-48 hours. For FLAG-TAK1 assays, cells were pretreated with low copper (100µM $CuSO_4$ for 1 hour). Cells were then pretreated as appropriate and stimulated with *E.coli* peptidoglycan (100ng/ml) for 10 minutes or not. Cells were lysed in 100µl/ml of lysis buffer (10% glycerol, 1% Triton X-100, 20mM Tris, 150mM NaCl, 25mM β-glycerolphosphate, 2mM EDTA, 1mM DTT, 1mM Sodium Orthovanadate, 1X Protease Inhibitor Cocktail), and kinases were immunoprecipitated with appropriate antibodies for 2-3 hours at 4°C; 75µg of total protein for FLAG-TAK1 with anti-FLAG M2 Agarose (Sigma), 75µg of total protein for endogenous TAK1 with anti-TAK1 antisera and 50µg of total protein for IKK with anti-IKKγ. Immunoprecipitated kinases were washed 2 times with 500µL of lysis buffer and 2 times 500µL with kinase reaction buffer (200mM HEPES, 200mM β-glycerolphosphate, 100mM $MgCl_2$, 500mM NaCl, 10mM DTT, 1mM Sodium Orthovanadate). Kinases were then added to 10µL of kinase reaction buffer containing 200µM cold ATP, 1µL ^{32g}P*-ATP, and substrate (1ug rMKK6-K28A for TAK1 KA, or 50ng rRelish for IKK KA). Kinase reactions were incubated at 30°C for 30 minutes and run on SDS-PAGE. SDS-PAGE gels were then fixed, dried, and autoradiographed.

Cloning

T7/FLAG Double tagged IMD was constructed in the pPAC-PL vector at *Kpn*I and *Not*I using standard cloning techniques. Subsequently, Act-T7-IMD D30A-FLAG and Act-T7-IMD A31V-FLAG were produced using QuikChange Site Directed Mutagenesis (Stratagene). AAPV-Imd (31-273) or the mutated form VAPV-Imd (31-273) were expressed using the Ubiquitin-fusion technique (Varshavsky, 2000).

Caspase Inhibitor Treatment

S2* cells were split $0.5x10^6$ cells per ml and allowed to incubate for ~20 hours at 27°C. 1µM 20-hydroxyecdysone was then added for and additional 24 hours. 100µM caspase inhibitor zVAD-FMK, dissolved in DMSO, was then added to cells for 30 minutes or 4 hours at 27°C before stimulation with *E.coli* peptidoglycan. Proteins were analyzed as described above.

IMD/DIAP2 Pull Down

S2 cells were transfected with pAc myc-Imd-HA or the pMT DHFR-HA-Ub-Imd (31-273) constructs with or without pMT-DIAP2-GTC. Expression was induced with 350µM $CuSO_4$ for 15 h and cells lysed in lysis buffer (50mM Tris, pH 7.5, 150mM NaCl, 1% TX-100, 10% glycerol, 1mM EDTA, Complete Protease Inhibitor Cocktail (Roche), 1 mM DTT). DIAP2-GTC was purified using GSH-Sepharose (GE Healthcare) and complexes eluted with 10mM Glutathione solution (in 50mM Tris-HCl pH 8.0). DIAP2 and interacting IMD proteins were analysed by Western Blot using antibodies against HA (myc-Imd-HA) (Roche), V5 (Imd (31-273) (AbD Serotec) and DIAP2 (Leulier *et al*., 2006).

Boiling SDS Immunoprecipitations

After stimulation with PGN S2* cells were harvested and spit. Half of the total cell pellet was lysed in lysis buffer as described above. The second half of the pellet was lysed in lysis buffer containing 1% SDS and immediately boiled for 10 minutes. Lysates from both treatments were then immunoprecipiated for IMD using anti-IMD sera as above. In the case of the boiled SDS lysis, the total SDS in the sample was diluted to below 0.05% before immunoprecipitation.

PREFACE TO CHAPTER III

This chapter is in preparation for publication:

Nicholas Paquette, Charles Sweet, Lindsay Wilson, Andrea Pereira, Bill Lane and Neal Silverman. *Serine/Threonine Acetylation of Drosophila TAK1 by the Y. pestis Effector YopJ*. (2009)

Charles Sweet performed IKK kinase analysis

Lindsay Wilson and Andrea Pereria performed *Drosophila* transgenic mapping and imaging

Bill Lane performed microcapillary reverse-phase HPLC nano-electrospray tandem mass spectrometry

Nicholas Paquette performed the remaining experiments

Nicholas Paquette and Neal Silverman designed the experiments and wrote the manuscript

CHAPTER III

Serine/Threonine Acetylation of *Drosophila* TAK1 by the *Y. pestis* Effector YopJ

Abstract

The Gram-negative bacteria *Yersinia pestis*, causative agent of plague, is both lethal and extremely virulent. One mechanism contributing to *Y. pestis* virulence is the presence of a type-three secretion system which injects effectors proteins, Yops, directly into the immune cells of the infected host. One of these Yop proteins, YopJ, has been shown to be highly pro-apoptotic and play a role in attenuation of mammalian NF-κB, p38 and JNK signal transduction pathways. Although the precise function of the protein remained elusive for some time, recent work has shown that YopJ acts as a serine/threonine acetyl-transferase targeting mitogen-activated protein (MAP) 2 kinases. Utilizing *Drosophila* cell culture and whole animals as a model system, we demonstrate YopJ mediated inhibition of one NF-κB signaling pathway (IMD), but not the other (Toll) . In fact, we show that TAK1, the critical MAP3K in the IMD pathway, is, targeted for YopJ-mediated serine/threonine acetylation. Acetylation of critical serine/threonine residues in the activation loop of *Drosophila* TAK1 blocks phosphorylation of the protein and subsequent kinase activation. These data present the first evidence that TAK1 is a target for YopJ mediated inhibition.

Introduction

The gram-negative bacteria *Yersinia pestis* is perhaps best known for its role as the causative agent of plague, responsible for millions of deaths throughout history. Although not often thought of as a 21st century disease, *Y. pestis* is endemic in rodents throughout the world, including a number of areas of the United States, particularly the southwest region where it can be found in prairie dogs and other mammals. *Y. pestis* is transmitted between hosts in two ways. The most common route of infection is through the bite of the flea , which causes a subcutaneous infection. The bacteria then travel to the lymph nodes of the infected host causing blisters (also known as bubos), the defining symptom of bubonic plague. The second route of infection occurs in pneumonic plague, when the bacteria are transmitted person-to-person by coughing, after the bacteria colonize the lungs of an infected individual.

One aspect which makes *Y. pestis* so virulent is the presence of a type three secretion system (T3SS) and a number of effector proteins known as Yersinia outer proteins (Yops) on the pCD1 plasmid (Iriarte and Cornelis, 1996). These bacterial effector proteins are injected by the T3SS directly into host immune cells (typically macrophages and dendritic cells) where they interfere with number of intracellular functions, such as cytoskeleton stability and various signal transduction pathways, greatly limiting the innate immune response (Marketon *et al*., 2005).

YopJ is one of six Yops that is injected into the immune cell cytoplasm and may play a large role in the down regulation of the innate immune response. YopJ has been shown to be both pro-apoptotic and to inhibit MAPK, TNF and NF-κB signaling pathways (Monack *et al*., 1997; Monack *et al*., 1998; Palmer *et al*., 1998; Schesser *et al*., 1998; Palmer *et al*., 1999). Although functionally identified to inhibit these pathways, the precise targets and mechanism employed by YopJ remained controversial for some time. Initially YopJ was proposed to act as a ubiquitin-like protein protease, cleaving the ubiquitin-like protein SUMO from its conjugated targets (Yoon *et al*., 2003). Subsequent evidence however suggested that YopJ acts as a deubiquitinase, removing critical polyubiquitin chains from the NF-κB/innate immune signaling pathway protein TRAF6, which is essential for downstream signaling (Sweet *et al*., 2007; Zhou *et al*., 2005). However, recent biochemical evidence from two groups, strongly argues that YopJ has a completely novel and unpredicted function; that of an serine/ threonine acetyltransferase. In this role YopJ acetylates serines and threonines of a family of mitogen-activated protein 2 (MAP2) kinases critical to mammalian innate immune signaling. This acetylation blocks their phosphorylation and subsequent activation of the kinases, thus neutralizing their innate immune signaling pathways (Mittal *et al*., 2006; Mukherjee *et al*., 2006).

It is clearly difficult to reconcile the drastically different functions attributed to YopJ. On the one hand, YopJ seems to act upstream during signaling blocking ubiquitination and pathway activation. While on the other hand YopJ appears to

block activation of downstream MAP2 kinases by acetylation. In either case the inhibitory activity would be sufficient to block immune signaling, consistent with previous literature (Monack *et al*., 1997; Monack *et al*., 1998; Palmer *et al*., 1998; Schesser *et al*., 1998; Palmer *et al*., 1999). A number of hypotheses therefore present themselves which could explain the discrepancy regarding the function of YopJ. First, YopJ could have two separate and distinct functions, working both as a ubiquitin protease and a serine/threonine acetyl-transferase. Secondly, YopJ mediated inhibition of kinases could disengage some feedback loop which is required for ubiquitination of upstream pathway components. Finally, these purported activities could be an artifact. as ,much of the published data is based on transient transfections or in vitro reactions. In order to further elucidate the molecular functions of YopJ we utilize *Drosophila* cell culture and whole animals as a model system to analyze YopJ mediated inhibition of NF-κB signaling.

Unlike mammals, *Drosophila* lack a fully developed adaptive immune system. Instead they rely almost entirely on innate immune signaling to defend against invading pathogens. One critical component of the *Drosophila* immune response is the rapid and robust production of a variety of antimicrobial peptides (AMPs) following infection. The production of AMPs is transcriptionally regulated by two innate immune pathways, the Toll pathway and the IMD pathway. The Toll pathway is activated by fungi and lysine type peptidoglycan (PGN), found in most Gram-positive bacteria which lead to the proteolytic cleavage of the cytokine Spätzle. Cleaved Spätzle binds the Toll receptor leading to the activation of an

adaptor complex containing the signaling proteins dMyD88, Tube, and the kinase Pelle. As a consequence the *Drosophila* IκB homologue Cactus is then phosphorylated, ubiquitinated, and degraded by the proteosome. The removal of Cactus then allows the NF-κB proteins Dif and Dorsal to translocate into the nucleus and activate AMP genes.

Conversely, the IMD immune signaling pathway is activated by the presence of DAP-type PGN common to most Gram-negative bacteria. When DAP-type PGN is bound by the peptidoglycan recognition protein (PGRP) it initiates an intracellular cascade in which cleavage of the proximal adapter protein IMD by the caspase DREDD leads to the K63-mediated polyubiquitination of IMD.(Kaneko *et al*., 2004 and Chapter 2). It is then proposed that this K63-polyubiquitin chain recruits the downstream kinases TAK1 and IKK. Once recruited to the ubiquitin scaffold TAK1 becomes activated and initiates two downstream arms of the IMD pathway. In the Relish/NF-κB arm , TAK1 phosphorylates and activates the IKK complex leading to the subsiquent phosphorylation of the NF-κB protein Relish (Silverman *et al*., 2003). In addition, the caspase DREDD is also responsible for the cleavage of Relish (Stöven *et al*., 2000). Once cleaved and phosphorylated, Relish translocates into the nucleus and activating AMP production. In the second arm of the IMD pathway, TAK1 phosphorylates the JNK kinase Hemipterous, which in turn phosphorylates the JNK protein Basket, leading to the activation of the AP1 transcription factor and production of various immune genes.

Both the *Drosophila* IMD and Toll pathways show a significant amount of homology to mammalian innate immune signaling pathways, and potentially both could be targets of YopJ mediated inhibition. However, we present evidence that only the IMD pathway is sensitive to YopJ mediated inhibition and furthermore that the presence of YopJ results in the serine/threonine acetylation of the MAP3 kinase TAK1 and subsequent inhibition of the kinase. This inhibition is sufficient to block downstream signaling of both the JNK and Relish/NF-κB branches of the IMD pathway. These data demonstrate that the MAP3 kinase TAK1 is a potent target of YopJ mediated inhibition and show YopJ mediated modification in living cells.

Results

YopJ blocks the IMD innate immune signaling pathway

In order to develop *Drosophila* as a model system for the study of YopJ-mediated innate immune inhibition, stable S2* cell lines inducibly expressing either wild type YopJ ($YopJ^{WT}$) or a catalytically inactive mutant (C172A, $YopJ^{CA}$) were generated. With the metallothionein promoter, addition of copper sulfate directly to the culture media induces the expression of $YopJ^{WT}$ or $YopJ^{CA}$ proteins, while in the absence of copper no protein is detected by western blot analysis (Figure 3.1A, bottom panel). After treatment with copper, these cells were stimulated with Spätzle or DAP-type PGN to activate the Toll or IMD pathways, respectively. Toll signaling was monitored by Northern blotting for *Drosomycin*

Figure 3.1

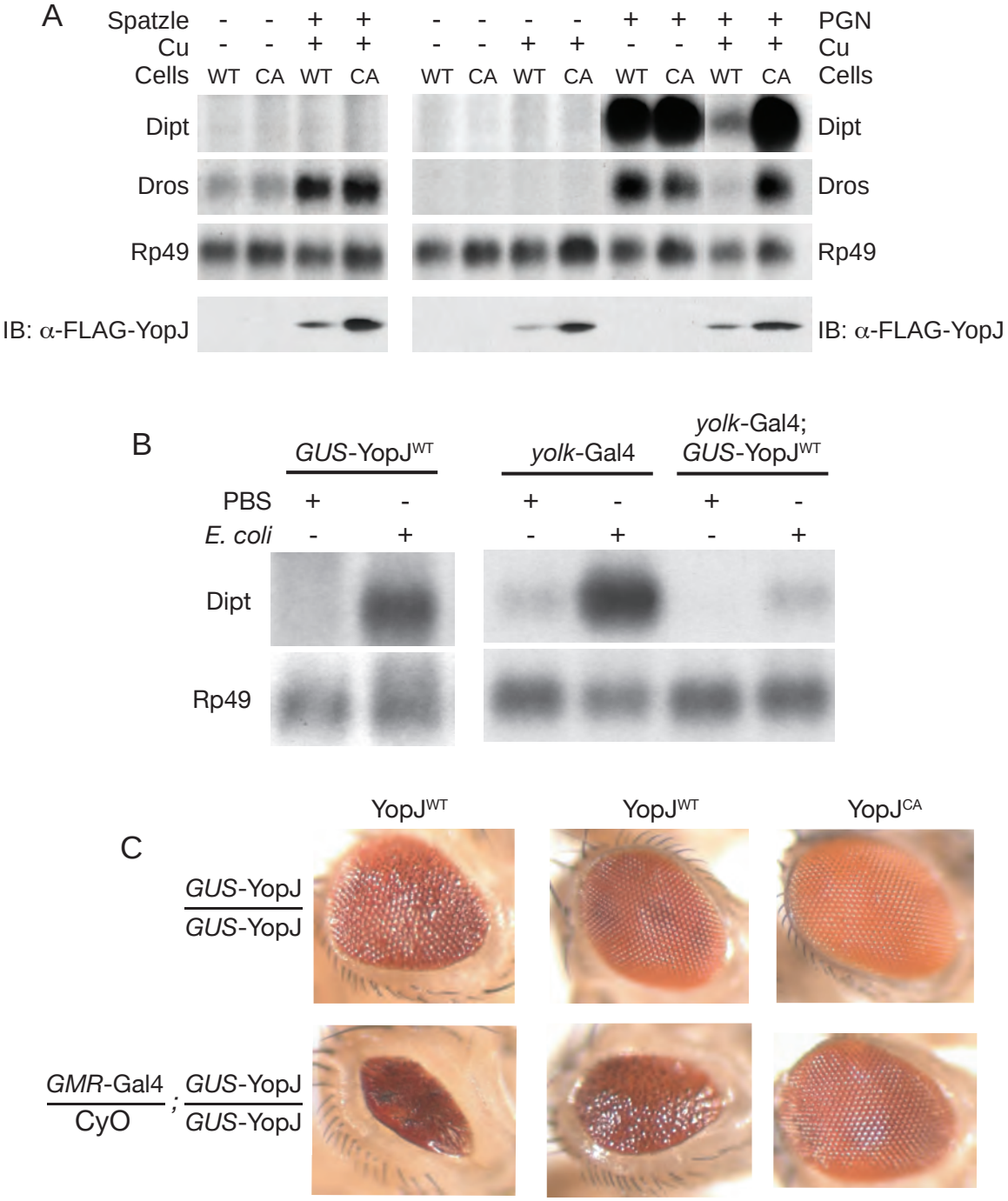
A
Spatzle
Cu
Cells
WT CA WT CA WT CA WT CA WT CA WT CA WT CA
PGN
Cu
Cells
Dipt
Dros
Rp49
IB: α-FLAG-YopJ
B
GUS-YopJWT
yolk-Gal4
yolk-Gal4; GUS-YopJWT
PBS
E. coli
Dipt
Rp49
C
YopJWT
YopJWT
YopJCA
GUS-YopJ / GUS-YopJ
GMR-Gal4 / CyO ; GUS-YopJ / GUS-YopJ

Figure 3.1 YopJ inhibits IMD but not Toll immune signaling

(A) S2* cells stably expressing YopJ^{WT} or YopJ^{CA} under control of the metallothionein promoter were pretreated with copper (to activate expression of YopJ) prior to stimulation with Spätzle (Left) or PGN (Right). Activation of immune signaling was monitored by Northern blotting of *Diptericin* and *Drosomycin* RNA. **(B)** Adult flies carrying transgenic pGUS-YopJ^{WT}, yolk-Gal4 driver, or yolk-Gal4; YopJ^{WT}, were pricked with a tungsten needle coated in either PBS or live *E. coli*. **(C)** Eyes of adult flies carrying transgenic pGUS-YopJ^{WT} or pGUS-YopJ^{CA} alone, or crossed to GMR-Gal4. Columns one and two represent two individual YopJ^{WT} insertion lines.

expression, while IMD signaling was monitored by probing for *Diptericin* (and to a lesser degree *Drosomycin*) (Figure 3.1A). Expression of YopJ had no effect on the Spätzle-induced expression of *Drosomycin,* while PGN-induced *Diptericin* and *Drosomycin* expression were dramatically inhibited. The failure to induced *Diptericin* was clearly linked to YopJ expression because $YopJ^{CA}$ was not inhibitory, and without copper pretreament *Diptericin* induction was robust. Together, these results demonstrate that YopJ is a potent inhibitor of IMD, but not Toll, signaling in *Drosophila* cells.

For studies in whole animals, we generated YopJ transgenic flies. Using the dual GMR/UAS promoter system (pGUS, Brodsky *et al*., 2000) we generated transgenic *Drosophila* which expressed wild type or mutant YopJ constitutively in the eye, and at any other location/time with appropriate Gal4 ‘drivers’. To monitor the effect of YopJ on the humoral systemic immune response, the fat body-specific *yolk*-Gal4 driver was used. After infection with live *E. coli,* control animals (female *yolk-gal4* driver flies or $YopJ^{WT}$ flies containing no Gal4 driver) showed robust IMD pathway activation as monitored by *Diptericin* RNA production. When the *yolk-gal4* driver was used to induce $YopJ^{WT}$ production in female fat bodies, IMD pathway activation was severely inhibited as seen by the reduction in *Diptericin* levels (Figure 3.1B), consistent with our cell culture data. Together these observations show that YopJ does not effect Toll signaling, yet blocks IMD signaling in both tissue culture and whole animals.

Interestingly constitutive GMR-mediated expression of YopJ^{WT} (from the pGUS transgene) in the eyes of adult flies led to the formation of a rough and reduced eye phenotype, which was not seen in YopJ^{CA} flies (Figure 3.1C). Multiple transgenic insertion lines were generated for both wild type and mutant YopJ. Although the penetrance of the rough eye phenotype varied between the YopJ^{WT} lines (as shown in Figure 3.1C, columns one and two), no phenotype was present in flies expressing YopJ^{CA}. The rough/reduced eyes found in YopJ^{WT} flies could be further enhanced by driving the higher expression of YopJ^{WT} via an additional *GMR-Gal4* driver. It is unlikely that the rough and reduced eye phenotype seen in adult *Drosophila* expressing YopJ^{WT} is due to inhibition of the IMD pathway. Unlike the Toll pathway, IMD pathway signaling is not involved in development and most IMD pathway mutants are viable to adulthood. It therefore seems likely that the developmental defects seen in YopJ^{WT} flies are a consequence of inhibition of other MAP kinase pathways important for eye development. Further work will be required in order to identify these kinases and determine if they are inhibited in a similar fashion to the IMD pathway.

Having established that YopJ^{WT} expression is sufficient to inhibit the IMD signaling pathway, we next determined the epistatic position of YopJ-mediated inhibition. Recent work by our group shows that cleavage and subsequent ubiquitination of IMD are crucial aspects of IMD pathway signaling (Chapter 2). As YopJ was proposed to act as a ubiquitin-protein protease, we examined if either of these IMD modifications were altered in stable cell lines expressing

YopJ (Sweet *et al*., 2007; Zhou *et al*., 2005). Similarly to previous experiments, addition of copper sulfate to culture media induced the expression of either $YopJ^{WT}$ or $YopJ^{CA}$ (Figure 3.2A). After stimulation with PGN comparable levels of IMD cleavage and ubiquitination were detected in both the $YopJ^{WT}$ and $YopJ^{CA}$ expressing cells in the presence or absence of copper treatment, indicating that YopJ has no effect on these upstream signaling events.

Next we examined activation of the *Drosophila* JNK kinase. Western blotting of lysates from cells expressing $YopJ^{WT}$ with anti-phospho-JNK antibody showed no phospho-JNK in these cells when stimulated with PGN, whereas JNK was phosphorylated normally in response to PGN in S2* cells and cells expressing $YopJ^{CA}$ (Figure 3.2B). Together with the inhibition of AMP gene induction, these data indicate that YopJ acts by inhibiting the IMD pathway downstream of IMD but upstream of JNK phosphorylation and Relish (NF-κB) activation. Orth and colleagues have argued that both NF-κB and JNK signaling are inhibited by YopJ by targeting different MAP2Ks for acetylation. An alternate possibility is that YopJ inhibits a protein upstream in the IMD pathway, that is required for both NF-κB and JNK activation, such as TAK1. This possibility is suggested by the reduction in the levels of phospho-IMD in cells expressing $YopJ^{WT}$ (Figure 3.2A, lane 6, middle panel). Although the function of phospho-IMD is not yet clear, our earlier work has established that it is dependent on TAK1 activity (Chapter 2).

Figure 3.2

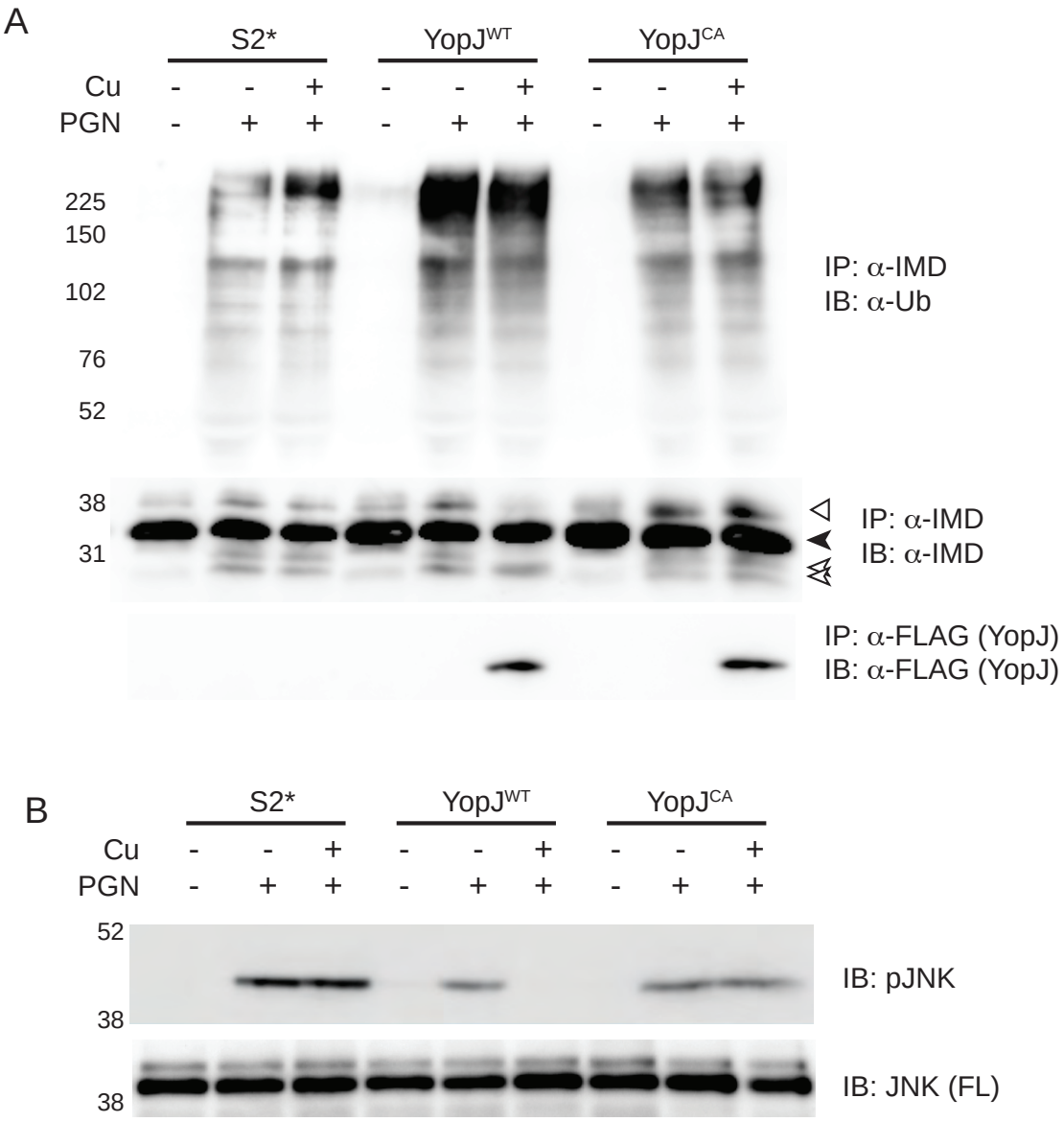
A
S2*
YopJWT
YopJCA
Cu - - + - - + - - +
PGN - + + - + + - + +
225
150
102
76
52
IP: α-IMD
IB: α-Ub
38
31
IP: α-IMD
IB: α-IMD
IP: α-FLAG (YopJ)
IB: α-FLAG (YopJ)
B
S2*
YopJWT
YopJCA
Cu - - + - - + - - +
PGN - + + - + + - + +
52
38
IB: pJNK
38
IB: JNK (FL)

Figure 3.2 YopJ functions between IMD and JNK

(A) Protein expression of YopJ^{WT} or YopJ^{CA} was induced in S2* cells prior to stimulation with PGN. Ubiquitination of IMD was monitored by IMD/ubiquitin co-immunoprecipitation. Anti-IMD blotting was used as a loading control and anti-FLAG-YopJ blot was used to verify the presence/absence of YopJ. ◀ marks unmodified full length IMD, ◁ highlights phosphorylated IMD,and ◁ marks the cleaved-IMD product **(B)** Phospho-JNK was monitored in lysates after treatment with PGN. Full length JNK blot serves as a loading control.

YopJ inhibits TAK1 activation

Hypothesizing that YopJ may be directly inhibiting the kinase TAK1, we next co-expressed both TAK1 and YopJ (WT or CA) in double stable S2* cells. In these cells, over expressed TAK1 and IKK kinase activities were monitored with IP-*in vitro* kinase assays using recombinant $MKK6^{K28A}$ (a mammalian TAK1 target) and recombinant Relish as substrates (respectively). In S2* cells, over expression of TAK1 alone was sufficient to activate the activity of both TAK1 and the downstream IKK complex (Figure 3.3A). When both TAK1 and $YopJ^{WT}$ were co-expressed, the activity of both kinases was inhibited, while co-expression of $YopJ^{CA}$ resulted in no discernible reduction in signal. Interestingly, when TAK1 was expressed alone, or in the presence of $YopJ^{CA}$ it migrated as a tight doublet at a molecular weight of approximately 100 kDa, whereas when expressed in concert with $YopJ^{WT}$ it ran slightly faster at a size of approximately 85kDa (Figure 3.3A). The predicted molecular for Drosophla TAK1 is 76 kDa. These data strongly indicated that YopJ directly interferes with the activity of TAK1 and that this interference was likely the result of some kind of post-translational modification.

In order to analyze the effect of YopJ on endogenous TAK1, IP-*in vitro* kinase assays were undertaken with a newly generated anti-TAK1 antibody. Cells expressing $YopJ^{WT}$ showed little TAK1 kinase activity above background, while cells expressing $YopJ^{CA}$ showed activity comparable to S2* cells (Figure 3.3B). These data support the results obtained with over expression of TAK1.

Figure 3.3

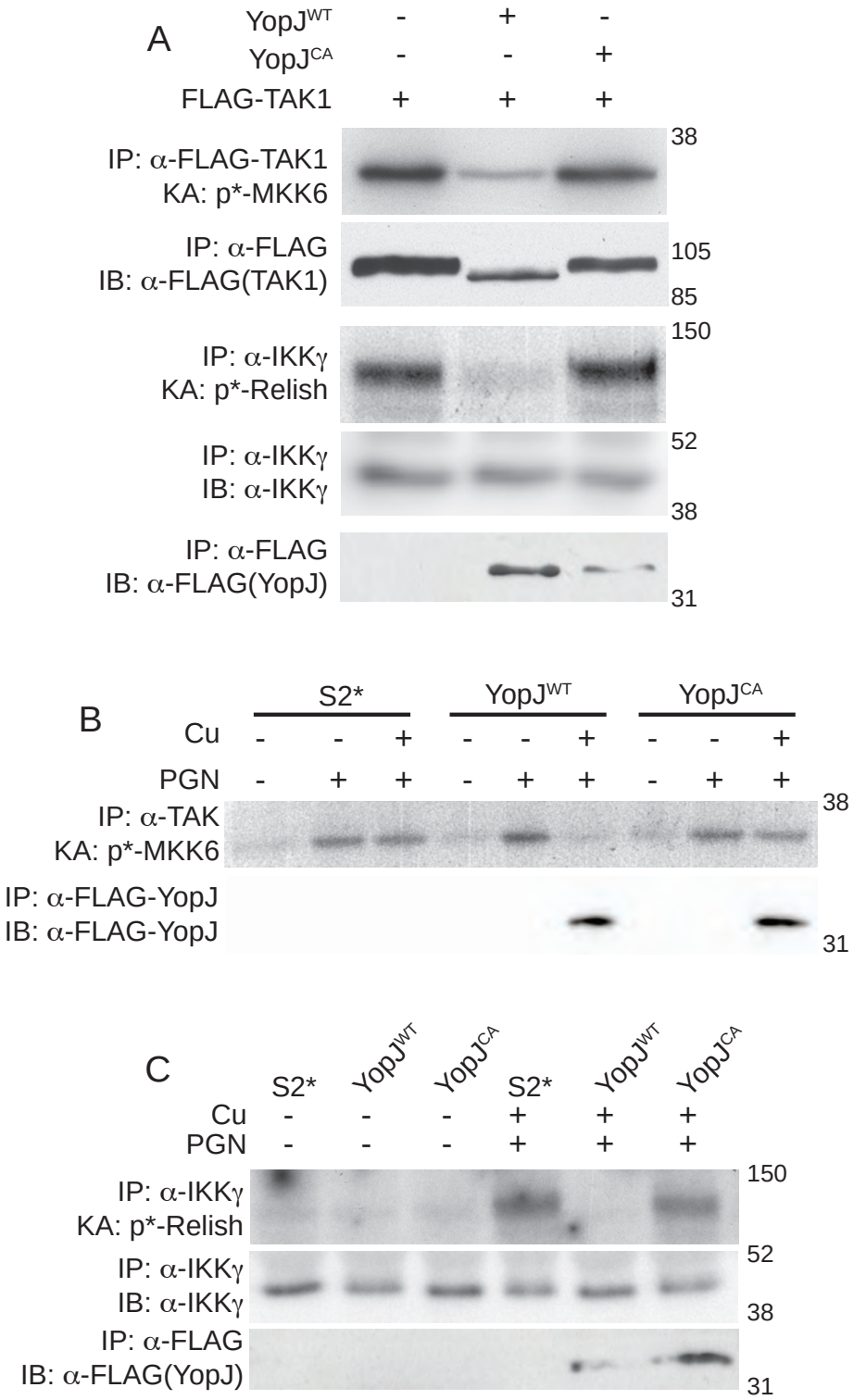
A
YopJWT - + -
YopJCA - - +
FLAG-TAK1 + + +
IP: α-FLAG-TAK1
KA: p*-MKK6
38
IP: α-FLAG
IB: α-FLAG(TAK1)
105
85
IP: α-IKKγ
KA: p*-Relish
150
IP: α-IKKγ
IB: α-IKKγ
52
38
IP: α-FLAG
IB: α-FLAG(YopJ)
31
B
S2*
YopJWT
YopJCA
Cu - - + - - + - - +
PGN - + + - + + - + +
IP: α-TAK
KA: p*-MKK6
38
IP: α-FLAG-YopJ
IB: α-FLAG-YopJ
31
C
S2*
YopJWT
YopJCA
S2*
YopJWT
YopJCA
Cu - - - + + +
PGN - - - + + +
IP: α-IKKγ
KA: p*-Relish
150
IP: α-IKKγ
IB: α-IKKγ
52
38
IP: α-FLAG
IB: α-FLAG(YopJ)
31

Figure 3.3 YopJ inhibits TAK1 kinase activity

(A) Activity of TAK1 and IKK was monitored by *in-vitro* kinase assay in S2* cells expressing metallothionein driven TAK1 with or without $YopJ^{WT}$ or $YopJ^{CA}$. Anti-FLAG (TAK1 and YopJ) and IKKγ blots serve as controls. **(B)** Activation of endogenous TAK1 was monitored in S2* cells expressing either $YopJ^{WT}$ or $YopJ^{CA}$. Anti-FLAG immunoblot serves as a control for the presence of YopJ **(C)** IKK kinase activity was monitored in S2* cells expressing $YopJ^{WT}$ or $YopJ^{CA}$ after stimulation with PGN. IKKγ blot serves as a kinase control.

Although our anti-TAK1 antibody is effective for immunopreciptiation, as monitored by endogenous TAK1 IP-kinase assays, it is not very useful for immunoblotting (data not shown) we have thus far been unable to detect endogenous TAK1 via immunoprecipitation/immunoblotting using this antibody. Therefore, we used an RNAi approach to demonstrate that the TAK1 IP-kinase assay is monitoring TAK1 acitivity. RNAi treatment targeting TAK1 was able to completely inhibit endogenous TAK1 kinase activity and accumulation of phospho-JNK after immune induction (Figure 3.4).

Consistent with YopJ mediated inhibition of endogenous TAK1 kinase activity, downstream IKK kinase activity is also absent in the presence of $YopJ^{WT}$ (Figure 3.3C). S2* cells treated with PGN show activation of IKK as monitored by and IP-*in vitro* kinase assay, with IKKγ antibody and recombinant Relish as a substrate, while expression of $YopJ^{WT}$ inhibits this activity. As expected expression of $YopJ^{CA}$ does not block the activity of IKK. Together these data show that wild type YopJ is able to inhibit the kinase activity of TAK1 and IKK after over expression of TAK1 as well as PGN induced activation. These results support the hypothesis that inhibition of TAK1, by YopJ, results in a reduction of downstream IKK activity.

TAK1 is post-translationally modified

In order to assess if the difference in TAK1 migration seen in the presence of $YopJ^{WT}$ was related to its lack of activity, we further analyzed the over

Figure 3.4

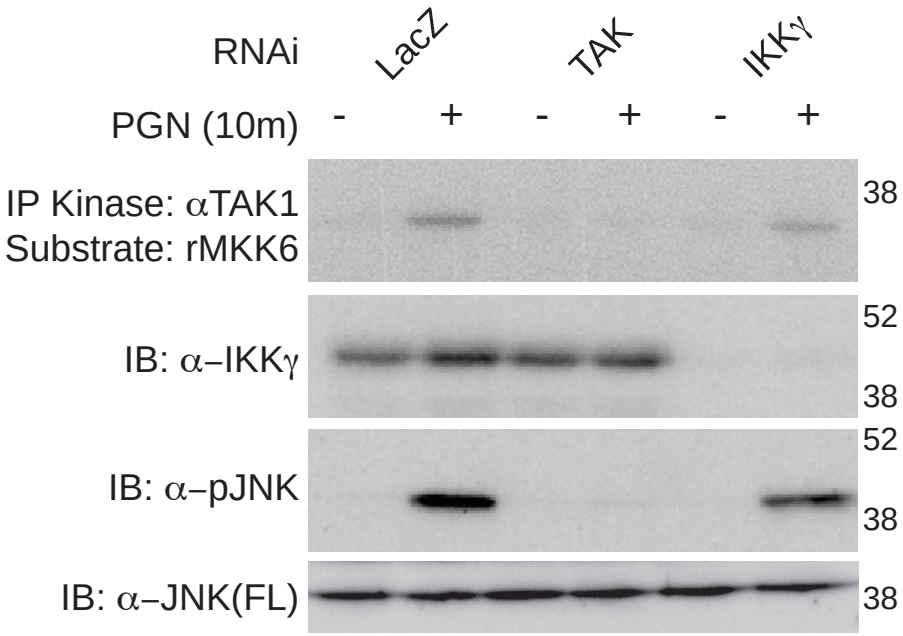
RNAi
LacZ
TAK
IKKγ
PGN (10m)
- + - + - +
IP Kinase: αTAK1
Substrate: rMKK6
38
IB: α–IKKγ
52
38
IB: α–pJNK
52
38
IB: α–JNK(FL)
38

Figure 3.4 Endogenous TAK1 kinase assay

Endogenous TAK1 kinase activity was monitored after treatment with RNAi to IMD pathway kinases prior to PGN stimulation. Anti-IKKγ blot serves as a control for IKKγ RNAi efficiency. Anti-phospho-JNK and FL-JNK blots serves as a control for TAK1 activity.

expressed FLAG-TAK1 protein. When optimized for higher resolution, immunoblot analysis showed that over expressed TAK1 alone, or TAK1 in the presence of YopJ^{CA} actually migrates as a doublet at approximately 95 and 105kDa while in the presence of YopJ^{WT} TAK1 runs faster at a lower molecular weight of approximately 85kDa (Figure 3.5A). When activated, mammalian TAK1 is auto-phosphorylated at three phospho-acceptor sites in its activation loop (Sakurai *et al*., 2000; Kishimoto *et al*., 2000). In order to determine if the observed *Drosophila* TAK1 bands represented phosphorylation events, we treated lysates expressing TAK1 in the presence or absence of YopJ with λ-protein phosphatase. When treated with λ-protein phosphatase the doublets observed in the TAK1 alone and TAK1 with YopJ^{CA} samples changed from approximately 95/105kDa to approximately 85/93kDa. In the presence of YopJ^{WT} however we found no change in the migration of TAK1 was detected (Figure 3.5B). These data indicate that active TAK1, (when expressed alone or with the inactive YopJ^{CA}) is phosphorylated, however no phosphorylation is present on TAK1 when co-expressed with YopJ^{WT}.

An alignment of *Drosophila* and mammalian TAK1 shows that three phospho-acceptor sites found in the activation loop of mammalian TAK1 (T184, T187, and S192) as well as the surrounding residues are all highly conserved in *Drosophila* TAK1 (Figure 3.5C). In mammals, mutations to any of these three residues to alanine is sufficient to ablate the activity of the protein and block downstream signaling (Yu *et al*., 2008; Prickett *et al*., 2008; Qiao *et al*., 2005). In

Figure 3.5

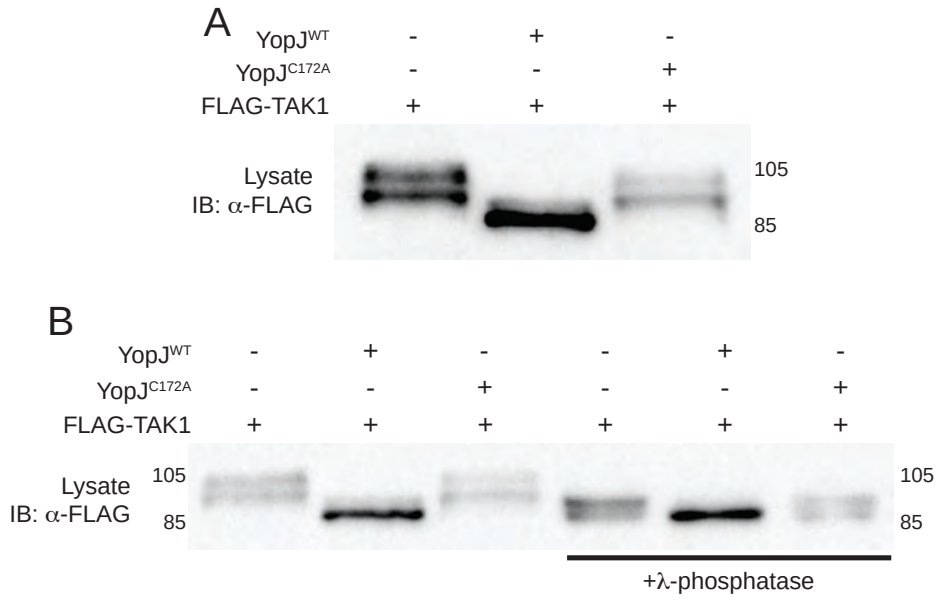
A
YopJWT - + -
YopJC172A - - +
FLAG-TAK1 + + +
Lysate
IB: α-FLAG
105
85
B
YopJWT - + - - + -
YopJC172A - - + - - +
FLAG-TAK1 + + + + + +
Lysate
IB: α-FLAG
105
85
105
85
+λ-phosphatase
C
hTAK1 175-DFGTACDIQTHMTNNKGSAAWMAPEV-200
dTAK1 159-DFGTVADKSTMMTNNRGSAAWMAPEV-184
D
dTAK1 159-DFGTVADKSTMMTNNRGSAAWMAPEV-184
dTAK1+YopJWT 159-DFGTVADKSTMMTNNRGSAAWMAPEV-184
dTAK1+YopJCA 159-DFGTVADKSTMMTNNRGSAAWMAPEV-184

Figure 3.5 YopJ acetylates TAK1

(A) High resolution anti-FLAG immunoblot of S2* cells over expressing FLAG-TAK1 in the presence of $YopJ^{WT}$ or $YopJ^{CA}$. **(B)** Anti-FLAG (TAK1) immunoblot of lysates from S2* cells expressing FLAG-TAK1 alone or in the presence of $YopJ^{WT}$ or $YopJ^{CA}$, were treated (or not) with λ-phosphatase. **(C)** Alignment of human and *Drosophila* TAK1 activation loops. Residues of mammalian TAK1 known to be phosphorylated are indicated (P). Conserved residues are boxed in grey. **(D)** Summary of MS/MS peptide analysis of *Drosophila* TAK1 activation loop. Phosphorylated (P) and acetylated (Ac) residues are indicated. A table containing all phospho-peptide and acetyl-peptide residues can be found in Supplemental Table 3.1. In both **(C)** and **(D)** conserved residues are boxed in grey.

order to confirm the phosphorylation of *Drosophila* TAK1 and determine which residues where phosphorylated, FLAG-TAK1 was isolated and prepared from samples containing over expressed TAK1 alone, with YopJ^{WT} or with YopJ^{CA}. These samples were then subjected to microcapillary reverse-phase HPLC nano-electrospray tandem mass spectrometry (MS/MS).

YopJ acetylates TAK1.

MS/MS peptide analysis identified a single phosphorylation in the activation loop of *Drosophila* TAK1, at S176 which aligns to S192 of the mammalian protein, when TAK1 was expressed alone or in the presence of YopJ^{CA}, (Figure 3.5D). A number of other phosphorylation sites were found outside the activation loop (see Table 3.6 for the full list of phospho-residues). Interestingly, no phosphorylation was seen in the activation loop of TAK1 when co-expressed with YopJ^{WT} and overall, phosphorylation as a whole was greatly reduced. Given that YopJ is thought to act as a serine/threonine acetyl transferase, TAK1 samples were then analyzed for acetylation. In the presence or absence of YopJ^{CA}, TAK1 displayed no detectible acetylation (see Table 3.6 for full list of acetyl-residues). However, in the presence of YopJ^{WT}, TAK1 showed remarkably heavy acetylation of both T168 and T171, which align to the critical threonines of the mammalian TAK1 activation loop, with minor acetylation of S167 and S176.

Table 3.6

MS/MS TAK1 Phospho-Residues

TAK Alone	TAK + YopJWT	TAK +YopJCA
S176	T149*	S65
S314	Y262*	S110
T321	S639*	S116
S390		T149
T394**		S176
S395**		S208
S396**		S307
S433*		S314
		T321
		Y369*
		T372*
		S390
		T394**
		S395**
		S396**
		S433

MS/MS TAK1 Acetyl-Residues

TAK Alone	TAK + YopJWT	TAK +YopJCA
None detected	S167*	None detected
	T168	
	T171	
	S176*	

Table 3.6 MS/MS TAK1 phospho- and acetyl-residues

A complete list of all phospo- (Top) and acetyl- (Bottom) residues identified in *Drosophila* TAK1. Complete data set is available upon request.

* Residues that require validation to determine modification

** Proximal serines and threonines of which one or more is phosphorylated but the data needs to be validated to distinguish the exact position

Predicting that phosphorylation of serine 176 of *Drosophila* TAK1 is critical for kinase activation we generated a TAK1^{S176A} mutant under the control of the metallothionein promoter. As shown previously, over expression of wild type TAK1 is sufficient to activate TAK1 kinase activity as monitored by IP-*in vitro* kinase activity. Over expression of TAK1^{S176A} however was unable to drive kinase activity (Figure 3.7A). Immuno-blotting showed that TAK1^{S176A} migrated slightly faster than wild type TAK1 at a molecular weight of approximately ~85kDa. To determine if this shift was the result of lack of phosphorylation, lysates expressing wild type TAK1 or TAK1^{S176A} were subjected to λ-protein phosphatase treatment. Wild type TAK1 samples migrated as a smear at approximately 95-105kDa, consistent with previous data (Figure 3.7B and 3.5A). When treated with λ-phosphatase this band collapsed to approximately 85kDa as seen previously (Figure 3.5B). Strikingly, TAK1^{S176A}, migrated at approximately 85kDa with and without λ phosphatase treatment indicating that the protein is not phosphorylated. These data demonstrate that phosphorylation of *Drosophila* TAK1 at serine 176 is required for kinase activation and acetylation of threonines 168 and T171 (and to a lesser degree serines 176 and 192) by YopJ block this phosphorylation rendering the kinase inactive.

Discussion

Data obtained from mammalian systems and a number of *in vitro* experiments, have identified the MAP2 kinase family, particularly the IKK

Figure 3.7

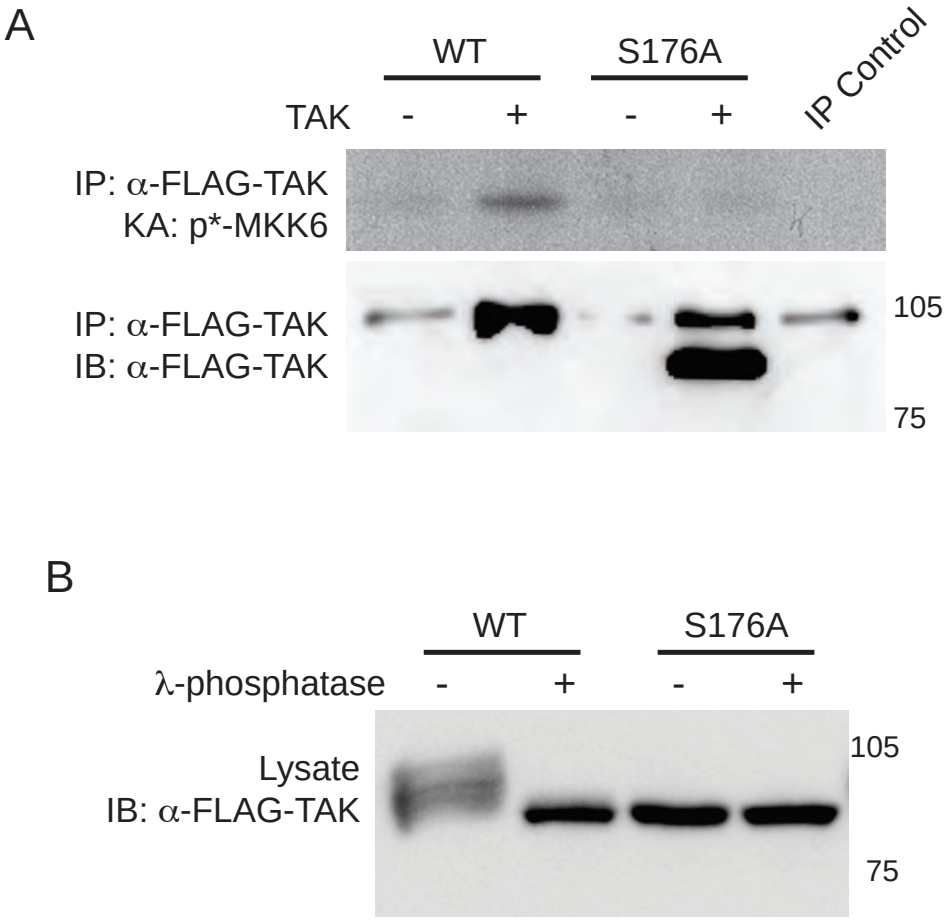
A
WT
S176A
IP Control
TAK
-
+
-
+
IP: α-FLAG-TAK
KA: p*-MKK6
IP: α-FLAG-TAK
IB: α-FLAG-TAK
105
75
B
WT
S176A
λ-phosphatase
-
+
-
+
Lysate
IB: α-FLAG-TAK
105
75

Figure 3.7 TAK1 S176A is required for kinase activation

(A) TAK1 Kinase activity was monitored in S2* cells over expressing wild type TAK1 or TAK1^{S176A} by *in-vitro* kinase assay. Anti-FLAG (TAK1) blot serves as a control. **(B)** Lysates from cells over expressing either wild type TAK1 or TAK1^{S176A} were treated with λ-phosphatase prior to SDS-PAGE.

complex, as the major target for YopJ mediated inhibition of NF-κB signaling via serine/threonine acetylation (Mittal *et al*., 2006; Mukherjee *et al*., 2006). The data presented here however shows that and additional target, the *Drosophila* MAP3 kinase TAK1, is also a potent target of the YopJ protein. We show that expression of YopJ is able to inhibit IMD, but not Toll, innate immune signaling. Inhibition of IMD pathway signaling by YopJ inhibits the activity of both TAK1 and IKK kinases after activation by both PGN stimulation or over expression of TAK1, while upstream events, such as IMD cleavage and ubiquitination, remain unaffected. YopJ also acetylates multiple serine and threonine residues in the TAK1 activation loop. This acetylation prevents the phosphorylation of TAK1 at serine 176, an event which is vital for activity of the kinase. We therefore conclude that TAK1 is a target of YopJ mediated inhibition by acetylation of critical activation-loop phosphorylation sites. Since TAK1 belongs to the broader class of MAP3 kinases, this work raises the possibility that YopJ may target other MAP3 kinases as well.

Consistent with the notion that YopJ may target other MAP2/3 kinases (perhaps outside the realm of immune signaling) transgenic flies expressing $YopJ^{WT}$ in the eye show a rough and reduced eye phenotype. IMD signaling is not implicated in development, thus this phenotype can not be attributed to interfering with immune signaling pathways. Instead, one or more developmentally relevant MAP2/3 kinases are also likely to be inhibited by YopJ and account for the eye phenotype. Further work will be required to determine

the precise identity of these proteins and the mechanism of YopJ's action upon them.

We believe that our data utilizing the *Drosophila* model system has three advantages over that previously described. First this work was undertaken exclusively in live cells or animals, an approach that because of the pro-apoptotic nature of YopJ has proven difficult within the context of a mammalian model. Utilizing the strong on/off *Drosophila* metallothionein promoter system, we have developed stable YopJ inducible cell lines, which provide better protein expression and greater overall consistency. Secondly, in order to study the function of YopJ, previous groups were forced to purify proteins separately and examine artificial interactions *in vitro* in the presence of massive amounts of acetyl-CoA. This method is subject to non-physiologically relevant artifacts, that may obscure accurate biochemical analysis. In our work, the proteins analyzed by MS/MS were produced and isolated from live cells, and represent a more physiologically relevant context. Lastly, the identity of TAK1 as the target for YopJ mediated inhibition seems more in line with the observations regarding the activity of YopJ (Mittal *et al*., 2006; Mukherjee *et al*., 2006). Targeted inactivation of TAK1/MAP3 kinases would allow for a much broader and more efficient method of immune pathway inhibition. Perhaps in concert with inhibition of MAP2 kinases, YopJ is able to effectively inhibit immune pathways in both mammals and insects.

Materials and methods

RNA analysis

Total RNA was isolated with the TRIzol reagent (Invitrogen) as previously described (Silverman *et al*., 2000) and expression of *Diptericin* and *Rp49* was analyzed by Northern blot analysis followed by autoradiography.

Protein and immunoprecipitation assays

S2* cells were lysed in buffer (10% glycerol, 1% Triton X-100, 20mM Tris, 150mM NaCl, 25mM β-glycerolphosphate, 2mM EDTA, 1mM DTT, 1mM Sodium Orthovanadate, 1X Protease Inhibitor Cocktail). For total protein analysis, 50-100µg of total protein were prepared as previously described (Kaneko *et al*., 2006) and immunoblotted with anti-FLAG-M5 (Sigma), anti-pJNK (Santa Cruz), anti-JNK(FL) or anti-IKKγ or anti-IMD. In order to optimize visualization of TAK1 10ug of total protein were run on an 8% SDS-PAGE minigel for 90 minutes at 140v. For immunoprecipitations, 600µg of total protein were precipitated with anti-IMD antisera in the presence of protein A agarose overnight at 4°C. Pellets were then washed twice in lysis buffer and prepared for SDS-PAGE. Samples were then analyzed by SDS-PAGE. 1/10 of the reaction use for blotted with anti-IMD antisera (as a loading control), while the remaining sample used for blotting with anti-Ubiquitin antibody (Santa Cruz).

Kinase assays

Activity of kinases was assayed as previously described (Silverman *et al*., 2000; Wang *et al*., 2001). Briefly, cultured S2* cells or S2* cells stably

transfected with inducible metallothionein FLAG-TAK1 were pretreated with 1µM 20-hydroxyecdysone for 24-48 hours. For FLAG-TAK1 assays, cells were pretreated with copper (500µM $CuSO_4$ for 4 hour). For endogenous TAK1 assays, cells were stimulated with *E. coli* peptidoglycan (100ng/ml) (or not) for 10 minutes. Cells were lysed in 100µl/ml of lysis buffer (10% glycerol, 1% Triton X-100, 20mM Tris, 150mM NaCl, 25mM β-glycerolphosphate, 2mM EDTA, 1mM DTT, 1mM Sodium Orthovanadate, 1X Protease Inhibitor Cocktail), and kinases were immunoprecipitated with appropriate antibodies for 2-3 hours at 4°C; 75µg of total protein was used to precipitate FLAG-TAK1 with anti-FLAG M2 Agarose (Sigma), 75µg of total protein for endogenous TAK1 with anti-TAK1 antisera and 50µg of total protein for IKK with anti-IKKγ. Immunoprecipitated kinases were washed 2 times with 500µL of lysis buffer and 2 times 500µL with kinase reaction buffer (200mM HEPES, 200mM β-glycerolphosphate, 100mM $MgCl_2$, 500mM NaCl, 10mM DTT, 1mM Sodium Orthovanadate). Kinases were then added to 10µL of kinase reaction buffer containing 200µM cold ATP, 1µL $^{32\gamma}$P*-ATP, and substrate (1ug rMKK6-K28A for TAK1 KA, or 50ng rRelish for IKK KA). Kinase reactions were incubated at 30°C for 30 minutes and run on SDS-PAGE. SDS-PAGE gels were then fixed, dried, and autoradiographed.

MS/MS peptide analysis

FLAG-TAK1 was immunoprecipitated from S2* cell via anti-FLAG (Sigma) as previously described. Samples were washed, run on SDS-PAGE and gels were

fixed and stained with coomassie brilliant blue. FLAG-TAK1 bands were isolated from these gels and sequence analysis was performed at the Harvard Microchemistry and Proteomics Analysis Facility by microcapillary reverse-phase HPLC nano-electrospray tandem mass spectrometry (µLC/MS/MS) on a Thermo LTQ-Orbitrap mass spectrometer.

PREFACE TO CHAPTER IV

This chapter is under revision in preparation for resubmission:

Alain C Jung*, Vanessa Gobert*, Rui Zhou[$], **Nicholas Paquette[$]**, Sophie Rutschmann, Marie-Claire Criqui, Marie-Céline Lafarge, Matthew Singer, David A Ruddy, Tom Maniatis, Jules A Hoffmann, Neal Silverman, Dominique Ferrandon, *Analysis of Drosophila TAB2 mutants reveals that IKK, but not JNK pathway activation, is essential in the host defense against Escherichia coli infections*.

*,[$] These authors contributed equally to this work

Nicholas Paquette generated and performed all experiments examining TAB2 RNAi

Nicholas Paquette and Neal Silverman assisted in writing of the manuscript.

CHAPTER IV

Analysis of *Drosophila TAB2* mutants reveals that IKK, but not JNK pathway activation, is essential in the host defense against *Escherichia coli* infections.

Abstract

We show that the *Drosophila TAK1 binding protein 2* (DmelTAB2) gene is required for the host defense against Gram-negative bacteria. In the IMD pathway, DmelTAB2 functions as an adaptor for TAK1, which activates both the JNK and the IKK/NF-κB pathways. Multiple mRNAs are transcribed from *DmelTAB2*. The longer isoform, which encodes the predicted full length protein, is dispensable for IKK/NF-κB signaling but is essential for JNK pathway activation. In contrast, mutations that disrupt all predicted DmelTAB2 isoforms affect both JNK and IKK signaling. Mutant flies that express only the shorter DmelTAB2 isoform are resistant to an *E. coli* challenge despite defective JNK pathway activation, whereas mutants that affect all forms of TAB2 are susceptible to infection. We conclude that the activation of the JNK pathway does not play an essential role in the *Drosophila* host defense against *E. coli* infections, while *DmelTAB2* is critical for NF-κB activation and antimicrobial peptide gene induction.

Introduction

Drosophila melanogaster is a strong model to study the role of innate immunity in the host defense. In addition to its powerful genetics, *Drosophila* lack an adaptive immune response. Thus, a phenotype of sensitivity to infections can be directly correlated with a reduced immune response. Once invading microorganisms are detected by appropriate Pattern Recognition Receptors (PRRs), two distinct NF-κB pathways are activated in the fat body, a functional equivalent of the mammalian liver (Hoffmann, 2003). The Toll pathway is required in the host defense against fungal and Gram-positive bacterial infections. It controls the activation of the NF-κB factor Dorsal-Related Immune Factor (DIF) through the destruction of its inhibitor, the IκB-like Cactus. This allows for DIF nuclear translocation, and the transcription of hundreds of genes, including those encoding the potent antifungal peptides Drosomycin and Metchnikowin. A second pathway, the Immune Deficiency (IMD) pathway, plays a major role in the response to Gram-negative infections. Following the stimulation of its microbial receptors PGRP-LC and PGRP-LE, the IMD pathway activates another NF-κB transcription factor, Relish, whose composite structure is evocative of that of mammalian p100 and p105 Rel precursors (Choe *et al*., 2002; Gottar *et al*., 2002; Hedengren *et al*., 1999; Kaneko *et al*., 2006; Leulier *et al*., 2003; Ramet *et al*., 2002). Relish is processed by a signal-dependent cleavage event, followed by the nuclear translocation of the N-terminal Rel domain, while the ankyrin repeat containing domain remains cytoplasmic (Stöven

et al., 2000). Relish activates the transcription of many target genes including those encoding the antibacterial peptides Diptericin and Drosocin, as well as Defensin, Cecropin, and Attacin. The Toll and IMD pathways jointly control the expression of the latter genes.

Downstream of the receptor proximal adaptor IMD two signaling pathways appear to converge on Relish and are both required for its full cleavage and activation. One pathway leads to phosphorylation of Relish via the DmelIKK complex. The second pathway, requiring the caspase DREDD, is required for Relish cleavage. DREDD is recruited into a complex with IMD through the adaptor protein FADD (Elrod-Erickson *et al*., 2000; Georgel *et al*., 2001; Hu and Yang, 2000; Leulier *et al*., 2000; Leulier *et al*., 2002; Naitza *et al*., 2002). Yet, it remains to be established whether DREDD directly cleaves Relish (Stöven *et al*., 2003). IKK complex activation is dependent on the Mitogen-activated Protein Kinase kinase kinase (MAP3K) TAK1, which also functions downstream of IMD (Silverman *et al*., 2003; Vidal *et al*., 2001; Zhou *et al*., 2005). Interestingly, cell-based experiments have revealed a second distinct function of the DREDD/ FADD complex in that it is also required for the activation of the IKK complex upstream of TAK1 and downstream of IMD (Zhou *et al*., 2005, Chapter 2).

Stimulation of the IMD pathway, either in flies or in S2 cell culture, also leads to the immediate and short-lived activation of the Jun kinase pathway (JNK) (Boutros *et al*., 2002; Park *et al*., 2004). The bifurcation takes place at the level of TAK1, which thus plays a dual role in JNK and IKK activation (Boutros *et*

al., 2002; Silverman *et al*., 2003). Interestingly, the TNF-like molecule Eiger induces the JNK pathway through TAK1 and possibly the MAP4K Misshapen and TRAF1 (Geuking *et al*., 2005). Thus, TAK1 appears to be at the intersection of these pathways, although it is not clear whether they function in the same tissues since Eiger is predominantly expressed in the nervous system (Igaki *et al*., 2002), whereas IMD activation essentially takes place in the fat body during a systemic infection.

We have undertaken a large scale genetic analysis of the *Drosophila* humoral immune response through Ethyl Methane Sulfonate (EMS) saturation mutagenesis of the second chromosome of *Drosophila melanogaster*, which represents 40% of the fly genome. We have previously reported the mutant phenotypes of *Dif* and *kenny* (Rutschmann *et al*., 2000a; Rutschmann *et al*., 2000b). Here, we report the isolation and characterization of null alleles of *galere* (*glr*), which maps to the *TAB2* locus. We find that mutant alleles of this locus can be grouped in two categories with strikingly distinct phenotypic properties depending on which TAB2 isoform is affected.

Results

Phenotype of *galere* mutant flies

We generated 27000 mutant fly lines by EMS mutagenesis and screened for those that failed to induce a *Diptericin-LacZ* reporter gene in response to an immune challenge with a mix of Gram-negative (*Escherichia coli*) and Gram-

positive (*Micrococcus luteus*) bacteria (Jung *et al*., 2001). Complementation analysis ascribed three lines to a new locus that we named *galere* (*glr*). Northern blot analysis confirmed that *Diptericin* expression was strongly decreased in *glr* flies after infection (Figure 4.1A). In addition, the expression level of other antibacterial peptide genes were either strongly (*Cecropin, Defensin*, Figure 4.1D&G) or partially decreased (*Drosocin, Attacin* Figure 4.1 B&C). Induction of the antifungal peptide gene *Drosomycin*, which is mostly dependent on the Toll pathway, was not altered in *glr* mutants (Figure 4.1F). Finally, *Metchnikowin* expression levels were not affected six hours after challenge, but we observed a mild decrease of its expression in *glr* mutants after 48 hours (Figure 4.1E), which is reminiscent of results obtained with *kenny* mutants (Rutschmann *et al*., 2000b). A noticeably dissimilar induction of *Diptericin* and *Drosocin* was observed in the *glr* mutants, which is not the case in other mutants affecting the IMD pathway.

We next examined the survival of wild-type and *glr* flies following infections with selected microorganisms. As illustrated in Figure 4.2A and B, the three *glr* mutant lines resisted fungal (*Beauveria bassiana*) and Gram-positive bacterial (*Enterococcus faecalis*) challenges like wildtype flies, indicating that the *glr* gene is not required for the host defense against these infections. In contrast, all three lines were sensitive to infection with *E. coli* (Figure 4.2C-E), less so than *kenny* flies. Furthermore, they died at the same intermediate rate as hypomorphic imd^{1} mutants, whereas null *imd* mutants succumbed more rapidly to this challenge

Figure 4.1

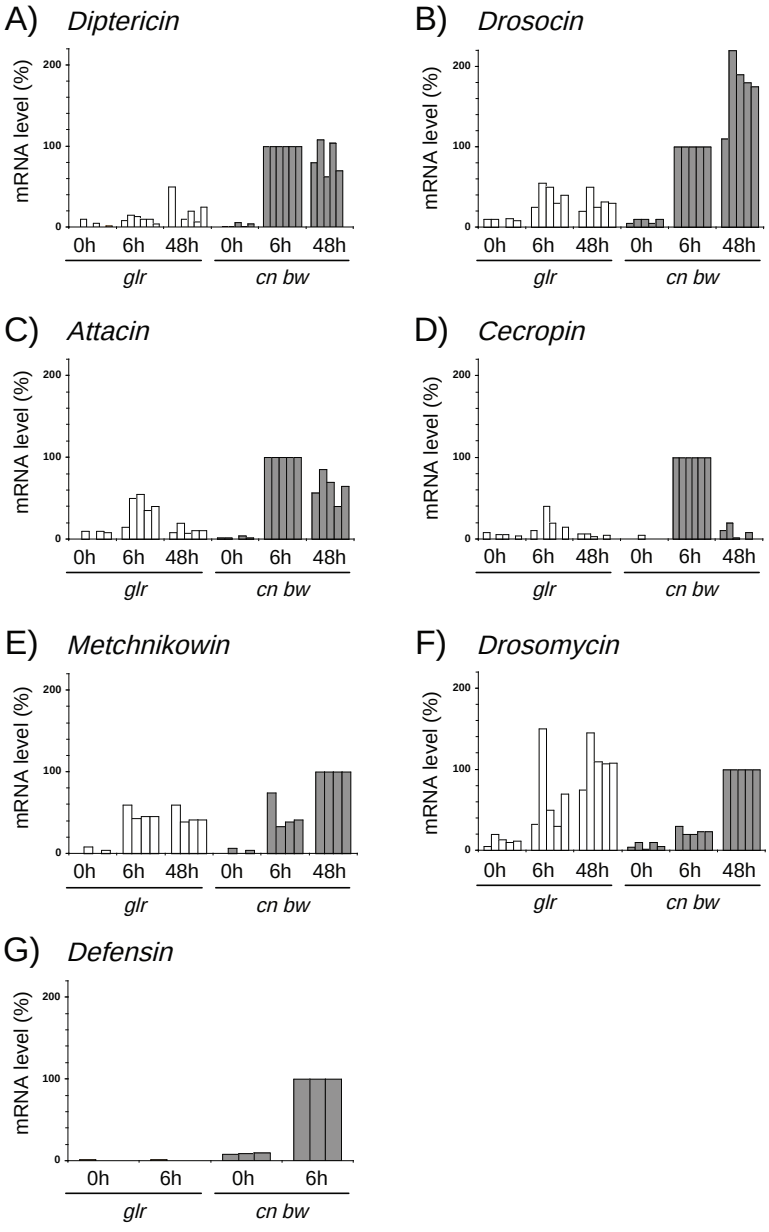
A) Diptericin
B) Drosocin
C) Attacin
D) Cecropin
E) Metchnikowin
F) Drosomycin
G) Defensin
mRNA level (%)
0
100
200
0h
6h
48h
glr
cn bw

Figure 4.1 The expression of antibacterial peptide genes is reduced in *galere* mutants

Quantification of Northern blot analysis of *galere* (*glr*) and wild-type *cn bw* flies, 0, 6 or 48 hours after challenge with a mix of Gram-positive (*M. luteus*) and Gram-negative (*E. coli*) bacteria. *cn bw* samples were used as 100% references at 6 or 48 hours, according to the kinetics of antimicrobial peptide gene expression. Each bar in a series corresponds to one independent Northern blot. **(A, D, G)** *Diptericin*, *Cecropin* and *Defensin* genes expression is drastically reduced in a *glr* background. Note that in some experiments, *Diptericin* mRNA levels in the *glr* mutants were higher at 48 hours than at six hours after infection, an observation that we had consistently made with the imd^{1} hypomorphic mutant (AJ, SR, unpublished observations). **(B, C)** Significant *Drosocin* and *Attacin* expression can be detected in *glr* flies. **(F)** *Drosomycin* expression is normal, whereas a mild decrease of *Metchnikowin* expression was observed 48 hours after induction **(E)**, as previously reported for *kenny* mutants.

Figure 4.2

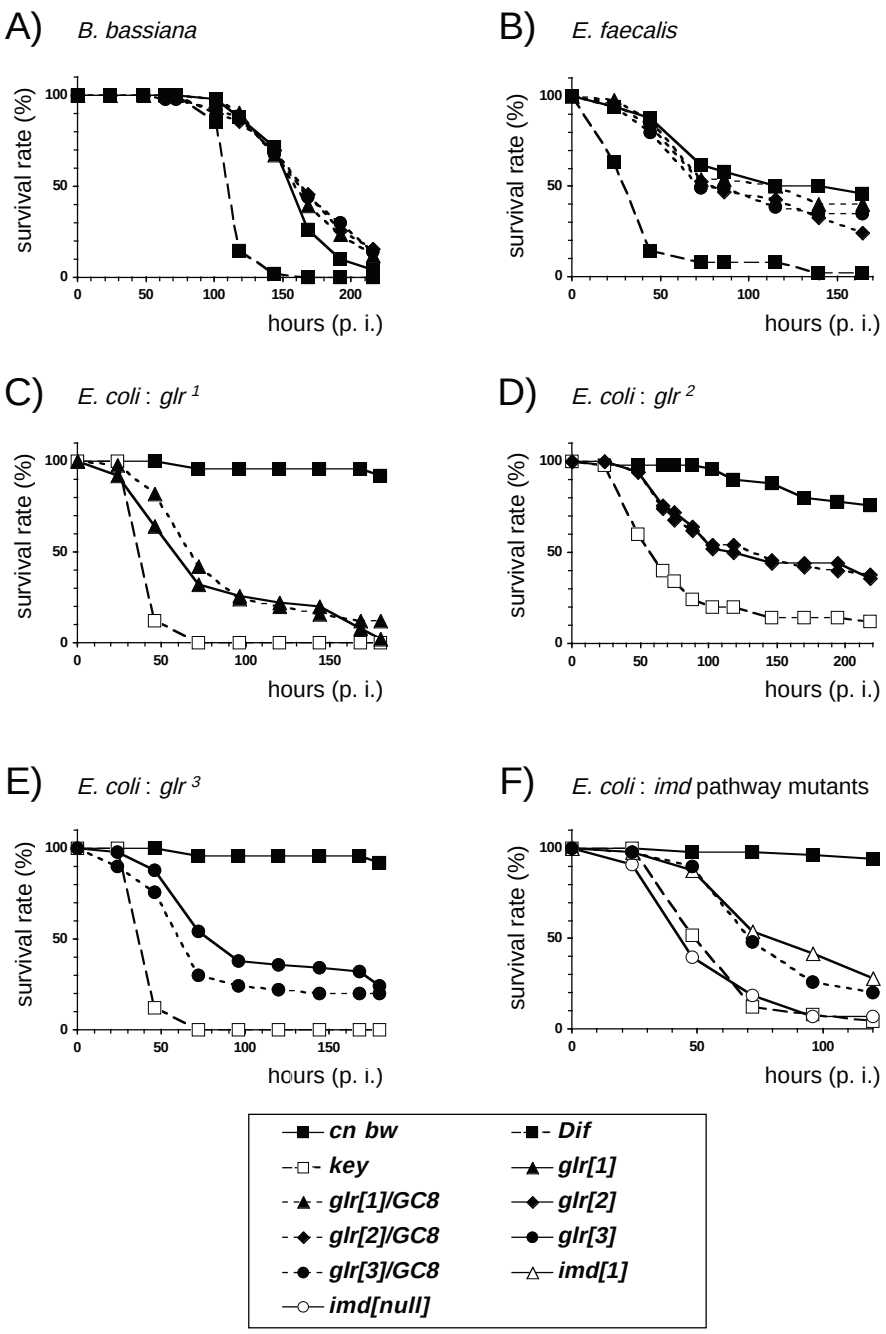
A) B. bassiana
B) E. faecalis
C) E. coli : glr 1
D) E. coli : glr 2
E) E. coli : glr 3
F) E. coli : imd pathway mutants
survival rate (%)
hours (p. i.)
cn bw
Dif
key
glr[1]
glr[1]/GC8
glr[2]
glr[2]/GC8
glr[3]
glr[3]/GC8
imd[1]
imd[null]

Figure 4.2 *galere* mutants are sensitive to Gram-negative bacterial infections

(A, B) *glr* mutants resist like wild-type to natural fungal (*Beauveria bassiana*) or Gram-positive bacterial (*Enterococcus faecalis*) infections ; *Dif* mutant flies succumb to these infections as expected. **(C-E)** Mutants for the three *glr* alleles are susceptible to Gram-negative bacterial infections, both in homo- or hemizygous conditions. **(F)** Although genetically null, *glr* mutant alleles display an intermediate sensitivity to Gram-negative bacterial infections, similar to that of the hypomorphic allele imd^{1}. *cn bw* : wild-type background control for the *glr*, *Dif* and *kenny* (*key*) mutants ; *GC8* : *Df(2R)GC8*, deficiency that uncovers the *glr* locus.

(Figure 4.2F). This intermediate sensitivity phenotype may be the consequence of the partial decrease of the induction of antimicrobial peptide (AMP) genes (Figure 4.1). An hypomorphic (non null) effect of the *glr* alleles may account for this mild phenotype. If this were the case, one would expect that hemizygous flies carrying one copy of the mutant allele and one deficiency chromosome devoid of the entire *glr* locus would display an increased sensitivity to infection compared to homozygous *glr* flies. However, the survival rates of homozygous (*glr/glr*) and hemizygous (*glr/Deficiency*) flies were nearly indistinguishable (Fig 4.2 C-E), indicating that the three *glr* alleles are genetic nulls.

galere is required in the IMD signal transduction pathway

Relish binds and activates the *Diptericin* promoter. Incubation of extracts from wild-type immune-challenged flies with a radiolabeled *Diptericin* promoter probe revealed a major retarded band that is absent when a mutant κB-site probe was used (Figure 4.3A). As for *imd*^{1}, *kenny*, and *Relish* mutants, this band is drastically reduced in extracts from challenged *glr* mutant flies. These data indicate that GLR is required in the IMD pathway to activate the Relish transcription factor. Moreover, the over expression of the *imd* gene using the Gal4-UAS system, which leads to the challenge-independent induction of *Diptericin* expression as previously reported (Figure 4.3B) (Georgel *et al*., 2001) was abolished in a *glr* mutant background. Similar results were obtained when

Figure 4.3

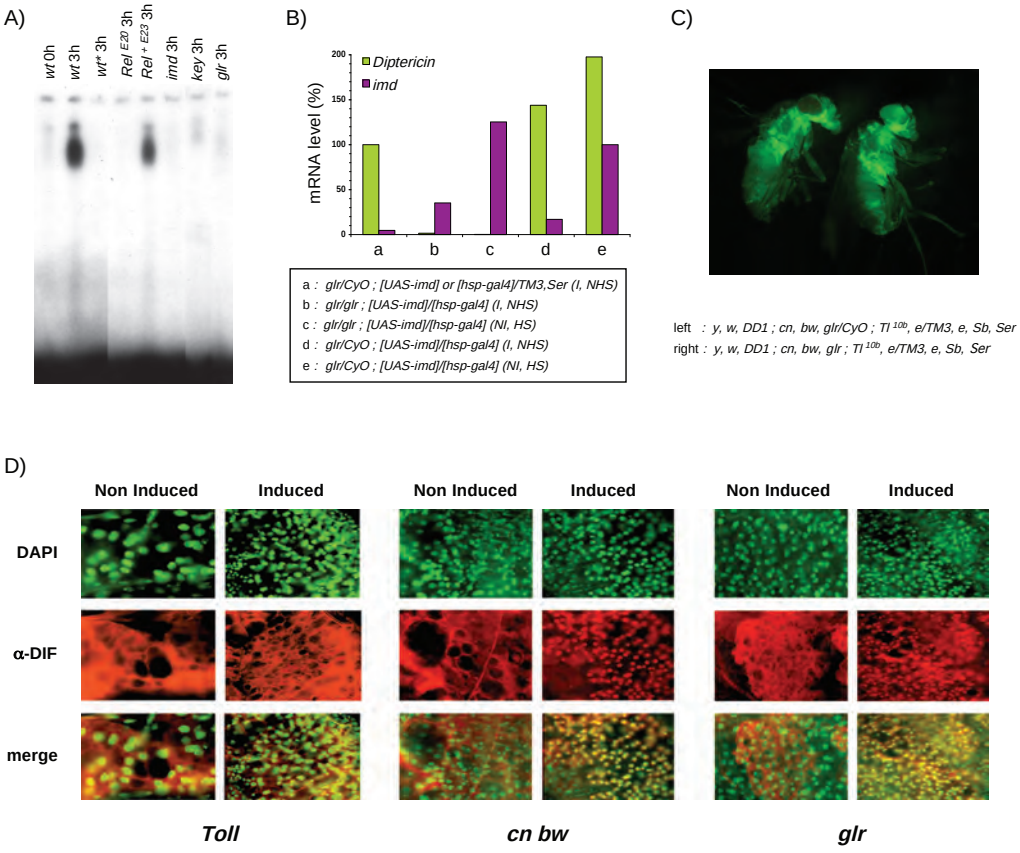
A)
wt 0h
wt 3h
wt* 3h
Rel E20 3h
Rel + E23 3h
imd 3h
key 3h
glr 3h
B)
Diptericin
imd
mRNA level (%)
200
150
100
50
0
a
b
c
d
e
a : glr/CyO ; [UAS-imd] or [hsp-gal4]/TM3,Ser (I, NHS)
b : glr/glr ; [UAS-imd]/[hsp-gal4] (I, NHS)
c : glr/glr ; [UAS-imd]/[hsp-gal4] (NI, HS)
d : glr/CyO ; [UAS-imd]/[hsp-gal4] (I, NHS)
e : glr/CyO ; [UAS-imd]/[hsp-gal4] (NI, HS)
C)
left : y, w, DD1 ; cn, bw, glr/CyO ; Tl 10b, e/TM3, e, Sb, Ser
right : y, w, DD1 ; cn, bw, glr ; Tl 10b, e/TM3, e, Sb, Ser
D)
Non Induced
Induced
Non Induced
Induced
Non Induced
Induced
DAPI
α-DIF
merge
Toll
cn bw
glr

Figure 4.3 *galere* is acting downstream of *imd* in the Gram-negative bacteria response signaling pathway

(A) *glr* is required for the binding of Relish to the *Diptericin* gene promoter. Fly extracts were incubated with a wild-type or a mutant (Dipt*) radiolabeled probe. The genotypes of the flies as well as the incubation time after immune challenge are indicated on top. Rel^{+E23} : background control for the Rel_{E20} null allele of *Relish.*

(B) Epistatic analysis between the *imd* and *glr* genes. Quantitative PCR was used to measure the steady-state levels of *Diptericin* and *imd* mRNAs. Flies in samples (a), (b), and (d) have been challenged for 6 hours with *E. coli* (I : induced, NI : noninduced); sample (a) flies are used as a 100% reference for *Diptericin* mRNA. *imd* over expression was obtained by heat-shocking flies (HS) that contain both an *hsp-gal4* and a *UAS-imd* transgenes (c), (e).

(C) *glr* is not involved in the Toll signaling pathway. In the fly on the left, the $Toll_{10b}$ gain-of function allele of the Toll receptor gene induces the challenge-independent of a *Drosomycin-GFP* reporter gene (*DD1*). GFP fluorescence is still observed in a *glr* mutant background (fly on the right).

(D) *glr* is not required for DIF nuclear uptake. After a septic injury, DIF translocates in the nucleus in wild-type (*cn bw*) and *glr* flies, whereas it is no longer the case in a *Toll* null background. The immunostaining of DIF appears in red ; in green, DAPI indicate the position of cell nuclei. The overlap of the two fluorescent signals yields a yellow color.

imd was over expressed in *glr* RNAi-treated S2 cells (Figure 4.4 and see below). We conclude that *glr* acts downstream of *imd* in this signaling pathway.

As shown above, *glr* flies were resistant to fungal and Gram-positive bacterial infections, suggesting that *glr* is not involved in the Toll pathway. This is further corroborated by the finding that DIF nuclear uptake was normal in *glr* mutant flies, but was abolished in a Toll null mutant background (Figure 4.3D). Furthermore, the constitutive expression of a *Drosomycin*-GFP reporter gene triggered by the Tl^{10b} gain-of-function allele of the Toll receptor gene was not abolished in a *glr* background (Figure 4.3C), whereas it is blocked in a *Dif* mutant background (Rutschmann *et al*., 2000b).

galere **encodes a** ***Drosophila*** **TAB2/TAB3 homolog**

We identified the *glr* locus by positional cloning (Figure 4.5). The three mutations affect the *CG7417* gene (Figure 4.6A), which encodes the *Drosophila* TAB2/TAB3 homologue since the predicted protein contains its three characteristic domains (Figure 4.7). The expression of a transgenic full-length CG7417 cDNA rescued the *glr3 Diptericin* inducibility phenotype (Figure 4.6B), thus demonstrating that the defect in IMD pathway activation is indeed due to the mutation in TAB2.

Figure 4.4

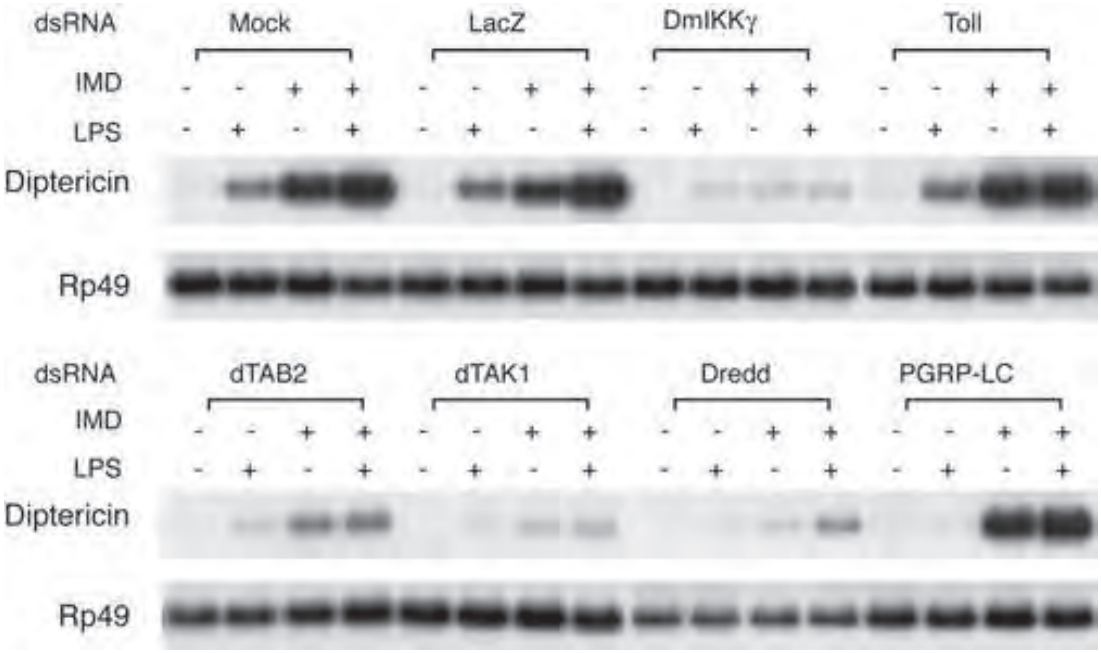
dsRNA
Mock
LacZ
DmIKKγ
Toll
IMD
LPS
Diptericin
Rp49
dsRNA
dTAB2
dTAK1
Dredd
PGRP-LC
IMD
LPS
Diptericin
Rp49

Figure 4.4 Galere/TAB2 functions downstream of IMD in S2 cells

IMD stable cells were transfected with various dsRNAs, then treated with various combinations of peptidoglycan and copper. Northern blotting analysis was performed to examine the expression of the antibacterial gene *Diptericin.*

Figure 4.5

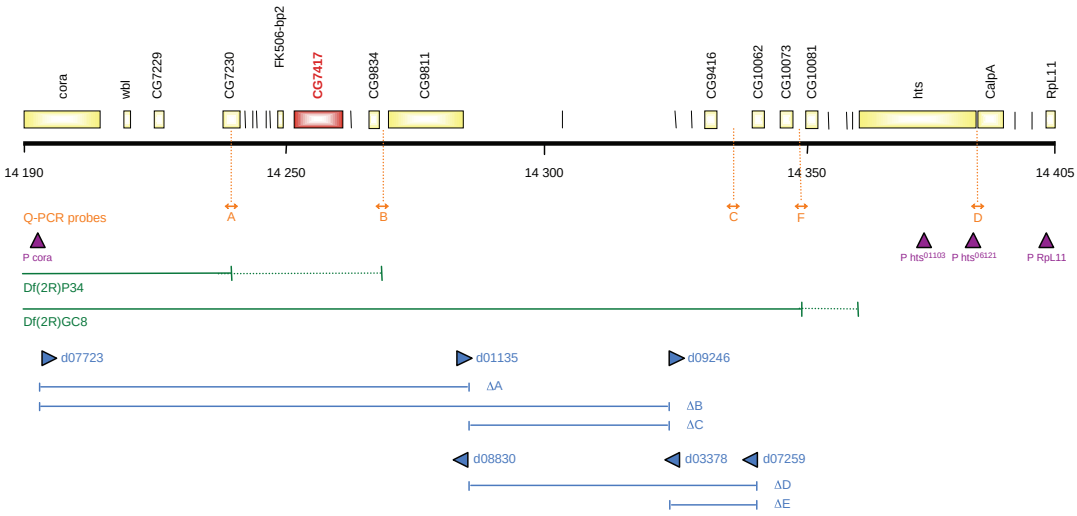
cora
wbl
CG7229
CG7230
FK506-bp2
CG7417
CG9834
CG9811
CG9416
CG10062
CG10073
CG10081
hts
CalpA
RpL11
14 190
14 250
14 300
14 350
14 405
Q-PCR probes
A
B
C
F
D
P cora
P hts01103
P hts06121
P RpL11
Df(2R)P34
Df(2R)GC8
d07723
d01135
d09246
ΔA
ΔB
ΔC
d08830
d03378
d07259
ΔD
ΔE

Figure 4.5 Positional cloning of the *glr* locus

We first mapped the position of *glr* to the 55A-56E interval by recombination mapping between the 2R loci *cn* and *bw*. This approximate position was confirmed by Single Nucleotide Polymorphism mapping. *glr* complemented all the deficiencies of the second chromosome deficiency kit that uncover this region. However, one 835 kbp interval, namely the 56C-56E region, was not covered by the deficiency kit and contains 75 predicted genes with no obvious similarity to known components of the NF-κB signaling cascade. We further restrained this interval by using the *Df(2R)GC8* deficiency which proximally overlaps the *Df(2R)P34* deficiency and removes an additional region distal to the *CG7229* gene (Konsolaki and Schupbach, 1998). *glr* complements only the latter deficiency ; this places the *glr* locus in the region uncovered only by *Df(2R)GC8*. We mapped by quantitative PCR the breakpoints of these two deficiencies (Chiang *et al*., 1999). The *Df(2R)P34* distal breakpoint mapped distal to *CG7230* while that of *Df(2R)GC8* was distal to *CG10073*. However, we found that *Df(2R)GC8* was unlikely to uncover the *hu-li-tai-shao* (*hts*) gene since it complemented two lethal P-alleles of *hts*. We further subdivided the 120,000 bp region comprised between *CG7230* and *hts* by generating flippasemediated deficiencies using FRT-site-containing P-elements in this region (Parks *et al*., 2004). *glr* complemented the *ΔC-ΔE, but not the ΔA and ΔB deficiencies, thus restraining the position* of glr to a 45.000 bp interval delimited by the CG7230 and CG9811 genes that contains 11 predicted genes. We noticed that one of these genes, CG7417, displayed very weak sequence similarity to mammalian TAB2. Indeed, the sequence conservation was mainly restricted to the Cterminal end of the protein and corresponds to a conserved motif known as little finger (NCBI : LOAD_little_fing.7.little-fing) or ZnF_RBZ (SMART : 00547.10 ; Zinc finger

Figure 4.5 Positional cloning of the *glr* locus (cont.)

domain in Ranbinding proteins). Recently, this motif was shown to interact specifically with K63-polyubiquitin chains (Kanayama *et al*., 2004). We therefore sequenced the CG7417 coding sequence both in wild-type and in the three mutant alleles. We found in each mutant allele a single point mutation that introduces a premature STOP codon in the gene : T to A at nucleotide 2681 (Cys_{786} of the 831-residue protein) for glr_1, C to T at nucleotide 2496 (Gln_{725}) for glr_2, and C to T at nucleotide 2326 (Gln_{669}) for glr_3. The finding that three independent mutations affect the coding sequence of one of the 11 candidate genes in the region which we delimited shows that *glr* mutations affect the CG7417 gene, a conclusion further supported by the rescue of the *glr* mutant phenotype by a transgene that expresses the wild-type gene (Figure 4.6B).

The figure shows the genetic map of the *glr* locus containing region. Scale : thousands bp, numbering according to Flybase. Genes in the region are drawn as boxes or vertical bars. Orange arrows and purple triangles represent respectively the Q-PCR probes and the lethal P element insertions used to map the distal breakpoints of the *Df(2R)P34* and *Df(2R)GC8* deficiencies (in green). Plain green lines correspond to the regions uncovered by those deficiencies, whereas dotted lines represent the interval containing their distal breakpoint. Deficiencies that were generated using the FRT-flippase system for further mapping are shown in blue ; blue triangles represent the modified P element insertions that were used to build those deficiencies. In red, the *CG7417 candidate gene presents a weak overall sequence similarity to the TAB2 and TAB3 genes* of vertebrates.

Figure 4.6

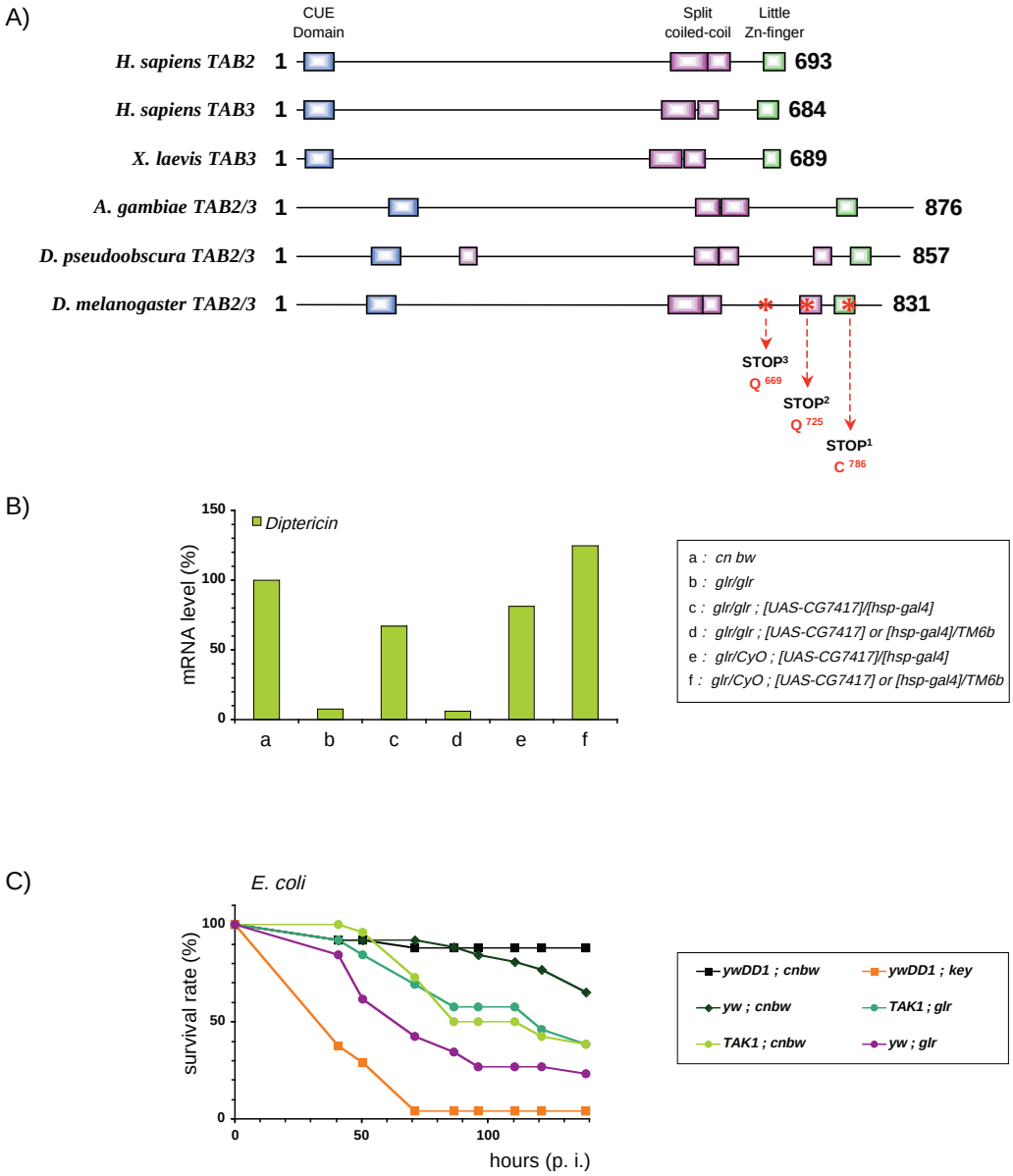
A)
CUE Domain
Split coiled-coil
Little Zn-finger
H. sapiens TAB2 1 693
H. sapiens TAB3 1 684
X. laevis TAB3 1 689
A. gambiae TAB2/3 1 876
D. pseudoobscura TAB2/3 1 857
D. melanogaster TAB2/3 1 831
STOP3 Q 669
STOP2 Q 725
STOP1 C 786
B)
Diptericin
mRNA level (%)
150
100
50
0
a b c d e f
a : cn bw
b : glr/glr
c : glr/glr ; [UAS-CG7417]/[hsp-gal4]
d : glr/glr ; [UAS-CG7417] or [hsp-gal4]/TM6b
e : glr/CyO ; [UAS-CG7417]/[hsp-gal4]
f : glr/CyO ; [UAS-CG7417] or [hsp-gal4]/TM6b
C)
E. coli
survival rate (%)
100
50
0
0
50
100
hours (p. i.)
ywDD1 ; cnbw
ywDD1 ; key
yw ; cnbw
TAK1 ; glr
TAK1 ; cnbw
yw ; glr

Figure 4.6 *galere* encodes the *Drosophila* homolog of TAK1 Binding Proteins 2 and 3

(A) The *Drosophila TAB2/3* homolog is mutated in *glr* flies. Structural representation of the TAB2 and TAB3 proteins in vertebrates and invertebrates. Three canonical domains define this family of proteins : a CUE domain (in blue), a split coiled-coil domain (in purple) and a little Zn finger (in green). *Drosophila* proteins have additional coiled-coil regions. Sequencing of the *CG7417* candidate gene from the three *glr* mutants revealed three independent point mutations in the coding sequence, that correspond to the premature introduction of a STOP codon and subsequent truncation of the mutant proteins, as indicated.
(B) Rescue of the *glr* mutant phenotype by a wild-type *glr* transgene. All flies have been challenged with *E. coli.* The genotypes of the flies are indicated in the legend. *glr* mutant flies that carry a wild-type cDNA under the control of UAS regulatory sequences express the *glr* gene at moderate levels, driven by the low constitutive expression provided by the *hsp*-Gal4 transgene in the absence of heat-shock (c). *glr* sibling flies obtained in the same cross that carry either the driver or the UAS transgene fail to express *Diptericin* (d), like *glr* mutant flies (b). Heterozygous sibling flies behave as wild-type (e, f).
(C) *TAK1;glr* double mutants display the same intermediate phenotype to Gram-negative bacterial infections as compared to either single mutant. *ywDD1 ; cn bw* : genetic background control in which the *kenny* (*key*) mutants have been generated ; the *TAK1* mutants have been generated in a *yw* context. To compare the *TAK1* and *glr* phenotypes, the genetic backgrounds of the first (*yw*) and second chromosomes (*cn bw*) have been homogenized using standard crosses. The slightly increased sensitivity of the *glr* simple mutants as compared to the *TAK1* and *TAK1; glr* mutants is not significant.

Figure 4.7

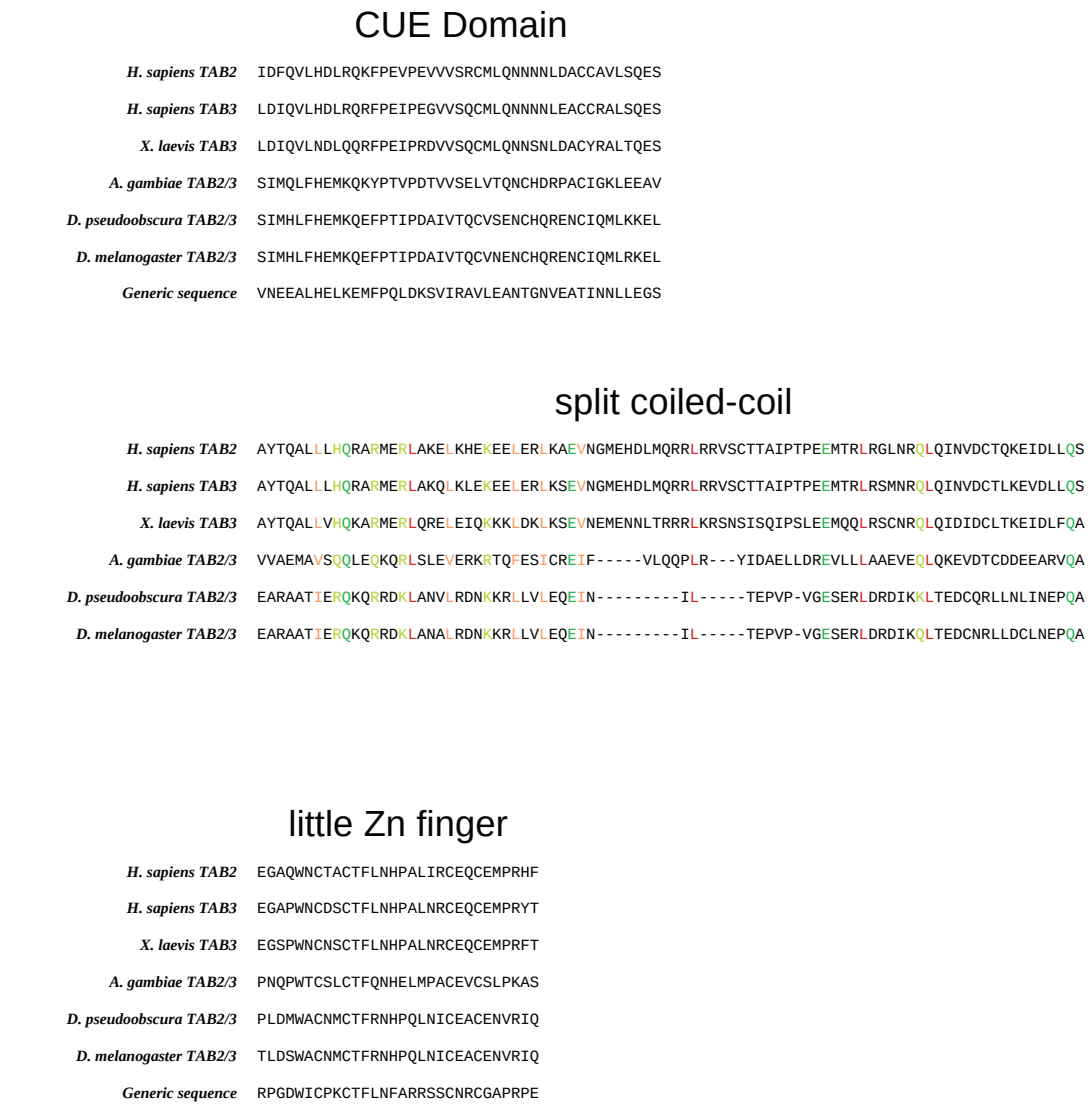
CUE Domain
H. sapiens TAB2 IDFQVLHDLRQKFPEVPEVVVSRCMLQNNNNLDACCAVLSQES
H. sapiens TAB3 LDIQVLHDLRQRFPEIPEGVVSQCMLQNNNNLEACCRALSQES
X. laevis TAB3 LDIQVLNDLQQRFPEIPRDVVSQCMLQNNSNLDACYRALTQES
A. gambiae TAB2/3 SIMQLFHEMKQKYPTVPDTVVSELVTQNCHDRPACIGKLEEAV
D. pseudoobscura TAB2/3 SIMHLFHEMKQEFPTIPDAIVTQCVSENCHQRENCIQMLKKEL
D. melanogaster TAB2/3 SIMHLFHEMKQEFPTIPDAIVTQCVNENCHQRENCIQMLRKEL
Generic sequence VNEEALHELKEMFPQLDKSVIRAVLEANTGNVEATINNLLEGS
split coiled-coil
H. sapiens TAB2 AYTQALLLHQRARMERLAKELKHEKEELERLKAEVNGMEHDLMQRRLRRVSCTTAIPTPEEMTRLRGLNRQLQINVDCTQKEIDLLQS
H. sapiens TAB3 AYTQALLLHQRARMERLAKQLKLEKEELERLKSEVNGMEHDLMQRRLRRVSCTTAIPTPEEMTRLRSMNRQLQINVDCTLKEVDLLQS
X. laevis TAB3 AYTQALLVHQKARMERLQRELEIQKKKLDKLKSEVNEMENNLTRRRLKRSNSISQIPSLEEMQQLRSCNRQLQIDIDCLTKEIDLFQA
A. gambiae TAB2/3 VVAEMAVSQQLEQKQRLSLEVERKRTQFESICREIF-----VLQQPLR---YIDAELLDREVLLLAAEVEQLQKEVDTCDDEEARVQA
D. pseudoobscura TAB2/3 EARAATIERQKQRRDKLANVLRDNKKRLLVLEQEIN---------IL-----TEPVP-VGESERLDRDIKKLTEDCQRLLNLINEPQA
D. melanogaster TAB2/3 EARAATIERQKQRRDKLANALRDNKKRLLVLEQEIN---------IL-----TEPVP-VGESERLDRDIKQLTEDCNRLLDCLNEPQA
little Zn finger
H. sapiens TAB2 EGAQWNCTACTFLNHPALIRCEQCEMPRHF
H. sapiens TAB3 EGAPWNCDSCTFLNHPALNRCEQCEMPRYT
X. laevis TAB3 EGSPWNCNSCTFLNHPALNRCEQCEMPRFT
A. gambiae TAB2/3 PNQPWTCSLCTFQNHELMPACEVCSLPKAS
D. pseudoobscura TAB2/3 PLDMWACNMCTFRNHPQLNICEACENVRIQ
D. melanogaster TAB2/3 TLDSWACNMCTFRNHPQLNICEACENVRIQ
Generic sequence RPGDWICPKCTFLNFARRSSCNRCGAPRPE

Figure 4.7 Alignments of the CUE, coiled-coil, and little Zn Finger domains that characterize the TAB2/TAB3 family

The CUE domain has been reported to bind to proteins that are mono- or polyubiquitinated (reviewed in (Di Fiore *et al*., 2003)). Indeed, the structures of two proteins that bind to ubiquitin have been published (Kang *et al*., 2003; Prag *et al*., 2003). The generic sequence of the PFAM CUE domain is shown. Residues from the Cue2-1 domain (*) and the Vps9 CUE domain (*: monomer; § : dimer) that interact directly with ubiquitin are indicated on top. Conserved residues of the TAB2/3 family are displayed in red (residues conserved in six sequences) and in orange (residues conserved in five out of six sequences). The apolar backbone of the domain is conserved (blue : conserved leucine or isoleucine residues present in the generic sequence; cyan : hydrophobic residues present at the same position). It is unlikely that the TAB2/3 CUE domains are able to bind to ubiquitin with high affinity since a key apolar residue (methionine shown in green in the generic sequence) that is involved in the interaction with an hydrophobic pocket defined by L8, I44, H68, and V70 of ubiquitin is replaced by charged residues. The same observation can be made about the distal di-leucine repeat where the leucine that binds to ubiquitin is replaced by polar or charged amino acids. However, the mouse TAB2 CUE domain has recently been shown to be able to bind to monoubiquitin and to be required for IL-1-induced TRAF6 ubiquitination and NF-κB pathway activation (Kanayama *et al*., 2004; Kishida *et al*., 2005).

The split coiled-coil domain has been shown to mediate the interaction of TAB2/3 with TAK1 (Geuking *et al*., 2005; Ishitani *et al*., 2003). Conserved leucine residues are shown in blue whereas apolar amino acids are indicated in cyan. Conserved charged or polar residues are displayed in light green (perfect

Figure 4.7 Alignments of the CUE, coiled-coil, and little Zn Finger domains that characterize the TAB2/TAB3 family (cont.)

conservation in darker green). There is no significant sequence conservation of this domain between insects and vertebrates (19% identity between GLR and human TAB3), whereas the domain is well conserved within vertebrates and within *Drosophila*. However, the *Anopheles gambiae* coiled-coil domain is highly divergent at the sequence level, both with *Drosophila* and vertebrates. Coiled-coil regions were predicted using the ISREC coils server (Lupas *et al*., 1991).

The Zn finger is highly conserved between members of the TAB2/3 family and together these domains may define a subfamily within the NCBI little finger family. Conserved cysteins are shown in bold. Red and orange colors are used as above. The *glr1* mutation affects this domain, and thus underscores its importance. However, since this mutation introduces a STOP codon, we cannot formally exclude that the truncation of the 44 residues that form the C-terminal domain distal to the Zn finger contributes to the mutant phenotype. Nevertheless, this possibility appears to be remote since this C-terminal extension is absent in vertebrates, is not conserved in the predicted mosquito sequences, and is less preserved between *D. melanogaster* and *D. pseudoobscura* (60% sequence identity) than the 95 % and 88% identity conservation for the CUE and coiled-coil domains respectively. TAB2 has been reported to be part of a N-CoR/TAB2/HDAC3 repressor complex on the chromatin that is exported out of the nucleus upon IL-1ß signaling (Baek *et al*., 2002). However, the nuclear export sequence and the MEKK phosphorylation sites of TAB2 that are required for export are not conserved in DmelTAB2. We conclude that this aspect of TAB2 biology is unlikely to occur also in *Drosophila*.

galere* and *TAK1* belong to the same branch downstream of *imd

Two peculiar features of the *glr* phenotype are its moderate sensitivity to *E. coli* infection and the intermediate levels of induction for certain AMP genes. By comparison null mutants of *imd* and *kenny* are highly susceptible to *E. coli* infection (Figure 4.2F) and exhibit almost no AMP gene induction. The intermediate *glr* phenotype is reminiscent of mutants carrying a null allele of *Drosophila TAK1*, the MAPKKK involved in the IMD pathway (Vidal *et al*., 2001) and (Figure 4.6C). This intermediate susceptibility to Gram-negative infections of *TAK1* and *glr* mutants suggests that an alternative secondary path functions downstream of IMD for the activation of the IKK complex. To determine whether *glr* and *TAK1* function in the same or distinct branches downstream of IMD, we generated *TAK1;glr* double mutants. If the two genes are required in distinct branches, the double-mutant combination should display a higher, additive, sensitivity to *E. coli* than either single mutant. In contrast, if the two gene products are involved in the same arm of the bifurcation, the phenotype of the double mutant should be similar to that of each single mutant. As shown in Figure 4.6C, we found that the latter hypothesis is correct and conclude that *TAK1* and *glr* function in the same branch. To further support this inference, we performed a yeast two-hybrid assay using DmelTAK1 as a bait and GLR as a prey and found a strong interaction, thus establishing that like in vertebrates *Drosophila* TAB2 and TAK1 bind directly to each other (Table 4.8, (Shibuya *et al*., 1996)). This interaction had been previously reported in a genome-wide yeast

Table 4.8

Drosophila TAB2 interacts with TAK1 in yeast two-hybrid assay

Bait	Prey		
	dTAB2	dTAK1	DmIKKγ $_{101-387}$
dTAK1	++++		
DmIKKβ			++

Table 4.8 TAK1 and Galere/TAB2 interact in yeast two-hybrid assays

The strength of potential interactions was qualitatively presented as “+”s, using the expression of the *Ade2* reporter gene as criteria.

two-hybrid screen and confirmed recently in co-immunoprecipitation experiments (Geuking *et al*., 2005; Giot *et al*., 2003). To further define the role of *glr* in the *imd* pathway, we analyzed its role in a S2* cell culture system (Zhou *et al*., 2005).

_galerel_TAB2 functions as an adaptor required for TAK1 activation

In the S2* embryonic macrophage cell line, IMD pathway stimulation by diaminopimelic acid-type peptidoglycan (DAP-PGN) induces the expression of *Diptericin* (Kaneko *et al*., 2004). As previously reported, treatment of S2* cells with dsRNA targeted at known members of the IMD pathway led to a strong decrease in the induction of *Diptericin* by PGN (Figure 4.9A). As expected, this was also the case when cells were treated with *TAB2* dsRNA (Gesellchen *et al*., 2005; Kleino *et al*., 2005; Zhuang *et al*., 2006). The induction of *Drosomycin* expression by the *Toll* pathway was not impaired by *TAB2* RNAi, consistent with the *in vivo* data (Figure 4.9B and Figures 4.1, 4.3). To establish that *TAB2* function is required in IKK activation, we monitored the challenge induced phosphorylation of Relish by immunoprecipitated IKK complex (Zhou *et al*., 2005). This phosphorylation is strongly reduced in S2 cells exposed to *TAB2* dsRNA, as for other mutants of the *imd* pathway (Figure 4.9C). This result indicates that like TAK1, TAB2 is required for the activation of the IKK complex by an immune challenge in *Drosophila* S2* cells. To define the function of TAB2 relative to TAK1, we asked whether *glr* was required for the induction of *Diptericin*

Figure 4.9

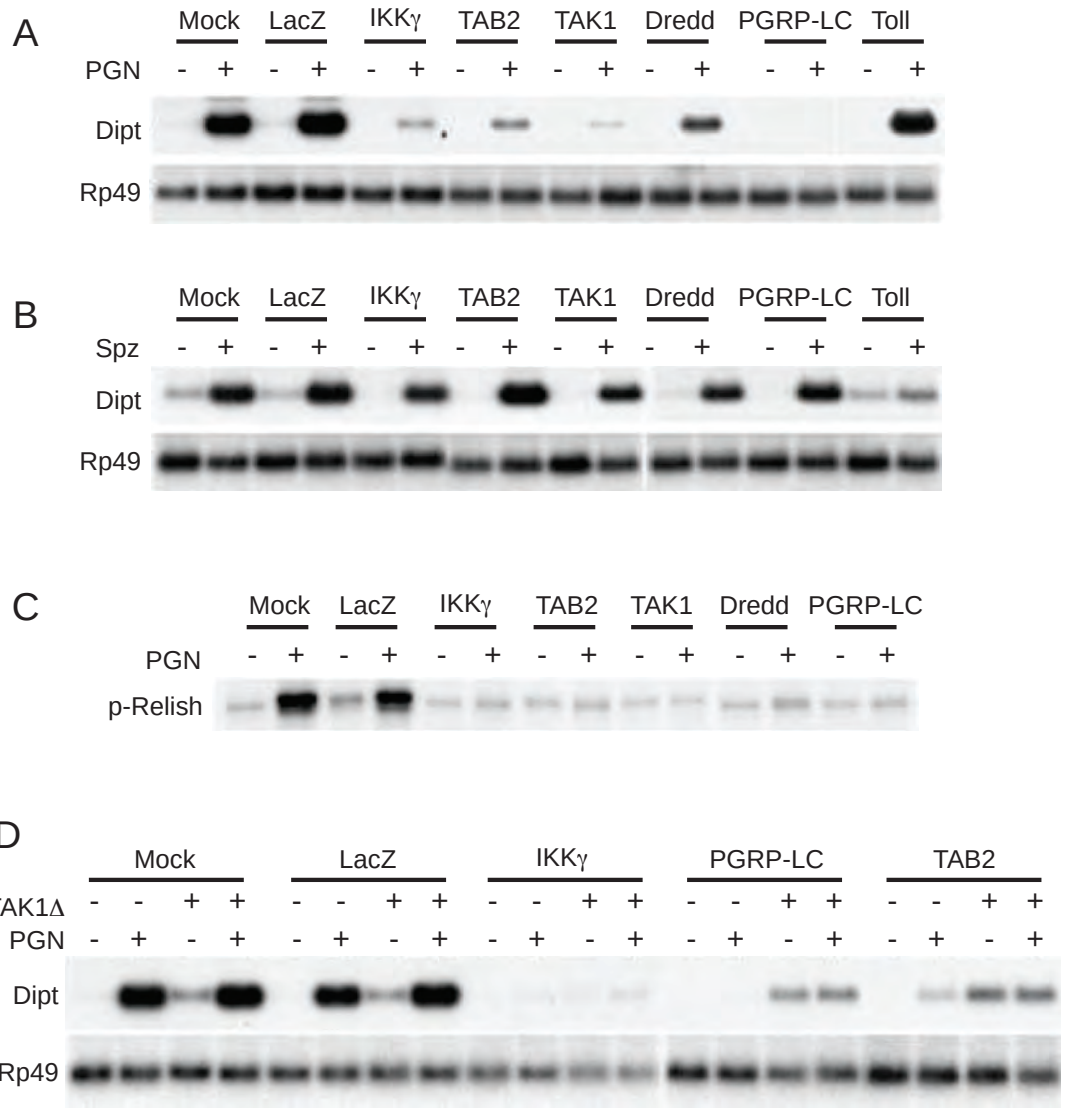
A
Mock
LacZ
IKKγ
TAB2
TAK1
Dredd
PGRP-LC
Toll
PGN
Dipt
Rp49
B
Spz
C
p-Relish
D
TAK1Δ

Figure 4.9 Galere/TAB2 functions upstream of the IKK complex in the IMD pathway

(A) *galere* is required for the antibacterial immune response. Various dsRNAs were transfected into S2 cells. Peptidoglycan-induced *Diptericin* gene activation was examined by Northern blotting. Rp49 serves as loading control.

(B) *galere* is not required for the antifungal immune response. DsRNA-transfected cells were treated with Spätzle-containing conditioned medium. *Drosomycin* gene expression was analyzed by Northern blotting.

(C) *galere* is required for peptidoglycan-induced IKK activation. DsRNA-transfected cells were treated with peptidoglycan for 15 minutes. The endogenous IKK complex was immunoprecipitated using antibody raised against DmelIKKγ. The immunoprecipitates were subsequently subjected to *in vitro* kinase assays using Relish as substrate.

(D) *galere* is not required for TAK1Δ-mediated antibacterial peptide gene activation. TAK1Δ stable cells were transfected with various dsRNAs, then treated with various combinations of peptidoglycan and copper. Northern blotting analysis was performed to examine the expression of the antibacterial gene *Diptericin*.

expression observed when an activated form of TAK1 is overexpressed in S2 cells (Figure 4.9D). The induction of *Diptericin* was not altered by *TAB2* RNAi and was similar to that observed after RNAi targeting *PGRP-LC* or *imd* (data not shown), two molecules that function upstream of TAK1 in the IMD pathway. In contrast, *FADD* and *DREDD* RNAi strongly reduced the induction of *Diptericin* in this system, consistent with their proposed role in Relish cleavage (Zhou *et al*., 2005). To more precisely define the role of TAB2, we assayed its role in TAK1 activation. To this end, we developed a TAK1 kinase activity assay in which we assessed the incorporation of radiolabeled ATP by epitope-tagged immunoprecipitated DmelTAK1 using as a substrate recombinant, kinase-dead, MKK6, a known target of human TAK1 (Wang *et al*., 2001). PGN-stimulation of S2* cells led to a significant and reproducible increase in the levels of DmelTAK1 activity, as monitored by this assay (Figure 4.10B). As expected, this level of TAK1 activity decreased to background level when cells were treated with dsRNA against the IMD pathway receptor gene *PGRP-LC* or with *TAK1* dsRNA, but *LacZ* dsRNA had little effect. In contrast, a significant phospho MKK6 signal was observed in cells treated with *IKK*γ dsRNA, consistent with the position of *kenny* downstream of *TAK1* in the IMD pathway. We found no significant activation of TAK1 in cells treated with *TAB2* exon4 dsRNA. Taken together, these data establish that TAB2 is an adaptor required for the activation of TAK1 by immune stimuli. A similar conclusion has been reached as regards the role of TAB2 in TAK1 activation by the Eiger pathway (Geuking *et al*., 2005).

Figure 4.10

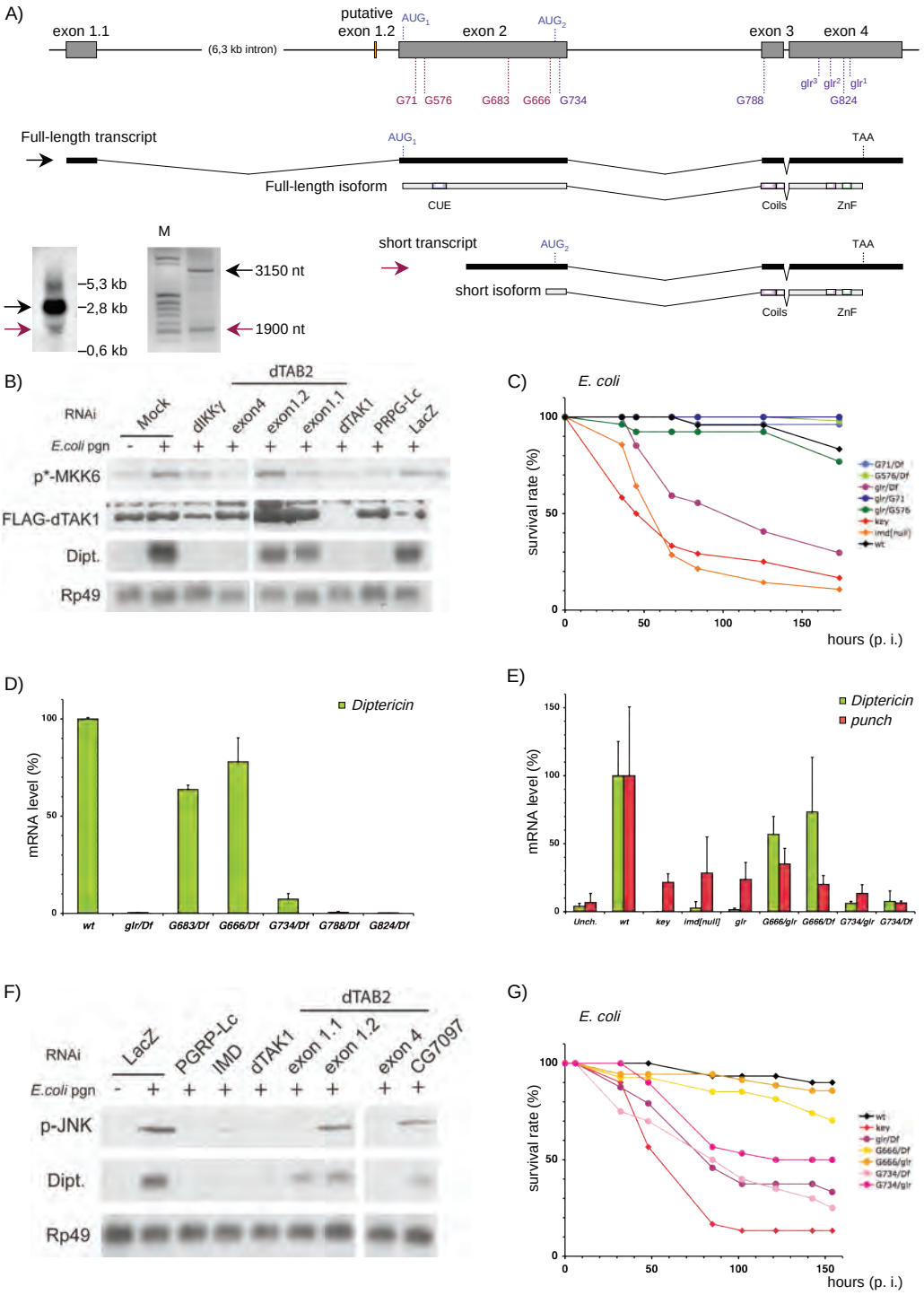
A)
exon 1.1
(6,3 kb intron)
putative exon 1.2
AUG1
exon 2
AUG2
exon 3
exon 4
G71 G576 G683 G666 G734
G788
glr3 glr2 glr1
G824
Full-length transcript
AUG1
TAA
Full-length isoform
CUE
Coils
ZnF
M
5,3 kb
2,8 kb
0,6 kb
3150 nt
1900 nt
short transcript
AUG2
TAA
short isoform
Coils
ZnF
B)
dTAB2
RNAi
Mock
dIKKγ
exon4
exon1.2
exon1.1
dTAK1
PRPG-Lc
LacZ
E.coli pgn
p*-MKK6
FLAG-dTAK1
Dipt.
Rp49
C)
E. coli
survival rate (%)
hours (p. i.)
D)
Diptericin
mRNA level (%)
wt
glr/Df
G683/Df
G666/Df
G734/Df
G788/Df
G824/Df
E)
Diptericin
punch
mRNA level (%)
Unch.
wt
key
imd[null]
glr
G666/glr
G666/Df
G734/glr
G734/Df
F)
dTAB2
RNAi
LacZ
PGRP-Lc
IMD
dTAK1
exon 1.1
exon 1.2
exon 4
CG7097
E.coli pgn
p-JNK
Dipt.
Rp49
G)
E. coli
survival rate (%)
hours (p. i.)

Figure 4.10 JNK pathway activation is dispensable in the *Drosophila* host defense against *E. coli*

(A) Scheme of the *TAB2* locus. The location of the STOP mutations used in this study are represented. The *glr* category of alleles is represented in blue while the other category, which affects the full-length protein isoform and only blocks JNK signaling, is represented in red. Two transcripts from the locus are shown, with the predicted protein product. The short isoform has been detected by Northern blot analysis (Inset left) and by 5' Race PCR (Inset right, M : size markers). Three ESTs (not shown : GH18828, GH24638, GH24933) further confirm its existence. The putative exon 1.2 is used as an alternative 5' exon in some ESTs. However, we could not detect any phenotypic consequence when its expression was targeted by RNAi in S2 cells (B, F).

(B) TAK1 activation assay. S2 cells expressing FLAG-tagged TAK1 were immunoprecipitated and incubated with human MKK6 and radiolabeled ATP. Kinase activity was monitored by autoradiography. The quantity of immunoprecipitated FLAG-tagged TAK1 was revealed by Western blot with a FLAG antibody. Finally, a fraction of the cell extract was used for Northern blot analysis and hybridized with a *Diptericin* and a *Rp49* probe.

(C) Survival experiments with a set of *TAB2* allelic combinations. The deficiency used in these studies was Df(2R)EXEL6069.

(D) Genetic characterization of *TAB2* alleles to map the distinct functions of the locus using *Diptericin* induction as a read-out. The *Dipt* mRNA levels were

Figure 4.10 JNK pathway activation is dispensable in the *Drosophila* host defense against *E. coli* (cont)

monitored 6 hours after an *E. coli* challenge using quantitative RT-PCR. The deficiency used in this panel and in E and G was ΔB (Figure 4.5).

(E) Analysis of IKK and JNK pathway activation. *Punch* and Dipt mRNA levels were monitored 3 hours after an *E. coli* challenge. *Punch* expression is dependent both on IKK and JNK pathway activation. Note that *Dipt* expression is moderately affected in the *G666* allele, whereas *Punch* mRNA levels are decreased almost as severely as in the *G734 TAB2* allele or *key*.

(F) JNK pathway activation is blocked when the long TAB2 isoform is targeted by dsRNA interference. RNAi-treated extracts of PGN-stimulated S2 cells were analyzed by Western blot analysis with a P-JNK specific antibody or analyzed by Northern blot analysis. Targeting the long TAB2 isoform, exon 1 dsRNA, did not affect *Diptericin* induction (see also lower panels of 6B).

(G) Survival experiments to an *E. coli* challenge. $TAB2^{G734}$ and not $TAB2^{G666}$ flies succumb to the infection.

JNK pathway activation is dispensable for host defense against *E. coli*

The TAK1-TAB2 complex is required both for IKK complex activation and for JNK pathway activation. In flies, 39 mutant alleles for TAB2 have been recovered in a suppressor screen for a JNK and TAK1-dependent eye phenotype induced by Eiger over expression in this tissue (Geuking *et al*., 2005). Interestingly, most of these mutations correspond to STOP codons distributed regularly along the putative *TAB2* ORF (Figure 4.10A), while all three *glr* alleles encode nonsense mutations clustering in the C-terminus of the gene. Therefore, we examined the susceptibility to *E. coli* infection of flies carrying nonsense mutations G71 and G576 that stop translation of TAB2 at residues 40 and 66 of the predicted protein, respectively. Strikingly, we found that $TAB2^{G71}$ and $TAB2^{G576}$ hemizygous or transheterozygous flies resisted infection, in contrast to $TAB2^{glr3}$ hemizygous flies (Figure 4.10C). In keeping with these unexpected results, $TAB2^{G71}$ and $TAB2^{G576}$ flies induced *Diptericin* expression normally (data not shown). We reasoned that shorter protein isoforms might originate from alternative start sites of transcription of the *TAB2* locus, thus bypassing the early STOP codons. Indeed, many *TAB2* ESTs have been isolated, some of which contain a 5' end starting within exon 2, past the initial AUG of the predicted full length protein (Figure 4.10A). We detected by Northern blot analysis the existence of three transcripts in adults, of approximate lengths 1.8 , 3.1 , and 5.2 kbp (Figure 4.10A). A full length sequenced cDNA (AJ277497) is 3.2 kbp and corresponds to the longest cDNA in the EST database. Two transcripts were

mapped in detail by 5' RACE RT-PCR in adult flies and S2 cells (Figure 4.10A). Interestingly, the shorter of these transcripts begins in the middle of exon 2 and lacks the first start codon (AUG^1, Figure 4.10A). Instead, this alternative transcript is predicted to utilize a later start codon (AUG^2 in Figure 4.10A) and to encode a shorter protein product of 355 C-terminal residues (Figure 4.10A). We hypothesized that this short transcript is sufficient for IMD signaling, while the results of Geuking *et al*. indicate that the longer product is required for the Eiger/ TAK/JNK pathway. We therefore decided to test several additional nonsense *TAB2* mutants to map the portions of this locus required for the IMD pathway. We found that $TAB2^{G683}$ (Gln330STOP) and $TAB2^{G666}$ (Gln458STOP) mutant flies are still able to induce *Diptericin* normally following *E. coli* infection, while the $TAB2^{G734}$ (Gln 486STOP), $TAB2^{G788}$ (Gln542STOP) and $TAB2^{G824}$ (Trp767STOP) flies induce negligible *Diptericin* induction (Figure 4.10D and 4.10A for allele map : red alleles functional, blue alleles nonfunctional IMD signaling). This mapping strategy thus delineates the aa458-486 interval in which a shorter ORF is expected to initiate translation. Interestingly, this 28-residue interval contains a ATG at position 476 (AUG^2 Figure 4.10A) that is the predicted initiation codon in the correct reading frame of the shortest transcript isolated by 5' RACE PCR.

We compared in more detail the phenotypes of the $TAB2^{G666}$ (Gln458STOP) and of the $TAB2^{G734}$ (Gln486STOP) mutants as regards JNK pathway and IKK complex activation using respectively *Punch* and *Diptericin* induction as known read-outs of these pathways (Silverman *et al*., 2003). We

determined that *Punch* maximum induction occurs 3 hours after an *E. coli* challenge and was markedly decreased in either the *TAB2*^{G666} (Gln458STOP) or the *TAB2*^{G734} (Gln486STOP) alleles, while *Diptericin* level was drastically reduced only in the latter (Figure 4.10E). *Punch* expression is also decreased in *kenny* mutants, thus showing that in adults *Punch* induction is controlled both by the IKK complex and the JNK pathway. These data indicate that the *TAB2*^{G666} allele strongly affects only JNK activation induced by a septic injury while the *TAB2*^{G734} mutant blocks the induction of both the JNK and the IKK pathways. Consistent with these interpretations, *Punch* expression is not reduced to background levels until both the JNK and NF-κB pathways are crippled, in the G734 and *glr* alleles. To confirm this interpretation, we differentially inactivated *TAB2* isoforms in S2* cells by using dsRNA that target either exon 1 or 4. Exon1 dsRNA is expected to mimic the *TAB2*^{G666} phenotype, since only the long isoform is targeted whereas exon4 dsRNA is expected to target both isoforms, thus recapitulating the effect of *TAB2*^{G734}. Only exon 4 dsRNA treatment abolished *Diptericin* induction (Figure 4.10B and 4.10F). In contrast, either exon 1 or exon 4 dsRNAs prevented TAK1 activation (Figure 4.10B) and JNK phosphorylation (Figure 4.10F). In conclusion, the full-length transcript is required only for JNK pathway activation, whereas IKK complex activation can be mediated by the short isoform alone.

The *TAB2*^{G666} allele allows the uncoupling of JNK pathway activation from IKK complex activation and thus provides the means to assess the relevance of JNK pathway activation to host defense. We therefore monitored the resistance

of *TAB2*^{G666} and *TAB2*^{G734} mutant flies to an *E.coli* infection. Figure 4.10G shows that only the latter are susceptible to this challenge while the former resist like wild-type flies. We conclude that JNK pathway activation does not play an essential role in host defense against *E. coli* infections.

Discussion

An important issue for understanding the NF-κB pathway in mammals is the role of TAB2 in TLR signaling and in the response to proinflammatory cytokines such as IL-1, TNFα. While data obtained in a cell culture system clearly implicate TAB2/3 in the response to cytokines (Ishitani *et al*., 2003), no evidence for a similar role has been obtained so far from the analysis of TAB2 knock-out mutant mice (Shim *et al*., 2005; Sanjo *et al*., 2003). Given the evolutionary conservation of the NF-κB pathway, our data in *Drosophila* suggest that the lack of phenotype in mice is indeed due to the redundancy of TAB2 and TAB3 (Ishitani *et al*., 2003).

The alleles of TAB2 with nonsense mutations in the first half of the gene (G71, G576, G683, and G666) are resistant to bacterial infection and induce fairly normal levels of AMP genes. These flies express an isoform of TAB2 lacking the CUE domain via the shorter transcript characterized above. Thus, as in mammals, the N-terminal CUE domain, one of three characteristic domains of TAB2 that have been conserved during evolution (Figure 4.6 and Figure 4.7), is dispensable for NF-κB signaling and host defense against infections (Kanayama

et al., 2004). In contrast, the “little Zn-finger” domain appears to be critical for NF-κB signaling, because a truncation removing this domain prevents immune activation (*glr*$_1$ allele).

In mammals, several components of the NF-κB pathway are posttranslationally modified by conjugation with K63-linked polyubiquitin chains via the E3 ubiquitin ligase TRAF6 and the E2 ubiquitin conjugating enzyme complex Ubc13-Uev1A (Chen, 2005). In TNF signaling, for instance, RIP1, TRAF2, and NEMO (IKKγ) are polyubiquitinated and it has been proposed that polyubiquitinated RIP1 serves as a platform to recruit both TAK1 and IKK complexes (Ea *et al*., 2006). Other ubiquitination complexes may also be involved in this pathway, because knockdown of *Ubc13* leads to a moderate reduction of NF-κB signaling (Yamamoto *et al*., 2006), while JNK signaling is abolished. Importantly, binding of both NEMO and TAB2/TAB3 to polyubiquitin chains is required for IKK complex activation *in vitro* (Ea *et al*., 2006; Wu *et al*., 2006). The binding of TAB2/TAB3 to K63-linked ubiquitin chains is mediated by their C-terminal “little Zn finger” (Kanayama *et al*., 2004). K63-polyubiquitination is also believed to play a role in the IMD pathway in *Drosophila* since the Bendless (Ubc13)/Uev1a E2 ubiquitin conjugating enzyme complex is required for IKK complex activation in S2*cells (Yamamoto *et al*., 2006; Zhou *et al*., 2005, Chapter 2). Our data further support the hypothesis that K63-polyubiquitin binding is critical for IMD signaling because the *TAB2*^{glr1} allele lacks an intact “little Zn finger” domain, and displays a phenotype equivalent to null.

We conclude that *Drosophila* TAB2 functions as an adaptor molecule for TAK1 function as : (i) TAK1 and TAB2 have the same non-additive phenotype, (ii) TAK1 and TAB2 interact directly (Geuking *et al*., 2005; Giot *et al*., 2003, this work), (iii) both TAK1 and TAB2 are required for the activation of the *Drosophila* IKK signaling complex and for that of the JNK pathway (Boutros *et al*., 2002; Silverman *et al*., 2003, this work), (iv) TAB2 is not required for *Diptericin* induction by an activated form of TAK1 but is required for TAK1 activation (Figure 4.10B). Finally, a similar conclusion has been reached in a study that addressed the role of the TAB2/TAK1 complex in JNK pathway activation by the *eiger/wengen* signaling cascade, which potentially intersects the *imd* pathway at the level of the TAK1/TAB2 complex (Geuking *et al*., 2005). The exact physiological role of this pathway triggered by the TNF-like molecule Eiger remains undefined, although it has been implicated in the production of a shock response to *Salmonella* infection (Brandt *et al*., 2004).

The genetic ablation of both *TAK1* and *TAB2* together leads to a strikingly mild phenotype, even though null alleles of genes acting either upstream (*imd*) or downstream (*kenny)* of TAK1 display a more severe phenotype (Figures 4.2F and 4.6C). These data suggest that two alternative paths occur downstream of *imd* and that these two branches re-converge on IKK. TAK1 and TAB2 belong to the same branch. Presumably, UBC13 and UEV1A also belong to this branch in which regulatory ubiquitination is likely to play a cardinal role. Relish can still be activated to some degree in the absence of a functional TAK1/TAB2 complex

since *Attacin* and *Drosocin* are still partially induced in *TAB2* mutants, but are not detectable in *Relish* mutants (Hedengren *et al*., 1999). This limited activation may partly account for the presence of Relish observed in the nuclei of TAK1 null mutant larvae (Delaney and Mlodzik, 2006). We predict that one or several genes constitute a second, partially redundant, branch that also converges on IKK. This second branch might then be responsible for the persistent activation of the IMD pathway. It has been shown in cell culture experiments that over expressed tagged TAK1 is degraded rapidly following Relish activation (Park *et al*., 2004). Yet, *Diptericin* and *Drosocin* are still expressed in wild-type flies at significant levels up to 48 hours after immune challenge (Figure 4.1), suggesting an alternative, longer-lived signaling pathway that functions independently of the TAK1/TAB2 complex. Candidates for this second sub-branch include the five other *Drosophila MAP3K* genes (Stronach, 2005), as may be the case in mammals. Indeed, the genetic ablation of TAK1 in mice does not lead to a total block of NF-κB signaling (Sato *et al*., 2006; Shim *et al*., 2005). In addition to TAK1, several MAP3K kinases such as NIK, MEKK1 and MEKK3 have been shown to activate the IKK signaling complex in mammalian cells (Schmidt *et al*., 2003). A potential alternative to the existence of a second branch downstream of RIP1 is that the IKK complexes that bind to polyubiquitinated RIP1 be sufficiently concentrated to allow for low level activation of the IKK complex independently of any MAP3K. This explanation may also hold in flies since several essential

residues in the NEMO Ub binding site are conserved in its fly homologue, Kenny (Ea *et al*., 2006).

The JNK pathway is activated briefly in response to immune stimuli both in flies and in cell culture systems (Boutros *et al*., 2002; Park *et al*., 2004). Its targets include structural and regulatory cytoskeletal genes. However, its physiological importance in the immune response remains unresolved. Conflicting reports concluded that the JNK pathway either down- regulates (Kim *et al*., 2005; Park *et al*., 2004), up-regulates (Delaney and Mlodzik, 2006; Kleino *et al*., 2005), or has no effect (Boutros *et al*., 2002; Silverman *et al*., 2003) on AMP gene induction in S2 cells. Following an *in vivo* study, it was recently proposed that the JNK pathway substantially controls the expression of AMP genes (Delaney and Mlodzik, 2006). However, this analysis was based on the experimental activation of the JNK pathway over a long time period, which did not recapitulate the brief activation of the JNK pathway observed in the septic injury model. Thus, the expression of AMP genes in this context may not represent a physiological situation. Moreover, the JNK loss-of-function clonal analysis, which reported a loss of AMP gene inducibility, was performed in larval fat body which is distinct from adult fat body. Finally, it cannot be excluded that the phenotype observed may be the indirect consequence of developmental effects of JNK loss-of function.

In our present report, we have analyzed several TAB2 mutant alleles and grouped them in two categories. The first category consists of mutations that

introduce STOP codons in the N-terminal half of the predicted full-length protein (JNK phenotype), affecting only the product of the long transcript and preventing JNK signaling. These mutants display only a slight reduction in AMP gene induction as opposed to a strong decrease of JNK pathway activation. In contrast, the second category of alleles (*glr*) introduces STOP codons in the C-terminal half, affecting all isoforms of the protein and strongly inhibiting *Diptericin* induction. For example, the *TAB2*^{G734} allele inserts a STOP codon near the predicted translation start of the short form and fails to support AMP genes induction. In this second category of mutant alleles, we observed that both JNK and IKK activation are strongly reduced. Thus, the difference between the first and second category of alleles is that IKK activation is prevented only in the latter while both groups of mutants display a severely decreased activation of the JNK pathway. The key observation is that only mutant alleles of the *glr* category succumb to an *E. coli* challenge. Since the mutants of the first category survive this infection even though JNK activation is prevented, we conclude that JNK pathway activation in *Drosophila* does not play an essential role in the host defense against *E. coli* infections.

Figure 4.11

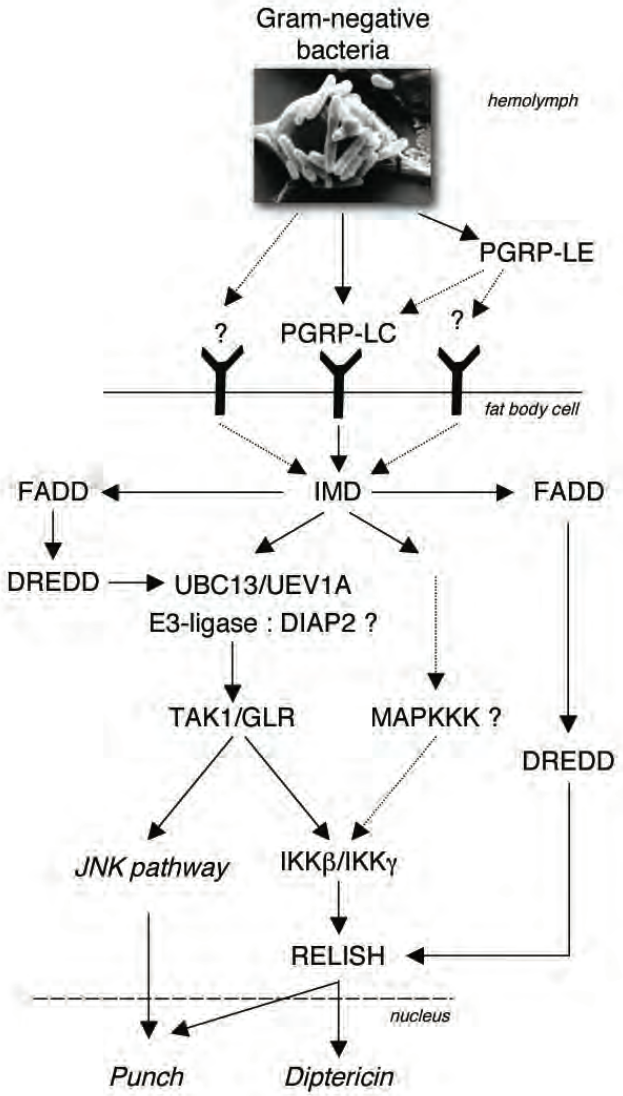
Gram-negative bacteria
hemolymph
PGRP-LE
?
PGRP-LC
?
fat body cell
FADD
IMD
FADD
DREDD
UBC13/UEV1A
E3-ligase : DIAP2 ?
TAK1/GLR
MAPKKK ?
DREDD
JNK pathway
IKKβ/IKKγ
RELISH
nucleus
Punch
Diptericin

Figure 4.11 Schematic representation of IKK signaling complex activation in the IMD pathway of *Drosophila*.

The proposed model of IMD pathway activation presented in the text

Materials and methods

Fly strains

Fly stocks were grown on standard cornmeal-agar medium at 25°C. The different genetics combinations used in this study were obtained using standard crosses with the following lines :

ywDD1 ; cn, bw : wild-type stock used for the mutagenesis in which glr_3 was generated (Jung *et al*., 2001). It carries on the X chromosome a *Diptericin-LacZ, Drosomycin-GFP* (*DD1*) reporter genes system. The glr_1 and glr_2 alleles have been generated in a *ywDD1 ; cn, bw, sp* context.

imd^1 : hypomorphic allele of the *imd* gene. *imd* null alleles will be described elsewhere.

$Tl^{9QRE1}/Df(3R)ro\text{-}XB3$: null Tl combination.

Df(2R)P34 : deficiency from the Bloomington public stock center,

Df(2R)GC8 : deficiency that distally overlaps Df(2R)P34 (Konsolaki and Schupbach, 1998).

$Toll^{10b}$*, e/TM3, e, Ser, Sb* : dominant female sterile gain-of-function allele of the Toll receptor gene, that constitutively signals to the nucleus.

Rel^{+E23} : background control for the Rel E20 null allele of Relish, (Hedengren *et al*., 1999)

yw : original stock used for the mutagenesis that generated the yw, DmelTAK1 mutants (Vidal *et al*., 2001).

P(LacW)corak08713, P(PZ)hts01103, P(LacW)htsk06121, P(LacW)RpL11k16914 : lethal P element insertions from the Bloomington stock center,

d07723, d01135, d09246, d08830, d03378 and d07259 : Flippase Recognition Target sequences containing P elements (Exelixis, Inc).

The G series of *TAB2* alleles as well as the *Df(2R)EXEL6069* deficiency are described in Geuking. *et al*. (2005).

The *UAS-glr* transgene was obtained by cloning a BglII-XhoI fragment from EST LD40663 into the same sites in the pUAS-T vector.

Microbial challenge and survival assays

Infections were performed as previously described (Rutschmann *et al*., 2000a). In this study we used the following microbial strains : *Escherichia coli 1106* (Gram-negative bacteria) alone or mixed with *Micrococcus luteus* (Gram-positive bacteria in the mix), *Enterococcus faecalis* (Gram-positive bacteria), and natural infections with *Beauveria bassiana* (entomopathogenic fungus). Each survival experiment was performed at least three times. For the double-mutants survival assay, backgrounds of the first and second chromosomes were homogenized, so as to be able to compare the phenotypes

Northern blots analysis

Northern blot analysis was carried out as previously described (Rutschmann *et al*., 2000a). Quantification was done with a BAS 2000 Bioimager and all results were standardized against the immune independent RP49 signal.

Immunolocalizations

One hour after infection with the mix of bacteria, flies were dissected and the fat body was stained with a specific rabbit anti-DIF antibody, as previously described (Rutschmann *et al*., 2000a).

Gel-shift experiments

These experiments were performed as described (Rutschmann *et al*., 2000a).

Real-Time Quantitative PCR

Quantification of transcripts : batches of 5 flies were frozen in liquid nitrogen. Total RNA extraction, R transcription and Real-Time PCR were performed as previously described (Gottar *et al*., 2002). Signals were standardized against the relevant RP49 signal, then the appropriate samples were given the value of 100%.

Deficiency mapping : Real-Time PCR experiments were run on genomic DNA

preparations of Df(2R)P34 and Df(2R)GC8 flies, using a Light Cycler **(**Roche**).** PCR reactions were set up according to the manufacturer's instructions in a 20 µL total volume. PCR steps : polymerase activation - 8 min, 45 cycles with : denaturation – 5 s at 95°C, annealing – 5 s at 60°C or 62°C (depending on the primers), elongation – 5 s at 72°C. Diptericin primers were used as a « 2 copies » positive control. Primers sequences are as follows :

Probe A : Forward (F) : 5'-CGTCGCCTTTATGGCATTAT-3'

Reverse (R) : 5’-TCGAGCAGGTAAGCGATTTT-3’

Probe B : F : 5’-ATTTGGGGGTTTCCTTGAAT-3’

R : 5’-AACAATTGCAGCACAATGGA-3’

Probe C : F : 5’-GCCAGACAAACGACACTTGA-3’

R : 5’-ACAAATTTGGCAACGAAAGC-3’

Probe F : F : 5’-TTGCCCTGGTCCTGAGTACA-3’

R : 5’-GCGAATTTCGATTTCTCACA-3’

Probe D : F : 5’-TGAAATAGGGCTGGCAAATC-3’

R : 5’-TGACTGCTATCGAATGTTTTGG-3’

Diptericin probe : F : 5’-GCTGCGCAATCGCTTCTACT-3’

R : 5’-TGGTGGAGTGGGCTTCATG-3’

Sequencing

Two different fragments of DNA were amplified by regular PCR reaction on *cn bw* and *glr* flies’ genomic DNA preparations. The first one corresponded to the second exon of *CG7417*, that contains the predicted ATG start codon ; we therefore used primers flanking this exon ; their sequence is as follows :

F : 5’-ATGGGAGGCGTTAGACAGAAAAAC-3’ and

R : 5’-ATGTATGTCCTCACGGCTCAGAAC-3’.

The second fragment corresponded to exons 3/4/5 genomic region. Primers were :

F : 5’-CCGAATGGGTGAACCGAGAAATC-3’ and

R : 5’-TGAACCCATCCCCAGCAATCC-3’.

The amplicons were then sequenced on an automated DNA sequencer

S2 cell culture, dsRNA analysis, kinase assays

These experiments have been performed as previously described (Zhou *et al*., 2005). The yeast two-hybrid experiment was performed following established protocol (Silverman *et al*., 2000).

5' RACE PCR

These experiments were performed using the Smart™ RACE cDNA amplification kit from BD Biosystem. The 3' primer was : 5' GTAAAGGGGCATGGTGGGACTACTGTC 3' and the 3' nested primer was 5' CTGCTCCTGCGTGGGATATGGGAAAAC 3':. This yielded bands of 520 bp (short transcript, Figure 4.10A) and 1750 bp (full-length transcript).

CHAPTER V

DISCUSSION

Overview

This thesis research has focused on understanding the molecular mechanisms of innate immune signal transduction in the *Drosophila* IMD pathway. In particular, the roles of ubiquitination and the MAP3 kinase TAK1 are central themes. The data shown elucidates the critical role that ubiquitination plays in *Drosophila* IMD innate immune signaling (Chapter 2). Furthermore, two novel mechanisms by which the kinase TAK1 can be regulated have also been described (Chapters 3 and 4).

As a whole the work presented in this thesis enables restructuring of the *Drosophila* IMD innate immune signaling pathway (Figure 5.1). Upon binding PGN, the PGRP-LC receptor sets in motion a series of events in which the adaptor protein IMD is cleaved by the caspase DREDD. Cleavage of IMD exposes an IAP binding motif containing a neo-N-terminal alanine at position 31, allowing IMD to interact with the BIR 2 & 3 domains of the ubiquitin E3 ligase DIAP2. In concert with the E2 conjugating enzymes, Uev1a, Bendless and Effete, IMD is then K63-polyubiquitinated. In a similar manner to that seen in mammalian NF-κB signaling, it is then proposed that this K63-polyubiquitin chain acts as a scaffold to recruit downstream TAK1 and IKK kinases. Containing a highly conserved K63-polyubiquitin binding domain, two isoforms of the TAK1 binding protein TAB2 have been demonstrated to be required for the differential activation of the downstream JNK and Relish/NF-κB arms of the IMD pathway. While both arms can utilize the long (full length) TAB2 isoform, the short isoform

Figure 5.1

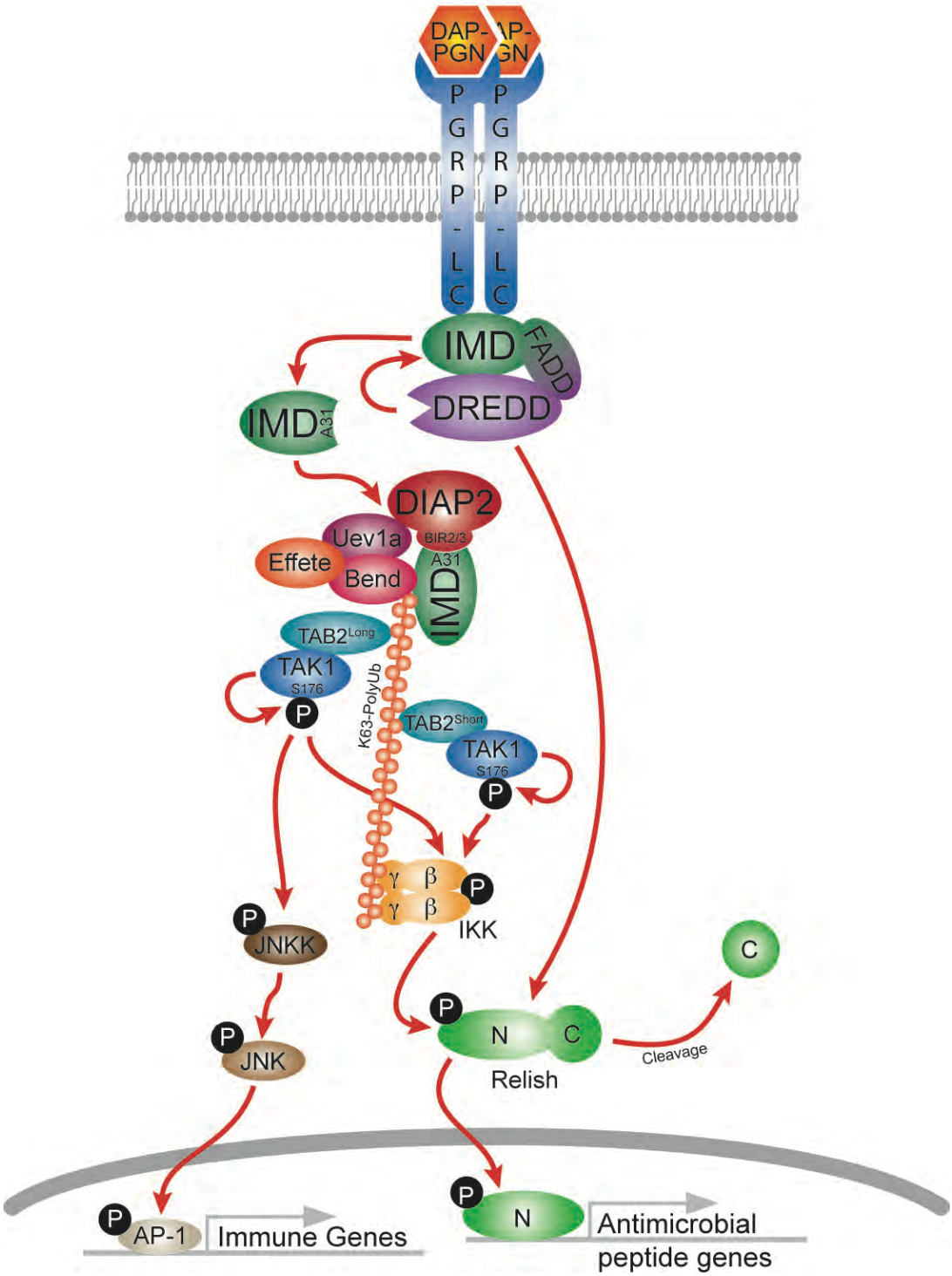
DAP-PGN
PGRP-LC
IMD
FADD
DREDD
IMD A31
DIAP2
Uev1a
BIR2/3
Effete
Bend
A31
IMD
TAB2Long
TAK1
S176
P
K63-PolyUb
TAB2Short
TAK1
S176
P
γ β
γ β
P
IKK
P
JNKK
P
JNK
P
N C
Relish
Cleavage
C
P
AP-1
Immune Genes
P
N
Antimicrobial
peptide genes

Figure 5.1 Comprehensive IMD signaling pathway model

A comprehensive model of IMD pathway signaling as described in the text.

is only able to promote activation of the Relish/NF-κB pathway. In addition, auto-phosphorylation of S176, within the activation loop of TAK1, is also required for activation of the kinase. In concert with TAB2, activated TAK1 can then initiate signaling to one or both downstream arms of the IMD pathway leading to the production of antimicrobial peptides and the activation of other immune regulated genes.

Regulation of IMD modification

As described in Chapter 2, within moments after stimulation with peptidoglycan (PGN), IMD becomes heavily modified, displaying cleaved, phosphorylated and ubiquitinated forms. However, mechanisms involved in regulation of these events remain unclear. Published work indicates that after activation, PGRP-LC receptor proteins come into proximity with one another (Chang *et al*., 2006). Furthermore, the intracellular domain of PGRP-LC is known to associate with the IMD (Aggarwal *et al*., 2008; Choe *et al*., 2005; Kaneko *et al*., 2006). In addition, unpublished work from our group indicates that DREDD (and FADD) also associates with the receptor complex. It can be proposed that activation of PGRP-LC, perhaps prebound to either IMD and/or DREDD, allows these proteins to come into close proximity facilitating the DREDD-mediated cleavage of IMD (Figure 5.2). Currently the protein domains required for these interactions are under active study.

Figure 5.2

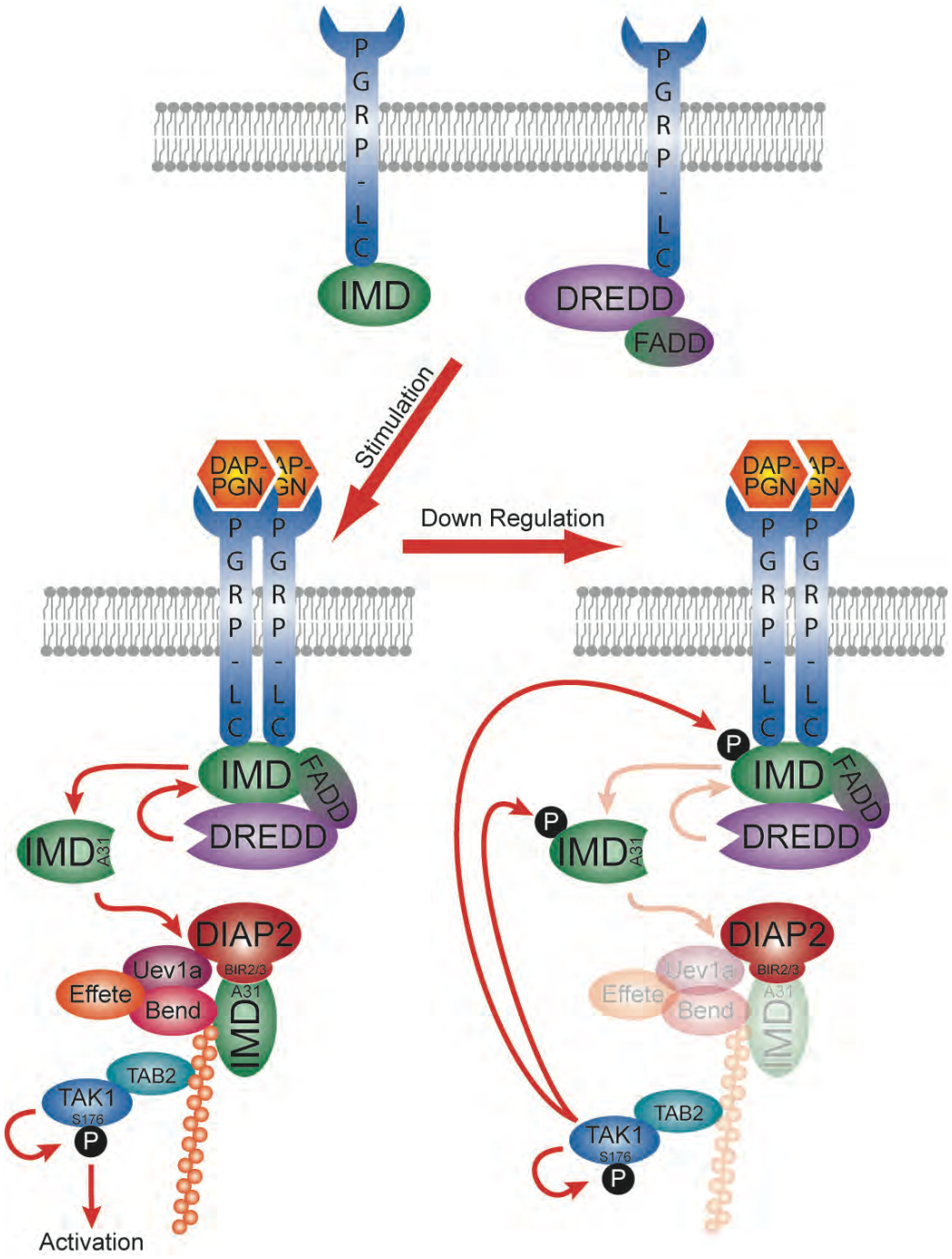
PGRP-LC
IMD
PGRP-LC
DREDD
FADD
Stimulation
Down Regulation
DAP-PGN
PGRP-LC
PGRP-LC
IMD
FADD
DREDD
IMD A31
DIAP2
Uev1a
BIR2/3
Effete
Bend
A31
IMD
TAB2
TAK1
S176
P
Activation

Figure 5.2 Down regulation of IMD signaling by phosphorylation

In an unstimulated state, PGRP-LC receptors may be bound to DREDD and/or IMD (top). Once stimulated the receptors co-localize inducing the DREDD mediated cleavage of IMD, activating signaling (bottom left). Once activated, TAK1 phosphorylates IMD in a negative feedback loop (bottom right). Phosphorylation of IMD may block cleavage and ubiquitination of the protein.

After cleavage, IMD binds DIAP2 and is K63-polyubiquitinated. As shown in Chapter 2, the kinetics behind this modification are rapid with polyubiquitination of IMD occurring within less than a minute after stimulation in S2* cells. Ubiquitination of IMD peaks at approximately 5 to 10 minutes and is largely dissipated by 30 minutes (Figure 2.6). The initial kinetics of IMD cleavage are nearly identical with cleavage occurring within one minute and peaking between 5 to 10 minutes. However, unlike ubiquitination, cleaved IMD is present for as long as 120 minutes after stimulation, long past the presence of ubiquitinated IMD (Figures 2.1B and 2.6). Interestingly, the association of IMD with DIAP2 shows a markedly different temporal pattern. This association occurs notably faster, peaking at 3 minutes, and begins to decrease immediately thereafter, in direct correlation with reduced levels of IMD ubiquitination (Figure 2.6). It is important to note that as levels of DIAP2/IMD association and IMD ubiquitination decrease, detectible phosphorylation of IMD increases. Occurring slightly slower, phosphorylation of IMD peaks at approximately 30 minutes post stimulation (Figure 2.1B and 2.6). As the presence of phosphorylated IMD seems to be inversely proportional to IMD ubiquitination an argument can be made that perhaps phosphorylation of IMD negatively regulates ubiquitination. Preliminary evidence indicates that this hypothesis may be correct. RNAi knocking down all IMD pathway kinases (TAK1, IKK, Hemipterous and Basket) indicates that only TAK1 appears to play a role in IMD phosphorylation. In addition, S2* cells which over express TAK1 show spontaneous phosphorylation

of IMD, yet fail to activate the IMD pathway. If these same cells, containing phosphorylated IMD, are then stimulated with PGN, the amount of cleaved and ubiquitinated IMD is greatly reduced compared to control cells not over expressing the kinase.

This preliminary data indicates that phosphorylation of IMD by TAK1 may play a negative regulatory role in regards to IMD ubiquitination, possibly by inhibiting the cleavage of IMD. However two lines of evidence complicate this issue. Firstly, is the presence of cleaved and phosphorylated IMD after stimulation (Figure 2.1B and 2.2). If phosphorylation of IMD blocks cleavage then how would a cleaved/phosphorylated form of IMD appear? One possible explanation is that TAK1 may be able to phosphorylate both full length and cleaved IMD. Therefore, while phosphorylation of the full length IMD may interfere with cleavage of the protein, phosphorylation of cleaved IMD may abrogate association with DIAP2 or the E2 conjugation proteins. Thus phosphorylation of IMD may play a dual role inhibiting pathway activation (Figure 5.2). Secondly, cleaved IMD is present in cell lysates after more than 120 minutes of stimulation with PGN, while ubiquitination is largely gone by 30 minutes (Figure 2.6). If cleavage of IMD is sufficient to initiate DIAP2 binding and ubiquitination, it remains unclear why this cleaved IMD is not ubiquitinated. Perhaps by 30 minutes after stimulation in S2* cells DIAP2 is saturated with cleaved IMD and although more IMD protein is cleaved it is unable to associate

with available DIAP2. Alternatively, another as of yet unidentified regulatory mechanism may play a role in the 'late' inhibition of IMD ubiquitination.

Ubiquitination of IMD

In Chapter 2, the *Drosophila* E2 ubiquitin conjugating enzyme Effete, homologous to mammalian Ubc5, is demonstrated to play an important role in the ubiquitination of IMD. In these experiments, RNAi knocking down expression of Effete, in concert with the E2 enzymes Uev1a and Bendless is able to block both IMD ubiquitination and pathway signaling as a whole. However, RNAi targeting these enzymes individually, or Uev1a and Bendless, show only partial phenotypes. While Uev1a and Bendless are known to associate *in-vivo,* it has not been determined if Effete also directly associates with this E2 complex (Zhou *et al*., 2005). These data indicate that these three E2 enzymes play a redundant or perhaps cooperative role in the ubiquitination of IMD.

In mammals, homologues to all three E2 enzymes, Uev1a, Bendless and Effete, have all been shown to play a role in ubiquitination during innate immune signaling. For example, mammalian Uev1a and Ubc13 (homologous to Bendless) have been shown to be important for K63-polyubiquitination. In particular, recent work illustrates that K63-polyubiquitin chains formed by mammalian Ubc13 after stimulation with IL-1 are required for IKK activity (Xu *et al*., 2009). Interestingly, the same study also showed that Ubc5-mediated polyubiquitin of RIP1 was required for IKK activity in the TNF pathway. In this

case however the polyubiquitin chains on RIP1 were not K63-mediated but some other unidentified linkage. Furthermore, Ubc5 was demonstrated to interact with the mammalian IAP protein cIAP1. Separately, Ubc5 has also been shown to produce unanchored polyubiquitin chains which are not conjugated to a target protein yet are sufficient to activate downstream TAK1 and IKK kinases both *in vitro* and in cell culture (Xia *et al*., 2009).

In light of the mammalian functions of these E2 proteins it can be proposed that after stimulation, IMD could be modified by the addition of multiple types of polyubiquitin chains. While Uev1a and Bendless may play a role in K63-polyubiquitination of IMD, Ubc5 (perhaps in concert with DIAP2) may promote a second form of polyubiquitination. Although IMD has been demonstrated to be K63-polyubiquitinated, this analysis does not eliminate the possible presence of other ubiquitin modifications. Multiple possibilities exist regarding the ubiquitination of IMD by Effete (Figure 5.3). First, Effete could promote polyubiquitination of IMD mediated by lysines other than lysine 48 or 63 of ubiquitin. Although K48- and K63-mediated polyubiquitination is widely described, ubiquitin also contains 5 other lysines (K6, K11, K27, K29, and K33) that could be utilized to generate polyubiquitin chains. Secondly, Effete may help promote the linear ubiquitination of IMD. Unlike lysine mediated polyubiquitin, linear ubiquitination occurs via the exposed N-terminus of a conjugated ubiquitin moiety. Identified in mammals, the role that linear ubiquitin plays during NF-κB signaling remains unclear. Lastly, Effete may promote the production of

Figure 5.3

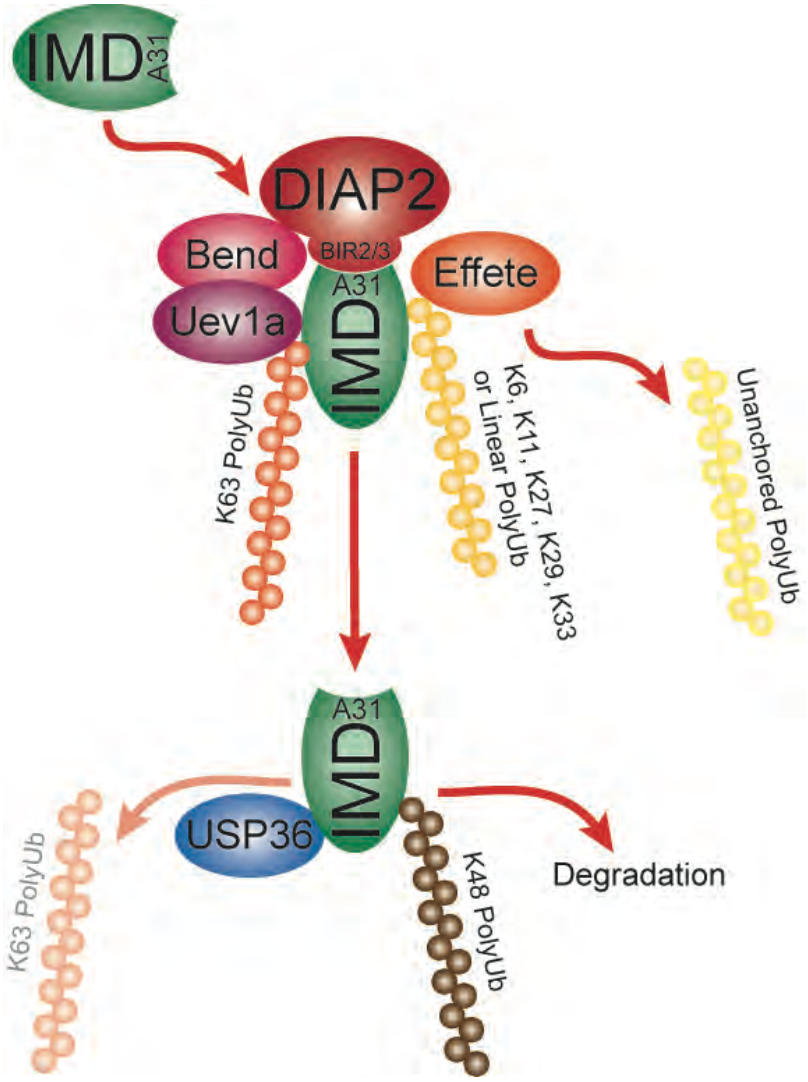
IMD
A31
DIAP2
BIR2/3
Bend
Uev1a
A31
IMD
Effete
K63 PolyUb
K6, K11, K27, K29, K33
or Linear PolyUb
Unanchored PolyUb
A31
IMD
USP36
K63 PolyUb
K48 PolyUb
Degradation

Figure 5.3 Ubiquitination of IMD

After binding DIAP2, cleaved IMD becomes ubiquitinated. The E2 enzymes Uev1a and Bendless are thought to mediate the production of K63-polyubiquitin chains. The Ubc5 homologue Effete may also promote the generation of other forms of lysine mediated or linear polyubiquitin on IMD. In concert with Effete, IMD may also serve as a source from which unanchored polyubiquitin chains are generated (Top). At a later time, the deubiquitinating enzyme USP36 removes K63-polyubiquitin chains from IMD. This promotes the production of K48-polyubiquitination and degradation of the protein (Bottom).

unanchored polyubiquitin, in a similar manner to the activity of Ubc5 observed in mammals. Although the mechanism behind production of unanchored polyubiquitin remains unclear, it is possible these chains could result from the cleavage of a polyubiquitin chain from a conjugated substrate protein, for example IMD. Further work is underway to determine if IMD is conjugated with any other types of polyubiquitin chains and to determine what role Effete plays in the additional modification. The possible presence of multiple types of polyubiquitination on IMD could also help explain the difficulty in identifying specific lysine residues of IMD required for signal transduction.

Deubiquitinating enzymes are also likely to play a significant role in the regulation of IMD pathway signaling. As mentioned earlier, the ubiquitination of IMD occurs rapidly and is largely gone by 30 minutes post PGN stimulation. Another group has identified a ubiquitin specific protease, USP36, which is able to remove the K63-polyubiquitin chains from IMD (Thevenon *et al*., 2009). By removing the IMD K63-polyubiquitin chains, USP36 is able to down regulate IMD signaling and appears to promote the K48-polyubiquitination and degradation of IMD (Figure 5.3) however the E2 and E3 enzymes involved in this event were not determined. In concert with the work described herein, these data illustrate the importance of proper regulation of polyubiquitin for IMD signaling.

Activation of TAK1

In Chapter 3, a single phospho-accepting-residue in the activation loop of TAK1, serine 176, was identified as being vital for kinase activity. In mammals, a model has been proposed in which TAK1 is activated by auto-phosphorylation within the activation loop in trans (Xia *et al*., 2009). Most likely, a similar event is also present in *Drosophila* (Figure 5.4A), however, this does not account for the additional phosphorylated residues identified outside the activation loop of *Drosophila* TAK1 after over expression and activation of the protein (Table 3.6). The manner in which these phosphorylations occur remains unclear. These sites may be auto-phosphorylated, in cis or trans, after phosphorylation within the activation loop, and be required for proper activation of the kinase. Alternatively, phosphorylation of downstream kinases by TAK1 could lead to feedback mediated phosphorylation of these sites.

Furthermore, data in Chapter 3 also illustrates that the acetylation of two highly conserved threonine residues, T168 and T171, within the activation loop of TAK1 is sufficient to block auto-phosphorylation and activation of the kinase. In mammals, but not *Drosophila*, these two theronines are also phosphorylated. It is unclear why acetylation of these two residues in *Drosophila* TAK1 is able to block the phosphorylation and activation of this kinase. One possible explanation is that these residues play a role in TAK-TAK trans-interactions required for auto-phosphorylation and activation (Figure 5.4A). If these threonines are modified by acetylation the TAK-TAK interaction may be abrogated, thus inhibiting auto-

Figure 5.4

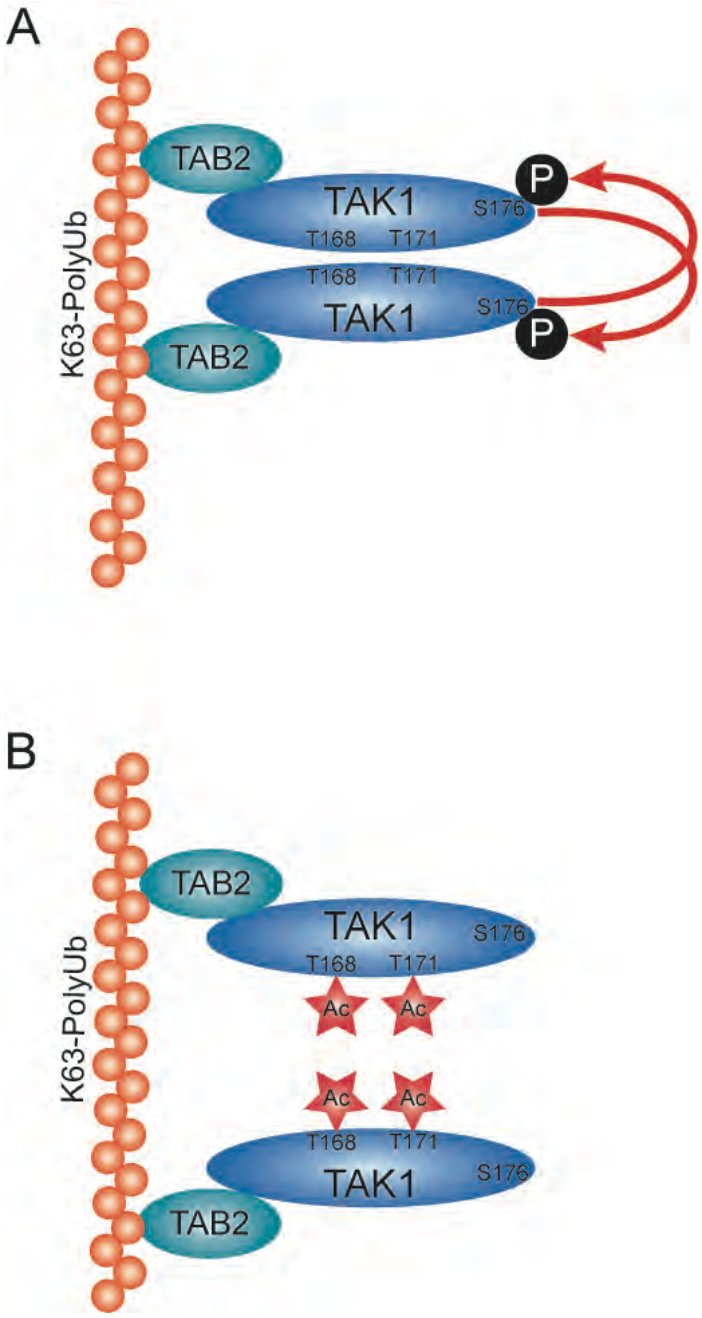
A
TAB2
TAK1
S176
T168
T171
P
T168
T171
TAK1
S176
P
TAB2
K63-PolyUb
B
TAB2
TAK1
S176
T168
T171
Ac
Ac
Ac
Ac
T168
T171
TAK1
S176
TAB2
K63-PolyUb

Figure 5.4 Activation of TAK1

(A) After binding the K63-polyubiquitin scaffold via TAB2, auto-phosphorylation (P) of TAK1 at serine 176 likely occurs in trans, in a similar manner to activation of mammalian TAK1. (B) Acetylation (Ac) of threonines 168 and 171, may block this TAK-TAK interaction rendering the kinases unable to cross activate, down-regulating the immune response.

phosphorylation and activity. Alternately, acetylation of these residues may force a conformational change in the activation loop rendering it inactive. An in depth analysis will be required to determine the functional effects of the multiple phosphorylations found on TAK1 and the manner in which they are generated.

Association with TAB2

There has been much controversy as to the role, if any, that JNK signaling plays during Relish/NF-κB antimicrobial peptide production. Several reports indicate that these two pathways may cross regulate, with each down-modulating the action of the other (Park *et al*., 2004; Kim *et al*., 2005). However, Delaney *et al.,* (2006) proposed a contradictory model in which TAK1/JNK activation is required for AMP gene induction in the larval fat body. The work described in Chapter 4 demonstrates that 2 forms of TAB2 are present in *Drosophila* and that RNAi treatment targeting the long (full length) isoform is able to uncouple JNK and Relish/NF-κB signaling. In these cells, JNK signaling is inhibited while AMP gene production proceeds as normal. Phenotypically similar TAB2 mutant flies (*TAB2*^{666}), also fail to robustly activate JNK signaling yet remain resistant to infection by *E. coli*. These data are consistent with the notion that JNK signaling is not required for activation of AMPs by the Relish/NF-κB arm of the IMD pathway.

In mammals TAB proteins have been shown to be critical components during NF-κB pathway activation by binding K63-polyubiquitin chains. Mediating

the association and activation of TAK1, the presence of TAB proteins is essential for signaling in both mammals and insects. Interestingly, in mammals, the TAB family protein TAB1 was shown to interact with the IAP protein XIAP. This interaction takes place utilizing the BIR1 domain of XIAP and is critical for TAK1 activation. As both TAB and IAP family members are involved in IMD pathway signaling a similar precedent may hold true. Unpublished work from our collaborators indicates that when co-expressed *Drosophila* TAB2 and DIAP2 associate, although the domains required for this interaction remain undetermined. TAB2 also appears to be critical for stabilization of IMD pathway components and viability of cells in culture. Treatment of S2* cells with RNAi targeting TAB2 for 3 days is sufficient to inhibit IMD pathway signaling. However, extended exposure (longer than 4 days) to TAB2 RNAi results in decreased TAK1 and DIAP2 protein levels, as well as decreased cell viability. This phenotype appears to be unique to TAB2 as RNAi treatment targeting other IMD pathway members does not display the same effects. These data strongly indicate that TAB2 associates with both TAK1 and DIAP2 prior to stimulation and that this association is critical for the stabilization of these two proteins.

Defining a mammalian counterpart

Vertebrate homologues of the *Drosophila* proteins described in this work have been implicated in immune signaling yet their interactions and functions in many cases remain largely unclassified. Lacking an adaptive immune response,

Drosophila serve as an important model system for the further understanding of innate immunity and host/pathogen interactions. To that end, this research helps to illuminate the mechanisms by which caspase mediated cleavage, ubiquitination, protein/protein interactions and kinase activation play a role in insect NF-κB signaling, and shed light onto how similar events may occur in mammals.

A similar scenario could be proposed for mammalian NF-κB signaling in which stimulation leads to the caspase-8 mediated cleavage of RIP1 exposing an IAP binding motif (IBM). This exposed IBM would then bind the BIR domains of cIAP1/2 promoting K63-polyubiquitination. Although IMD is considered to be similar to RIP1, the two proteins share little sequence homology outside their death domains. Unlike IMD, RIP1 also contains a kinase domain which is dispensable for NF-κB pathway activation. Therefore, RIP1 may not be the functional IMD homologue involved in capase mediated cleavage during mammalian signaling, instead TRAFs or some alternative protein may undertake this role. For such a hypothesis to hold true, these proteins must contain a caspase cleavage site immediately adjacent to an IBM. Although *in-silico* analysis of both mouse and human TRAF2, TRAF6, RIP1 and RIP2 proteins identifies a number of possible caspase cleavage sites, no obvious IBMs are seen in tandem. However, this does not eliminate the possibility that an atypical IBM is present or that another protein is cleaved and ubiquitinated. Further

research within mammalian systems is currently underway to determine whether a similar paradigm holds true.

REFERENCES

Aggarwal, K. et al. (2008). Rudra interrupts receptor signaling complexes to negatively regulate the IMD pathway. PLoS Pathog 4: e1000120.

Akira, S., Uematsu, S., and Takeuchi, O. (2006). Pathogen recognition and innate immunity. Cell 124: 783–801.

Amerik, A.Y., and Hochstrasser, M. (2004). Mechanism and function of deubiquitinating enzymes. Biochim Biophys Acta 1695: 189–207.

Asling, B., Dushay, M.S., and Hultmark, D. (1995). Identification of early genes in the Drosophila immune response by PCR-based differential display: the Attacin A gene and the evolution of attacin-like proteins. Insect Biochem Mol Biol 25: 511–518.

Bachmair, A., Finley, D., and Varshavsky, A. (1986). In vivo half-life of a protein is a function of its amino-terminal residue. Science 234: 179–186.

Baek, S.H. et al. (2002). Exchange of N-CoR corepressor and Tip60 coactivator complexes links gene expression by NF-kappaB and beta-amyloid precursor protein. Cell 110: 55–67.

Balachandran, S., Thomas, E., and Barber, G.N. (2004). A FADD-dependent innate immune mechanism in mammalian cells. Nature 432: 401–405.

Belvin, M.P., Jin, Y., and Anderson, K.V. (1995). Cactus protein degradation mediates Drosophila dorsal-ventral signaling. Genes Dev 9: 783–793.

Bergmann, A. et al. (1996). A gradient of cytoplasmic Cactus degradation establishes the nuclear localization gradient of the dorsal morphogen in Drosophila. Mech Dev 60: 109–123.

Bernassola, F., Karin, M., Ciechanover, A., and Melino, G. (2008). The HECT family of E3 ubiquitin ligases: multiple players in cancer development. Cancer Cell 14: 10–21.

Bertrand, M.J. et al. (2009). Cellular inhibitors of apoptosis cIAP1 and cIAP2 are required for innate immunity signaling by the pattern recognition receptors NOD1 and NOD2. Immunity 30: 789–801.

Bertrand, M.J. et al. (2008). cIAP1 and cIAP2 facilitate cancer cell survival by functioning as E3 ligases that promote RIP1 ubiquitination. Mol Cell 30: 689–700.

Bidere, N., Snow, A.L., Sakai, K., Zheng, L., and Lenardo, M.J. (2006). Caspase-8 regulation by direct interaction with TRAF6 in T cell receptor-induced NF-kappaB activation. Curr Biol 16: 1666–1671.

Bischoff, V. et al. (2004). Function of the Drosophila pattern-recognition receptor PGRP-SD in the detection of Gram-positive bacteria. Nat Immunol 5: 1175–1180.

Boman, H.G., Nilsson, I., and Rasmuson, B. (1972). Inducible antibacterial defence system in Drosophila. Nature 237: 232–235.

Boutros, M., Agaisse, H., and Perrimon, N. (2002). Sequential Activation of Signaling Pathways during Innate Immune Responses in Drosophila. Dev Cell 3: 711–722.

Brandt, S.M. et al. (2004). Secreted Bacterial Effectors and Host-Produced Eiger/ TNF Drive Death in aSalmonella-Infected Fruit Fly. PLoS Biol 2: e418.

Brey, P.T. (1998). The contributions of the Pasteur school of insect immunity in Molecular mechanisms of immune responses in insects. (London: Chapman &Hall).

Brodsky, M.H. et al. (2000). Drosophila p53 binds a damage response element at the reaper locus. Cell 101: 103–113.

Burns, K. et al. (1998). MyD88, an adapter protein involved in interleukin-1 signaling. J Biol Chem 273: 12203–12209.

Cao, Z., Henzel, W.J., and Gao, X. (1996). IRAK: a kinase associated with the interleukin-1 receptor. Science 271: 1128–1131.

Chang, C.I., Chelliah, Y., Borek, D., Mengin-Lecreulx, D., and Deisenhofer, J. (2006). Structure of Trachael Cytotoxin in Complex with a Heterodimeric Pattern-Recognition Receptor. Science 311: 1761–1764.

Chang, L., and Karin, M. (2001). Mammalian MAP kinase signalling cascades. Nature 410: 37–40.

Chaves-Carballo, E. (2005). Carlos Finlay and yellow fever: triumph over adversity. Mil Med 170: 881–885.

Chen, W., White, M.A., and Cobb, M.H. (2002). Stimulus-specific requirements for MAP3 kinases in activating the JNK pathway. J Biol Chem 277: 49105–49110.

Chen, Z.J. (2005). Ubiquitin signalling in the NF-kappaB pathway. Nat Cell Biol 7: 758–765.

Chen, Z.J., Parent, L., and Maniatis, T. (1996). Site-specific phosphorylation of IkBa by a novel ubiquitination-dependent protein kinase activity. Cell 84: 853–862.

Cheng, H. et al. (2007). Regulation of IRAK-4 kinase activity via autophosphorylation within its activation loop. Biochem Biophys Res Commun 352: 609–616.

Cheung, P.C., Nebreda, A.R., and Cohen, P. (2004). TAB3, a new binding partner of the protein kinase TAK1. Biochem J 378: 27–34.

Chiang, P.W., Wei, W.L., Gibson, K., Bodmer, R., and Kurnit, D.M. (1999). A fluorescent quantitative PCR approach to map gene deletions in the Drosophila genome. Genetics 153: 1313–1316.

Chiu, Y.H., Zhao, M., and Chen, Z.J. (2009). Ubiquitin in NF-kappaB Signaling. Chem Rev

Choe, K.M., Lee, H., and Anderson, K.V. (2005). Drosophila peptidoglycan recognition protein LC (PGRP-LC) acts as a signal-transducing innate immune receptor. Proc Natl Acad Sci U S A 102: 1122–1126.

Choe, K.M., Werner, T., Stöven, S., Hultmark, D., and Anderson, K.V. (2002). Requirement for a peptidoglycan recognition protein (PGRP) in Relish activation and antibacterial immune responses in Drosophila. Science 296: 359–362.

Chun, H.J. et al. (2002). Pleiotropic defects in lymphocyte activation caused by caspase-8 mutations lead to human immunodeficiency. Nature 419: 395–399.

De Gregorio, E., Spellman, P.T., Rubin, G.M., and Lemaitre, B. (2001). Genome-wide analysis of the Drosophila immune response by using oligonucleotide microarrays. Proc Natl Acad Sci U S A 98: 12590–12595.

De Gregorio, E., Spellman, P.T., Tzou, P., Rubin, G.M., and Lemaitre, B. (2002). The Toll and Imd pathways are the major regulators of the immune response in Drosophila. Embo J 21: 2568–2579.

Delaney, J.R., and Mlodzik, M. (2006). TGF-beta activated kinase-1: new insights into the diverse roles of TAK1 in development and immunity. Cell Cycle 5: 2852–2855.

Delaney, J.R. et al. (2006). Cooperative control of Drosophila immune responses by the JNK and NF-kappaB signaling pathways. Embo J 25: 3068–3077.

Deng, L. et al. (2000). Activation of the IkappaB kinase complex by TRAF6 requires a dimeric ubiquitin-conjugating enzyme complex and a unique polyubiquitin chain. Cell 103: 351–61.

Deveraux, Q.L., and Reed, J.C. (1999). IAP family proteins--suppressors of apoptosis. Genes Dev 13: 239–252.

Di Fiore, P.P., Polo, S., and Hofmann, K. (2003). When ubiquitin meets ubiquitin receptors: a signalling connection. Nat Rev Mol Cell Biol 4: 491–497.

Dimarcq, J.L. et al. (1994). Characterization and transcriptional profiles of a Drosophila gene encoding an insect defensin. A study in insect immunity. Eur J Biochem 221: 201–209.

Drier, E.A., and Steward, R. (1997). The dorsoventral signal transduction pathway and the Rel-like transcription factors in Drosophila. Semin Cancer Biol 8: 83–92.

Dunne, A., and O'Neill, L.A. (2003). The interleukin-1 receptor/Toll-like receptor superfamily: signal transduction during inflammation and host defense. Sci STKE 2003: re3.

Dushay, M.S., Åsling, B., and Hultmark, D. (1996). Origins of immunity: Relish, a compound Rel-like gene in the antibacterial defense of Drosophila. Proc. Natl. Acad. Sci. USA 93: 10343–10347.

Ea, C.K., Deng, L., Xia, Z.P., Pineda, G., and Chen, Z.J. (2006). Activation of IKK by TNFalpha requires site-specific ubiquitination of RIP1 and polyubiquitin binding by NEMO. Mol Cell 22: 245–257.

Ekengren, S., and Hultmark, D. (1999). Drosophila cecropin as an antifungal agent. Insect Biochem Mol Biol 29: 965–972.

Elrod-Erickson, M., Mishra, S., and Schneider, D. (2000). Interactions between the cellular and humoral immune responses in drosophila. Curr Biol 10: 781–784.

Erturk-Hasdemir, D. et al. (2009). Two roles for the Drosophila IKK complex in the activation of Relish and the induction of antimicrobial peptide genes. Proc Natl Acad Sci U S A 106: 9779–9784.

Ferrandon, D., Imler, J.L., Hetru, C., and Hoffmann, J.A. (2007). The Drosophila systemic immune response: sensing and signalling during bacterial and fungal infections. Nat Rev Immunol 7: 862–874.

Ferrandon, D. et al. (1998). A drosomycin-GFP reporter transgene reveals a local immune response in Drosophila that is not dependent on the Toll pathway. Embo J 17: 1217–1227.

Fitzgerald, K.A. et al. (2003). IKKepsilon and TBK1 are essential components of the IRF3 signaling pathway. Nat Immunol 4: 491–496.

Fitzgerald, K.A. et al. (2001). Mal (MyD88-adapter-like) is required for Toll-like receptor-4 signal transduction. Nature 413: 78–83.

Geetha, T., Kenchappa, R.S., Wooten, M.W., and Carter, B.D. (2005). TRAF6-mediated ubiquitination regulates nuclear translocation of NRIF, the p75 receptor interactor. Embo J 24: 3859–3868.

Georgel, P. et al. (2001). Drosophila immune deficiency (IMD) is a death domain protein that activates antibacterial defense and can promote apoptosis. Dev Cell 1: 503–514.

Gesellchen, V., Kuttenkeuler, D., Steckel, M., Pelte, N., and Boutros, M. (2005). An RNA interference screen identifies Inhibitor of Apoptosis Protein 2 as a regulator of innate immune signalling in Drosophila. EMBO Rep 6: 979–984.

Geuking, P., Narasimamurthy, R., and Basler, K. (2005). A genetic screen targeting the tumor necrosis factor/Eiger signaling pathway: identification of

Drosophila TAB2 as a functionally conserved component. Genetics 171: 1683–1694.

Gillespie, S.K., and Wasserman, S.A. (1994). Dorsal, a Drosophila Rel-like protein, is phosphorylated upon activation of the transmembrane protein Toll. Mol Cell Biol 14: 3559–3568.

Giot, L. et al. (2003). A protein interaction map of Drosophila melanogaster. Science 302: 1727–1736.

Glickman, M.H., and Ciechanover, A. (2002). The ubiquitin-proteasome proteolytic pathway: destruction for the sake of construction. Physiol Rev 82: 373–428.

Gobert, V. et al. (2003). Dual activation of the Drosophila Toll pathway by two pattern recognition receptors. Science 302: 2126–2130.

Gottar, M. et al. (2002). The Drosophila immune response against Gram-negative bacteria is mediated by a peptidoglycan recognition protein. Nature 416: 640–644.

Hacker, H., and Karin, M. (2006). Regulation and function of IKK and IKK-related kinases. Sci STKE 2006: re13.

Hacker, H. et al. (2006). Specificity in Toll-like receptor signalling through distinct effector functions of TRAF3 and TRAF6. Nature 439: 204–207.

Hedengren, M. et al. (1999). Relish, a central factor in the control of humoral but not cellular immunity in Drosophila. Mol. Cell 4: 827–837.

Heimpel, A.M., and Harshbarger, J.C. (1965). Symposium on microbial insecticides. V. Immunity in insects. Bacteriol Rev 29: 397–405.

Hershko, A. (1983). Ubiquitin: roles in protein modification and breakdown. Cell 34: 11–12.

Hicke, L. (2001). Protein regulation by monoubiquitin. Nat Rev Mol Cell Biol 2: 195–201.

Hoffmann, A., and Baltimore, D. (2006). Circuitry of nuclear factor kappaB signaling. Immunol Rev 210: 171–186.

Hoffmann, J.A. (2003). The immune response of Drosophila. Nature 426: 33–38.

Holland, P.M., Suzanne, M., Campbell, J.S., Noselli, S., and Cooper, J.A. (1997). MKK7 is a stress-activated mitogen-activated protein kinase kinase functionally related to hemipterous. J Biol Chem 272: 24994–24998.

Horng, T., Barton, G.M., Flavell, R.A., and Medzhitov, R. (2002). The adaptor molecule TIRAP provides signalling specificity for Toll-like receptors. Nature 420: 329–333.

Hsu, H., Huang, J., Shu, H.B., Baichwal, V., and Goeddel, D.V. (1996a). TNF-dependent recruitment of the protein kinase RIP to the TNF receptor-1 signaling complex. Immunity 4: 387–396.

Hsu, H., Shu, H.B., Pan, M.G., and Goeddel, D.V. (1996b). TRADD-TRAF2 and TRADD-FADD interactions define two distinct TNF receptor 1 signal transduction pathways. Cell 84: 299–308.

Hu, S., and Yang, X. (2000). dFADD, a novel death domain-containing adapter protein for the Drosophila caspase DREDD. J Biol Chem 275: 30761–3074.

Hu, X., Yagi, Y., Tanji, T., Zhou, S., and Ip, Y.T. (2004). Multimerization and interaction of Toll and Spatzle in Drosophila. Proc Natl Acad Sci U S A 101: 9369–9374.

Huh, J.R. et al. (2007). The Drosophila inhibitor of apoptosis (IAP) DIAP2 is dispensable for cell survival, required for the innate immune response to gram-negative bacterial infection, and can be negatively regulated by the reaper/hid/grim family of IAP-binding apoptosis inducers. J Biol Chem 282: 2056–2068.

Hultmark, D. et al. (1983). Insect immunity. Attacins, a family of antibacterial proteins from Hyalophora cecropia. Embo J 2: 571–576.

Idriss, H.T., and Naismith, J.H. (2000). TNF alpha and the TNF receptor superfamily: structure-function relationship(s). Microsc Res Tech 50: 184–195.

Igaki, T. et al. (2002). Eiger, a TNF superfamily ligand that triggers the Drosophila JNK pathway. Embo J 21: 3009–3018.

Iriarte, M., and Cornelis, G.R. (1996). Molecular determinants of Yersinia pathogenesis. Microbiologia 12: 267–280.

Irving, P. et al. (2001). A genome-wide analysis of immune responses in Drosophila. Proc Natl Acad Sci U S A 98: 15119–15124.

Ishitani, T. et al. (2003). Role of the TAB2-related protein TAB3 in IL-1 and TNF signaling. Embo J 22: 6277–6288.

Jang, I.H. et al. (2006). A Spatzle-processing enzyme required for toll signaling activation in Drosophila innate immunity. Dev Cell 10: 45–55.

Jiang, Z., Ninomiya-Tsuji, J., Qian, Y., Matsumoto, K., and Li, X. (2002). Interleukin-1 (IL-1) receptor-associated kinase-dependent IL-1-induced signaling complexes phosphorylate TAK1 and TAB2 at the plasma membrane and activate TAK1 in the cytosol. Mol Cell Biol 22: 7158–7167.

Jung, A.C., Criqui, M.C., Rutschmann, S., Hoffmann, J.A., and Ferrandon, D. (2001). Microfluorometer assay to measure the expression of beta-galactosidase and green fluorescent protein reporter genes in single Drosophila flies. Biotechniques 30: 594–8, 600-1.

Kambris, Z. et al. (2006). Drosophila immunity: a large-scale in vivo RNAi screen identifies five serine proteases required for Toll activation. Curr Biol 16: 808–813.

Kanayama, A. et al. (2004). TAB2 and TAB3 activate the NF-kappaB pathway through binding to polyubiquitin chains. Mol Cell 15: 535–548.

Kaneko, T. et al. (2004). Monomeric and Polymeric Gram-Negative Peptidoglycan but Not Purified LPS Stimulate the Drosophila IMD Pathway. Immunity 20: 637–649.

Kaneko, T. et al. (2006). PGRP-LC and PGRP-LE have essential yet distinct functions in the drosophila immune response to monomeric DAP-type peptidoglycan. Nat Immunol 7: 715–723.

Kang, R.S. et al. (2003). Solution structure of a CUE-ubiquitin complex reveals a conserved mode of ubiquitin binding. Cell 113: 621–630.

Kawagoe, T. et al. (2008). Sequential control of Toll-like receptor-dependent responses by IRAK1 and IRAK2. Nat Immunol 9: 684–691.

Kawai, T., Adachi, O., Ogawa, T., Takeda, K., and Akira, S. (1999). Unresponsiveness of MyD88-deficient mice to endotoxin. Immunity 11: 115–122.

Keating, S.E., Maloney, G.M., Moran, E.M., and Bowie, A.G. (2007). IRAK-2 participates in multiple toll-like receptor signaling pathways to NFkappaB via activation of TRAF6 ubiquitination. J Biol Chem 282: 33435–33443.

Khush, R.S., Cornwell, W.D., Uram, J.N., and Lemaitre, B. (2002). A ubiquitin-proteasome pathway represses the Drosophila immune deficiency signaling cascade. Curr Biol 12: 1728–1737.

Kim, H.M. et al. (2007). Crystal structure of the TLR4-MD-2 complex with bound endotoxin antagonist Eritoran. Cell 130: 906–917.

Kim, T. et al. (2005). Downregulation of lipopolysaccharide response in Drosophila by negative crosstalk between the AP1 and NF-kappaB signaling modules. Nat Immunol 6: 211–218.

Kim, Y.-S. et al. (2000). Lipopolysaccharide-activated kinase, an essential component for the induction of the antimicrobial peptide genes in *Drosophila melanogaster* cells. J. Biol. Chem. 275: 2071–2079.

Kirisako, T. et al. (2006). A ubiquitin ligase complex assembles linear polyubiquitin chains. Embo J 25: 4877–4887.

Kishida, S., Sanjo, H., Akira, S., Matsumoto, K., and Ninomiya-Tsuji, J. (2005). TAK1-binding protein 2 facilitates ubiquitination of TRAF6 and assembly of TRAF6 with IKK in the IL-1 signaling pathway. Genes Cells 10: 447–454.

Kishimoto, K., Matsumoto, K., and Ninomiya-Tsuji, J. (2000). TAK1 mitogen-activated protein kinase kinase kinase is activated by autophosphorylation within its activation loop. J Biol Chem 275: 7359–7364.

Kleino, A. et al. (2005). Inhibitor of apoptosis 2 and TAK1-binding protein are components of the Drosophila Imd pathway. Embo J 24: 3423–3434.

Kollewe, C. et al. (2004). Sequential autophosphorylation steps in the interleukin-1 receptor-associated kinase-1 regulate its availability as an adapter in interleukin-1 signaling. J Biol Chem 279: 5227–5236.

Komander, D. et al. (2009). Molecular discrimination of structurally equivalent Lys 63-linked and linear polyubiquitin chains. EMBO Rep 10: 466–473.

Konsolaki, M., and Schupbach, T. (1998). windbeutel, a gene required for dorsoventral patterning in Drosophila, encodes a protein that has homologies to vertebrate proteins of the endoplasmic reticulum. Genes Dev 12: 120–131.

Kovalenko, A. et al. (2003). The tumour suppressor CYLD negatively regulates NF-kappaB signalling by deubiquitination. Nature 424: 801–805.

Krikos, A., Laherty, C.D., and Dixit, V.M. (1992). Transcriptional activation of the tumor necrosis factor alpha-inducible zinc finger protein, A20, is mediated by kappa B elements. J Biol Chem 267: 17971–17976.

Kylsten, P., Samakovlis, C., and Hultmark, D. (1990). The cecropin locus in Drosophila; a compact gene cluster involved in the response to infection. Embo J 9: 217–224.

Lamothe, B. et al. (2007). Site-specific Lys-63-linked tumor necrosis factor receptor-associated factor 6 auto-ubiquitination is a critical determinant of I kappa B kinase activation. J Biol Chem 282: 4102–4112.

Laplantine, E. et al. (2009). NEMO specifically recognizes K63-linked poly-ubiquitin chains through a new bipartite ubiquitin-binding domain. Embo J

Lee, T.H., Shank, J., Cusson, N., and Kelliher, M.A. (2004). The kinase activity of Rip1 is not required for tumor necrosis factor-alpha-induced IkappaB kinase or p38 MAP kinase activation or for the ubiquitination of Rip1 by Traf2. J Biol Chem 279: 33185–33191.

Lemaitre, B., and Hoffmann, J. (2007). The Host Defense of Drosophila melanogaster. Annu Rev Immunol 25: 697–743.

Lemaitre, B., Nicolas, E., Michaut, L., Reichhart, J.M., and Hoffmann, J.A. (1996). The dorsoventral regulatory gene cassette spätzle/Toll/cactus controls the potent antifungal response in Drosophila adults. Cell 86: 973–983.

Lemaitre, B., Reichhart, J.M., and Hoffmann, J.A. (1997). Drosophila host defense: differential induction of antimicrobial peptide genes after infection by various classes of microorganisms. Proc. Natl. Acad. Sci. USA 94: 14614–14619.

Lemmers, B. et al. (2007). Essential role for caspase-8 in Toll-like receptors and NFkappaB signaling. J Biol Chem 282: 7416–7423.

Leulier, F., Lhocine, N., Lemaitre, B., and Meier, P. (2006). The Drosophila inhibitor of apoptosis protein DIAP2 functions in innate immunity and is essential to resist gram-negative bacterial infection. Mol Cell Biol 26: 7821–7831.

Leulier, F. et al. (2003). The Drosophila immune system detects bacteria through specific peptidoglycan recognition. Nat Immunol 4: 478–484.

Leulier, F., Rodriguez, A., Khush, R.S., Abrams, J.M., and Lemaitre, B. (2000). The *Drosophila* caspase Dredd is required to resist Gram-negative bacterial infection. EMBO Reports 1: 353–358.

Leulier, F., Vidal, S., Saigo, K., Ueda, R., and Lemaitre, B. (2002). Inducible expression of double-stranded RNA reveals a role for dFADD in the regulation of the antibacterial response in Drosophila adults. Curr Biol 12: 996–1000.

Levashina, E.A. et al. (1995). Metchnikowin, a novel immune-inducible proline-rich peptide from Drosophila with antibacterial and antifungal properties. Eur J Biochem 233: 694–700.

Levitin, A., and Whiteway, M. (2008). Drosophila innate immunity and response to fungal infections. Cell Microbiol 10: 1021–1026.

Li, S., Wang, L., and Dorf, M.E. (2009). PKC phosphorylation of TRAF2 mediates IKKalpha/beta recruitment and K63-linked polyubiquitination. Mol Cell 33: 30–42.

Li, X. et al. (1999). Mutant cells that do not respond to interleukin-1 (IL-1) reveal a novel role for IL-1 receptor-associated kinase. Mol Cell Biol 19: 4643–452.

Liehl, P., Blight, M., Vodovar, N., Boccard, F., and Lemaitre, B. (2006). Prevalence of local immune response against oral infection in a Drosophila/ Pseudomonas infection model. PLoS Pathog 2: e56.

Ligoxygakis, P., Pelte, N., Hoffmann, J.A., and Reichhart, J.M. (2002). Activation of Drosophila Toll during fungal infection by a blood serine protease. Science 297: 114–116.

Lim, J.H. et al. (2006). Structural Basis for Preferential Recognition of Diaminopimelic Acid-type Peptidoglycan by a Subset of Peptidoglycan Recognition Proteins. J Biol Chem 281: 8286–8295.

Liu, Z.P., Galindo, R.L., and Wasserman, S.A. (1997). A role for CKII phosphorylation of the cactus PEST domain in dorsoventral patterning of the Drosophila embryo. Genes Dev 11: 3413–3422.

Lu, Y., Wu, L.P., and Anderson, K.V. (2001). The antibacterial arm of the drosophila innate immune response requires an IkappaB kinase. Genes Dev 15: 104–10.

Lupas, A., Van Dyke, M., and Stock, J. (1991). Predicting coiled coils from protein sequences. Science 252: 1162–1164.

Marketon, M.M., DePaolo, R.W., DeBord, K.L., Jabri, B., and Schneewind, O. (2005). Plague bacteria target immune cells during infection. Science 309: 1739–1741.

Mercurio, F. et al. (1997). IKK-1 and IKK-2: cytokine-activated IkB kinases essential for NF- kB activation. Science 278: 860–866.

Meylan, E. et al. (2004). RIP1 is an essential mediator of Toll-like receptor 3-induced NF-kappa B activation. Nat Immunol 5: 503–507.

Michaut, L. et al. (1996). Determination of the disulfide array of the first inducible antifungal peptide from insects: drosomycin from Drosophila melanogaster. FEBS Lett 395: 6–10.

Michel, T., Reichhart, J.M., Hoffmann, J.A., and Royet, J. (2001). Drosophila Toll is activated by Gram-positive bacteria through a circulating peptidoglycan recognition protein. Nature 414: 756–759.

Mittal, R., Peak-Chew, S.Y., and McMahon, H.T. (2006). Acetylation of MEK2 and I kappa B kinase (IKK) activation loop residues by YopJ inhibits signaling. Proc Natl Acad Sci U S A 103: 18574–18579.

Mollah, S. et al. (2007). Targeted mass spectrometric strategy for global mapping of ubiquitination on proteins. Rapid Commun Mass Spectrom 21: 3357–3364.

Monack, D.M., Mecsas, J., Bouley, D., and Falkow, S. (1998). Yersinia-induced apoptosis in vivo aids in the establishment of a systemic infection of mice. J Exp Med 188: 2127–2137.

Monack, D.M., Mecsas, J., Ghori, N., and Falkow, S. (1997). Yersinia signals macrophages to undergo apoptosis and YopJ is necessary for this cell death. Proc Natl Acad Sci U S A 94: 10385–10390.

Mukherjee, S. et al. (2006). Yersinia YopJ acetylates and inhibits kinase activation by blocking phosphorylation. Science 312: 1211–1214.

Mukhopadhyay, D., and Riezman, H. (2007). Proteasome-independent functions of ubiquitin in endocytosis and signaling. Science 315: 201–205.

Naitza, S. et al. (2002). The Drosophila immune defense against gram-negative infection requires the death protein dFADD. Immunity 17: 575–581.

Nicolas, E., Reichhart, J.M., Hoffmann, J.A., and Lemaitre, B. (1998). In vivo regulation of the IkappaB homologue cactus during the immune response of Drosophila. J Biol Chem 273: 10463–10469.

O'Neill, L.A., and Bowie, A.G. (2007). The family of five: TIR-domain-containing adaptors in Toll-like receptor signalling. Nat Rev Immunol 7: 353–364.

Oganesyan, G. et al. (2006). Critical role of TRAF3 in the Toll-like receptor-dependent and -independent antiviral response. Nature 439: 208–211.

Ordureau, A. et al. (2008). The IRAK-catalysed activation of the E3 ligase function of Pellino isoforms induces the Lys63-linked polyubiquitination of IRAK1. Biochem J 409: 43–52.

Palmer, L.E., Hobbie, S., Galan, J.E., and Bliska, J.B. (1998). YopJ of Yersinia pseudotuberculosis is required for the inhibition of macrophage TNF-alpha production and downregulation of the MAP kinases p38 and JNK. Mol Microbiol 27: 953–965.

Palmer, L.E., Pancetti, A.R., Greenberg, S., and Bliska, J.B. (1999). YopJ of Yersinia spp. is sufficient to cause downregulation of multiple mitogen-activated protein kinases in eukaryotic cells. Infect Immun 67: 708–716.

Park, B.S. et al. (2009). The structural basis of lipopolysaccharide recognition by the TLR4-MD-2 complex. Nature 458: 1191–1195.

Park, J.M. et al. (2004). Targeting of TAK1 by the NF-kappa B protein Relish regulates the JNK-mediated immune response in Drosophila. Genes Dev 18: 584–594.

Parks, A.L. et al. (2004). Systematic generation of high-resolution deletion coverage of the Drosophila melanogaster genome. Nat Genet 36: 288–292.

Perkins, N.D. et al. (1997). Regulation of NF-kappaB by cyclin-dependent kinases associated with the p300 coactivator. Science 275: 523–527.

Petroski, M.D., and Deshaies, R.J. (2005). Function and regulation of cullin-RING ubiquitin ligases. Nat Rev Mol Cell Biol 6: 9–20.

Pili-Floury, S. et al. (2004). In vivo RNA interference analysis reveals an unexpected role for GNBP1 in the defense against Gram-positive bacterial infection in Drosophila adults. J Biol Chem 279: 12848–12853.

Prag, G. et al. (2003). Mechanism of ubiquitin recognition by the CUE domain of Vps9p. Cell 113: 609–620.

Prickett, T.D. et al. (2008). TAB4 stimulates TAK1-TAB1 phosphorylation and binds polyubiquitin to direct signaling to NF-kappaB. J Biol Chem 283: 19245–19254.

Qiao, B., Padilla, S.R., and Benya, P.D. (2005). Transforming growth factor (TGF)-beta-activated kinase 1 mimics and mediates TGF-beta-induced stimulation of type II collagen synthesis in chondrocytes independent of Col2a1 transcription and Smad3 signaling. J Biol Chem 280: 17562–17571.

Qin, J., Jiang, Z., Qian, Y., Casanova, J.L., and Li, X. (2004). IRAK4 kinase activity is redundant for interleukin-1 (IL-1) receptor-associated kinase phosphorylation and IL-1 responsiveness. J Biol Chem 279: 26748–26753.

Qiu, P., Pan, P.C., and Govind, S. (1998). A role for the Drosophila Toll/Cactus pathway in larval hematopoiesis. Development 125: 1909–1920.

Rahighi, S. et al. (2009). Specific recognition of linear ubiquitin chains by NEMO is important for NF-kappaB activation. Cell 136: 1098–1109.

Ramet, M., Lanot, R., Zachary, D., and Manfruelli, P. (2002a). JNK signaling pathway is required for efficient wound healing in Drosophila. Dev Biol 241: 145–156.

Ramet, M., Manfruelli, P., Pearson, A., Mathey-Prevot, B., and Ezekowitz, R.A. (2002b). Functional genomic analysis of phagocytosis and identification of a Drosophila receptor for E. coli. Nature 416: 644–648.

Reach, M. et al. (1996). A gradient of cactus protein degradation establishes dorsoventral polarity in the Drosophila embryo. Dev Biol 180: 353–364.

Ribeiro, P.S. et al. (2007). DIAP2 functions as a mechanism-based regulator of drICE that contributes to the caspase activity threshold in living cells. J Cell Biol 179: 1467–1480.

Rothwarf, D.M., Zandi, E., Natoli, G., and Karin, M. (1998). IKKg is an essential regulatory subunit of the IkB kinase complex. Nature 395: 297–300.

Rutschmann, S. et al. (2000a). The Rel protein DIF mediates the antifungal but not the antibacterial host defense in Drosophila. Immunity 12: 569–580.

Rutschmann, S. et al. (2000b). Role of Drosophila IKK gamma in a toll-independent antibacterial immune response. Nat Immunol 1: 342–347.

Sakurai, H., Miyoshi, H., Mizukami, J., and Sugita, T. (2000). Phosphorylation-dependent activation of TAK1 mitogen-activated protein kinase kinase kinase by TAB1. FEBS Lett 474: 141–145.

Salmena, L. et al. (2003). Essential role for caspase 8 in T-cell homeostasis and T-cell-mediated immunity. Genes Dev 17: 883–895.

Samakovlis, C., Åsling, B., Boman, H.G., Gateff, E., and Hultmark, D. (1992). In vitro induction of cecropin genes--an immune response in a Drosophila blood cell line. Biochem. Biophys. Res. Commun. 188: 1169–1175.

Samakovlis, C., Kimbrell, D.A., Kylsten, P., Engstrom, A., and Hultmark, D. (1990). The immune response in Drosophila: pattern of cecropin expression and biological activity. Embo J 9: 2969–2976.

Sanjo, H. et al. (2003). TAB2 is essential for prevention of apoptosis in fetal liver but not for interleukin-1 signaling. Mol Cell Biol 23: 1231–1238.

Santamaria, P., and Nusslein-Volhard, C. (1983). Partial rescue of dorsal, a maternal effect mutation affecting the dorso-ventral pattern of the Drosophila embryo, by the injection of wild-type cytoplasm. Embo J 2: 1695–1699.

Sato, M., Umetsu, D., Murakami, S., Yasugi, T., and Tabata, T. (2006). DWnt4 regulates the dorsoventral specificity of retinal projections in the Drosophila melanogaster visual system. Nat Neurosci 9: 67–75.

Sato, S. et al. (2003). Toll/IL-1 receptor domain-containing adaptor inducing IFN-beta (TRIF) associates with TNF receptor-associated factor 6 and TANK-binding kinase 1, and activates two distinct transcription factors, NF-kappa B and IFN-regulatory factor-3, in the Toll-like receptor signaling. J Immunol 171: 4304–4310.

Schesser, K. et al. (1998). The yopJ locus is required for Yersinia-mediated inhibition of NF-kappaB activation and cytokine expression: YopJ contains a eukaryotic SH2-like domain that is essential for its repressive activity. Mol Microbiol 28: 1067–1079.

Schmidt, C. et al. (2003). Mechanisms of proinflammatory cytokine-induced biphasic NF-kappaB activation. Mol Cell 12: 1287–1300.

Senger, K. et al. (2004). Immunity regulatory DNAs share common organizational features in Drosophila. Mol Cell 13: 19–32.

Sharma, S. et al. (2003). Triggering the interferon antiviral response through an IKK-related pathway. Science 300: 1148–1151.

Shi, Y. (2004). Caspase activation, inhibition, and reactivation: a mechanistic view. Protein Sci 13: 1979–1987.

Shibuya, H. et al. (1996). TAB1: an activator of the TAK1 MAPKKK in TGF-beta signal transduction. Science 272: 1179–1182.

Shim, J.H. et al. (2005). TAK1, but not TAB1 or TAB2, plays an essential role in multiple signaling pathways in vivo. Genes Dev 19: 2668–2681.

Silverman, N., and Maniatis, T. (2001). NF-kappaB signaling pathways in mammalian and insect innate immunity. Genes Dev 15: 2321–2342.

Silverman, N. et al. (2003). Immune activation of NF-kappaB and JNK requires Drosophila TAK1. J Biol Chem 278: 48928–48934.

Silverman, N. et al. (2000). A Drosophila IkappaB kinase complex required for Relish cleavage and antibacterial immunity. Genes Dev 14: 2461–271.

Sluss, H.K., Han, Z., Barrett, T., Davis, R.J., and Ip, Y.T. (1996). A JNK signal transduction pathway that mediates morphogenesis and an immune response in Drosophila. Genes Dev 10: 2745–258.

Spencer, E., Jiang, J., and Chen, Z.J. (1999). Signal-induced ubiquitination of IkBa by the F-box protein Slimb/bTrCP. Genes & Dev. 13: 284–294.

Steiner, H., Hultmark, D., Engstrom, A., Bennich, H., and Boman, H.G. (1981). Sequence and specificity of two antibacterial proteins involved in insect immunity. Nature 292: 246–248.

Steinhaus, E.A. (1940). THE MICROBIOLOGY OF INSECTS: With Special Reference to the Biologic Relationships between Bacteria and Insects. Bacteriol Rev 4: 17–57.

Stenbak, C.R. et al. (2004). Peptidoglycan molecular requirements allowing detection by the Drosophila immune deficiency pathway. J Immunol 173: 7339–7348.

Stöven, S., Ando, I., Kadalayil, L., Engström, Y., and Hultmark, D. (2000). Activation of the *Drosophila* NF-kB factor Relish by rapid endoproteolytic cleavage. EMBO Rep 1: 347–352.

Stöven, S. et al. (2003). Caspase-mediated processing of the Drosophila NF-{kappa}B factor Relish. Proc Natl Acad Sci U S A

Stronach, B. (2005). Dissecting JNK signaling, one KKKinase at a time. Dev Dyn 232: 575–584.

Su, H. et al. (2005a). Requirement for caspase-8 in NF-kappaB activation by antigen receptor. Science 307: 1465–1468.

Su, H. et al. (2005b). Requirement for caspase-8 in NF-kappaB activation by antigen receptor. Science 307: 1465–1468.

Sun, H. et al. (2008). TIPE2, a negative regulator of innate and adaptive immunity that maintains immune homeostasis. Cell 133: 415–426.

Sun, L., Deng, L., Ea, C.K., Xia, Z.P., and Chen, Z.J. (2004). The TRAF6 ubiquitin ligase and TAK1 kinase mediate IKK activation by BCL10 and MALT1 in T lymphocytes. Mol Cell 14: 289–301.

Sun, S.C., Asling, B., and Faye, I. (1991). Organization and expression of the immunoresponsive lysozyme gene in the giant silk moth, Hyalophora cecropia. J Biol Chem 266: 6644–6649.

Sun, X., Yin, J., Starovasnik, M.A., Fairbrother, W.J., and Dixit, V.M. (2002a). Identification of a novel homotypic interaction motif required for the phosphorylation of receptor-interacting protein (RIP) by RIP3. J Biol Chem 277: 9505–9511.

Sun, X., Yin, J., Starovasnik, M.A., Fairbrother, W.J., and Dixit, V.M. (2002b). Identification of a novel homotypic interaction motif required for the phosphorylation of receptor-interacting protein (RIP) by RIP3. J Biol Chem 277: 9505–9511.

Suzuki, N., Suzuki, S., and Yeh, W.C. (2002). IRAK-4 as the central TIR signaling mediator in innate immunity. Trends Immunol 23: 503–506.

Sweet, C.R., Conlon, J., Golenbock, D.T., Goguen, J., and Silverman, N. (2007). YopJ targets TRAF proteins to inhibit TLR-mediated NF-kappaB, MAPK and IRF3 signal transduction. Cell Microbiol 9: 2700–2715.

Takaesu, G. et al. (2000). TAB2, a novel adaptor protein, mediates activation of TAK1 MAPKKK by linking TAK1 to TRAF6 in the IL-1 signal transduction pathway. Mol Cell 5: 649–58.

Takahashi, K. et al. (2006). Roles of caspase-8 and caspase-10 in innate immune responses to double-stranded RNA. J Immunol 176: 4520–4524.

Takehana, A. et al. (2002). Overexpression of a pattern-recognition receptor, peptidoglycan-recognition protein-LE, activates imd/relish-mediated antibacterial defense and the prophenoloxidase cascade in Drosophila larvae. Proc Natl Acad Sci U S A 99: 13705–13710.

Takehana, A. et al. (2004). Peptidoglycan Recognition Protein (PGRP)-LE and PGRP-LC act synergistically in *Drosophila* immunity. Embo J 23: 4690–4700.

Tanji, T., Hu, X., Weber, A.N., and Ip, Y.T. (2007). Toll and IMD pathways synergistically activate innate immune response in Drosophila. Mol Cell Biol

Tauszig-Delamasure, S., Bilak, H., Capovilla, M., Hoffmann, J.A., and Imler, J.L. (2002). Drosophila MyD88 is required for the response to fungal and Gram-positive bacterial infections. Nat Immunol 3: 91–97.

Tenev, T., Zachariou, A., Wilson, R., Ditzel, M., and Meier, P. (2005). IAPs are functionally non-equivalent and regulate effector caspases through distinct mechanisms. Nat Cell Biol 7: 70–77.

Thevenon, D. et al. (2009). The *Drosophila* Ubiquitin Specific Protease dUSP36/Scny targets IMD to prevent constitutive immune signalling. Cell Host and Microbes

Tokunaga, F. et al. (2009). Involvement of linear polyubiquitylation of NEMO in NF-kappaB activation. Nat Cell Biol 11: 123–132.

Towb, P., Galindo, R.L., and Wasserman, S.A. (1998). Recruitment of Tube and Pelle to signaling sites at the surface of the Drosophila embryo. Development 125: 2443–250.

Trompouki, E. et al. (2003). CYLD is a deubiquitinating enzyme that negatively regulates NF-kappaB activation by TNFR family members. Nature 424: 793–796.

Tzou, P. et al. (2000). Tissue-specific inducible expression of antimicrobial peptide genes in Drosophila surface epithelia. Immunity 13: 737–748.

Tzou, P., Reichhart, J.M., and Lemaitre, B. (2002). Constitutive expression of a single antimicrobial peptide can restore wild-type resistance to infection in immunodeficient Drosophila mutants. Proc Natl Acad Sci U S A 99: 2152–2157.

Valanne, S., Kleino, A., Myllymaki, H., Vuoristo, J., and Ramet, M. (2007). Iap2 is required for a sustained response in the Drosophila Imd pathway. Dev Comp Immunol

Varshavsky, A. (2000). Ubiquitin fusion technique and its descendants. Methods Enzymol 327: 578–593.

Vaux, D.L., and Silke, J. (2005). IAPs, RINGs and ubiquitylation. Nat Rev Mol Cell Biol 6: 287–297.

Verhagen, A.M., Coulson, E.J., and Vaux, D.L. (2001). Inhibitor of apoptosis proteins and their relatives: IAPs and other BIRPs. Genome Biol 2: REVIEWS3009.

Vidal, S. et al. (2001). Mutations in the Drosophila dTAK1 gene reveal a conserved function for MAPKKKs in the control of rel/NF-kappaB-dependent innate immune responses. Genes Dev 15: 1900–1912.

Wang, C. et al. (2001). TAK1 is a ubiquitin-dependent kinase of MKK and IKK. Nature 412: 346–351.

Weber, A.N. et al. (2003). Binding of the Drosophila cytokine Spatzle to Toll is direct and establishes signaling. Nat Immunol 4: 794–800.

Werner, T., Borge-Renberg, K., Mellroth, P., Steiner, H., and Hultmark, D. (2003). Functional diversity of the Drosophila PGRP-LC gene cluster in the response to lipopolysaccharide and peptidoglycan. J Biol Chem 278: 26319–26322.

Wesche, H., Henzel, W.J., Shillinglaw, W., Li, S., and Cao, Z. (1997). MyD88: an adapter that recruits IRAK to the IL-1 receptor complex. Immunity 7: 837–847.

Wicker, C. et al. (1990). Insect immunity. Characterization of a Drosophila cDNA encoding a novel member of the diptericin family of immune peptides. J Biol Chem 265: 22493–22498.

Windheim, M., Stafford, M., Peggie, M., and Cohen, P. (2008). Interleukin-1 (IL-1) induces the Lys63-linked polyubiquitination of IL-1 receptor-associated kinase 1 to facilitate NEMO binding and the activation of IkappaBalpha kinase. Mol Cell Biol 28: 1783–1791.

Wooff, J., Pastushok, L., Hanna, M., Fu, Y., and Xiao, W. (2004). The TRAF6 RING finger domain mediates physical interaction with Ubc13. FEBS Lett 566: 229–233.

Wu, C.J., Conze, D.B., Li, T., Srinivasula, S.M., and Ashwell, J.D. (2006). Sensing of Lys 63-linked polyubiquitination by NEMO is a key event in NF-kappaB activation [corrected]. Nat Cell Biol 8: 398–406.

Wu, G. et al. (2000). Structural basis of IAP recognition by Smac/DIABLO. Nature 408: 1008–1012.

Wu, L.P., and Anderson, K.V. (1998). Regulated nuclear import of Rel proteins in the Drosophila immune response. Nature 392: 93–97.

Xia, Z.P. et al. (2009). Direct activation of protein kinases by unanchored polyubiquitin chains. Nature 461: 114–119.

Xu, M., Skaug, B., Zeng, W., and Chen, Z.J. (2009). A Ubiquitin replacement strategy in human cells reveals distinct mechanisms of IKK activation by TNFalpha and IL-1beta. Mol Cell 36: 302–314.

Yamamoto, M. et al. (2006). Key function for the Ubc13 E2 ubiquitin-conjugating enzyme in immune receptor signaling. Nat Immunol 7: 962–970.

Yamamoto, M. et al. (2003). Role of adaptor TRIF in the MyD88-independent toll-like receptor signaling pathway. Science 301: 640–643.

Yamin, T.T., and Miller, D.K. (1997). The interleukin-1 receptor-associated kinase is degraded by proteasomes following its phosphorylation. J Biol Chem 272: 21540–21547.

Yoon, S., Liu, Z., Eyobo, Y., and Orth, K. (2003). Yersinia effector YopJ inhibits yeast MAPK signaling pathways by an evolutionarily conserved mechanism. J Biol Chem 278: 2131–2135.

Yu, Y. et al. (2008). Phosphorylation of Thr-178 and Thr-184 in the TAK1 T-loop is required for interleukin (IL)-1-mediated optimal NFkappaB and AP-1 activation as well as IL-6 gene expression. J Biol Chem 283: 24497–24505.

Zandi, E., Rothwarf, D.M., Delhase, M., Hayakawa, M., and Karin, M. (1997). The IkappaB kinase complex (IKK) contains two kinase subunits, IKKalpha and IKKbeta, necessary for IkappaB phosphorylation and NF-kappaB activation. Cell 91: 243–252.

Zettervall, C.J. et al. (2004). A directed screen for genes involved in Drosophila blood cell activation. Proc Natl Acad Sci U S A 101: 14192–14197.

Zhou, H. et al. (2005a). Yersinia virulence factor YopJ acts as a deubiquitinase to inhibit NF-kappa B activation. J Exp Med 202: 1327–1332.

Zhou, R. et al. (2005b). The role of ubiquitnation in Drosophila innate immunity. J Biol Chem

Zhuang, Z.H. et al. (2006). Drosophila TAB2 is required for the immune activation of JNK and NF-kappaB. Cell Signal 18: 964–970.